AD 289 613

Best
Available
Copy

63-1-5

MEMORANDUM
RM-2826-PR
NOVEMBER 1962

THE THERMODYNAMIC PROPERTIES AND SHOCK-WAVE CHARACTERISTICS OF A MODEL VENUS ATMOSPHERE

W. C. Strahle

PREPARED FOR:

UNITED STATES AIR FORCE PROJECT RAND

The RAND Corporation
SANTA MONICA • CALIFORNIA

MEMORANDUM
RM-2826-PR
NOVEMBER 1962

THE THERMODYNAMIC PROPERTIES AND SHOCK-WAVE CHARACTERISTICS OF A MODEL VENUS ATMOSPHERE

W. C. Strahle

This research is sponsored by the United States Air Force under Project RAND — Contract No. AF 49(638)-700 — monitored by the Directorate of Development Planning, Deputy Chief of Staff, Research and Technology, Hq USAF. Views or conclusions contained in this Memorandum should not be interpreted as representing the official opinion or policy of the United States Air Force. Permission to quote from or reproduce portions of this Memorandum must be obtained from The RAND Corporation.

The RAND Corporation
1700 MAIN ST • SANTA MONICA • CALIFORNIA

PREFACE

This Project RAND Memorandum extends the study reported in RM-2292, _Thermodynamic Properties of Carbon Dioxide to 24,000°K - With Possible Application to the Atmosphere of Venus._ Whereas that earlier study assumed an atmosphere of pure carbon dioxide, the present study assumes an atmospheric composition of 85 per cent carbon dioxide and 15 per cent nitrogen by volume.

The calculated thermodynamic properties of this mixture, as well as the normal-shock-wave properties at selected altitudes, are presented as an aid to studies of the aerodynamic phenomena of high-speed vehicle entry into the atmosphere of Venus.

ACKNOWLEDGMENTS

The author is very grateful for the many instructive discussions with J. L. Raymond, S. H. Dole, and F. R. Gilmore. The assistance of Jeannine McGann and Carolyn Huber with the calculations and graphs is also greatly appreciated.

SUMMARY

In this Memorandum a model for the atmosphere of Venus is developed which may be useful for design studies of early atmospheric-entry vehicles and for wind-tunnel simulation application. This atmosphere, derived from many questionable assumptions and scant experimental data, consists of 85 per cent carbon dioxide and 15 per cent nitrogen by volume.

The thermodynamic properties of the derived atmospheric composition are presented over the temperature-pressure range of 150°K to 24,000°K and 10^{-4} atm to 10^{2} atm. To further assist in aerodynamic entry calculations, normal-shock-wave characteristics of such an atmosphere are also presented. The fact that nitrogen is present has important consequences in the thermodynamic properties and electron concentrations over the full temperature and pressure range. The effects are of the order of the percentage of nitrogen addition to pure carbon dioxide.

A graphical method of obtaining obtaining oblique-shock-wave data and a method of obtaining electron concentrations at low temperatures are included as appendixes.

CONTENTS

SYMBOLS

A	area, cm^2
C	specific heat, $\frac{Btu}{lb\text{-}mole\ ^oR}$, $\frac{cal}{g\text{-}mole\ ^oK}$
E	specific internal energy, cal/g-mole
e	specific internal energy, cal/g
F	Gibbs free energy, cal/g-mole
g	acceleration of gravity, cm/sec^2
H	specific enthalpy, cal/g-mole
h	specific enthalpy, cal/g
$\bar{H}$	specific enthalpy in Ref. 10, Btu/lb-mole
K_p	equilibrium constant for partial pressures
L	Avogadro's number, particles/g-mole
M	molecular weight (of mixture if without a subscript), g/g-mole
M_o	molecular weight of "cold" undissociated mixture, g/g-mole
m	mass, g
n	number of g-moles = $\sum_i n_i$
p	pressure, atm
p_o	standard pressure, 1 atm
q	polytropic exponent
R	universal gas constant, $\frac{Btu}{lb\text{-}mole\ ^oR}$, $\frac{cal}{g\text{-}mole\ ^oK}$
r	radius from center of planet, Km
S	specific entropy, cal/g-mole ^oK
s	specific entropy, cal/g ^oK
T	temperature, ^oK
T_o	standard temperature, 273.16^oK

u	velocity component normal to a two-dimensional oblique shock wave, ft/sec
v	velocity component parallel to a two-dimensional oblique shock wave, ft/sec
w	free-stream velocity in two-dimensional flow $= \sqrt{u^2 + v^2}$, ft/sec
β	two-dimensional oblique-shock-wave inclination angle to free stream ($\leq 90^{\circ}$)
γ	ratio of specific heats $= C_p/C_v$
θ	two-dimensional oblique-shock-wave flow deflection angle
ρ	density, g/cm^3
ρ_o	density at p_o, T_o, and M_o, g/cm^3
Φ	entropy function tabulated in Ref. 10, Btu/lb-mole $^{\circ}R$

<u>SUBSCRIPTS</u>

E	earth
i	i^{th} species
o	standard temperature, 0 $^{\circ}K$ unless as specified by T_o
p	constant pressure
s	surface of planet
V	Venus
v	constant volume
1	state upstream of shock wave
2	state aft of shock wave

<u>SUPERSCRIPT</u>

o	standard pressure, 1 atm

I. INTRODUCTION

In order that design studies may be carried out concerning space-vehicle entry into planetary atmospheres, it is necessary that the atmospheric composition-pressure-density relation with altitude for a particular atmosphere in question be known to a fair degree of precision. Since shock-wave, deceleration, and aerodynamic-heating calculations are all dependent upon this relation, it must at least be bracketed within reasonable limits.[1] This study is concerned with estimating this relation for the atmosphere of Venus.

Unfortunately, very little is known concerning this atmosphere. Through theoretical arguments, spectroscopic, photometric, and radiometric measurements, several theories have been advanced, no two of which, however, appear to be the same.[1-8] An attempt is made here to bring about reasonable agreement between two theories that are approached from different viewpoints. The resulting atmospheric model could then be used as a tentative mean which could be compared to other theoretical and experimental models until more experimental data are gathered and a better understanding of the Venus atmosphere develops. The establishment of this mean model atmosphere and its thermodynamic and aerodynamic characteristics is the objective of this study.

The first theory on the Venus atmosphere which is considered is that of Dole.[3] The partial pressures given in Ref. 3 correspond to a per cent by volume equal to the reported per cent by weight. Since the molecular weight of N_2 and CO_2 are markedly different, this cannot be the case. Two methods for calculating atmospheric composition have been employed. Using the basic data on pp. 4-6 and the theory of Dole, the probable range of atmospheric compositions has been recalculated; a probable average composition

according to this theory has also been calculated. The second method employed makes use of some of the available experimental data, one of Dole's basic assumptions, and one assumption concerning the pressure-density relation of the Venus atmosphere below the cloud layer. The assumptions involved are open to debate and the experimental data are highly uncertain, but the remarkable result is that the two methods yield quantitative estimates of the atmospheric composition in close agreement with each other. It is taken as the basic statement of this Memorandum that these methods do yield a reasonable quantitative estimate of the atmospheric composition. The composition arrived at is 85 per cent CO_2 and 15 per cent N_2 by volume, and the atmosphere is then modeled; i.e., the pressure-temperature-altitude relation is derived. The thermodynamic properties of the chosen composition are calculated over the temperature-pressure ranges of $150^{\circ}K$ to $24{,}000^{\circ}K$ and 10^{-4} atm to 10^{2} atm, respectively. Finally, normal shock-wave properties are presented for selected altitudes in the chosen atmospheric model.

The appendices include a method of obtaining oblique shock-wave properties from normal shock-wave properties and a method of obtaining electron concentrations at low temperatures. The first is useful when it is impractical to compute and plot oblique shock charts because of uncertainty in the characteristics of a particular atmosphere. The second is useful for determining the temperature and pressure influence on the electromagnetic environment, for example, of radio signals to or from an entry vehicle.

II. A TENTATIVE ATMOSPHERE FOR VENUS

CONDITIONS AND ASSUMPTIONS

Two methods will be used to deduce the composition of the Venus atmosphere; one is that of Dole,(3) while the other is based on a few selected experimental measurements. The first approach will merely require that slight numerical refinements be made in Dole's paper; the trace of argon mentioned in the paper will be neglected, but the theory will be assumed correct. The second approach will require assumptions concerning both the validity of some highly speculative experimental data and the pressure-temperature-altitude relation below the Venus cloud layer. More will be said later concerning the acceptance of these data and the assumptions involved in choosing the final model. However, before continuing with the derivation it is necessary to state that this is not intended to be a rigorous, absolute derivation of the composition of the Venus atmosphere. It is solely intended to provide some justification for assuming a particular model atmosphere. The discussion at the end of this section will shed some light on the difficulties associated with the acceptance of this model; as for acceptance of some of the experimental data, the reader may consult the referenced literature.

First, some general assumptions pertinent to both methods are necessary. The constituents of the atmosphere will be assumed to obey the perfect gas law, $p/\rho = RT/M$. The gas mixture will be assumed to be of constant composition throughout the atmosphere; this neglects "settling" of heavier constituents, diffusion, photodissociation, and ionization. The complete gas mixture is assumed to be in hydrostatic equilibrium in a constant gravitational field, with centrifugal force due to planetary

rotation being neglected. Now, as pointed out in Ref. 1, all of these assumptions except the perfect gas law may be far from realizable, especially at high altitudes. However, they introduce far less uncertainty than do the assumptions to follow, and they are fairly good assumptions for the altitude range of aerodynamic interest.

Following Dole, the amount of N_2 in the Venus atmosphere will be assumed equal to that in Earth's, but scaled down to make allowance for the difference in the sizes of the planets. Since the atmospheric gases are mainly generated at or near the surface of a planet, relative masses of N_2 in the two atmospheres will be scaled in proportion to the surface areas of the two planets. Moreover, the Venus atmosphere is assumed to consist of only CO_2 and N_2, the trace constituents being neglected. These two assumptions are basically deduced by Dole, and they are basic to both the numerical refinements in Dole's paper and to the second method.

The second method will require, in addition to the above, that the atmosphere of Venus exist in adiabatic equilibrium from the surface to "the top of the cloud layer." This is another very basic and important assumption.

The numerical data consistent both with what is known of Earth and Venus and with the above assumptions are presented below. For detailed information on these data, the reader is directed to the references. The composition of the Venus atmosphere will then be calculated from considerations of these two methods or approaches and the data below.

BASIC DATA

A. Composition of air by volume for Earth(9)

O_2 = 20.946 per cent

$N_2 = 78.084$ per cent

+ trace elements

B. Molecular weights (chemical scale)[9]

$$M_{N_2} = 28.016 \text{ g/g-mole}$$

$$M_{CO_2} = 44.011 \text{ g/g-mole}$$

$$M_{Air} = 28.967 \text{ g/g-mole}$$

C. Specific heats (450°K)[10]

$$(c_p)_{N_2} = 7.017 \text{ cal/g-mole }^{\circ}\text{K}$$

$$(c_v)_{N_2} = 5.031 \text{ cal/g-mole }^{\circ}\text{K}$$

$$(c_p)_{CO_2} = 10.280 \text{ cal/g-mole }^{\circ}\text{K}$$

$$(c_v)_{CO_2} = 8.294 \text{ cal/g-mole }^{\circ}\text{K}$$

D. Mass of CO_2 per unit area of Earth's surface (in the atmosphere, sea water, carbonates, coal, etc.)[3]

$$\left(\frac{m_{CO_2}}{A_s}\right)_E = 7.23 - 9.66 \text{ kg/cm}^2\text{, estimated limits}$$

$$\left(\frac{m_{CO_2}}{A_s}\right)_{E_{Average}} = 8.445 \text{ kg/cm}^2 \text{ (computed from Ref. 3)}$$

E. Planetary data

$$m_V/m_E = 0.819 \text{ (averaged from Ref. 3)}$$

$$r_{s_V}/r_{s_E} = 0.950$$ (estimated from Ref. 3, including an estimate for the height of the cloud layer)

$$r_{s_E} = 6371 \text{ km}$$[11]

$$g_{s_V}/g_{s_E} = 0.90748 \text{ (computed from above)}$$

$$g_{s_E} = 980.665 \text{ cm/sec}^2 \text{ (11)}$$

F. Experimental (and highly uncertain) data concerning the atmosphere of Venus

Surface temperature

$$T_s = 600^\circ K \text{ (12)}$$

Temperature of reflecting layer above which there are 1000 m-atm* of CO_2

$$T_1 = 300^\circ K \text{ (2,13)}$$

Temperature at or near the "cloud top," but assumed to be above the 300°K reflecting layer (data compiled from original references in Ref. 6)

$$T_2 = 235^\circ K$$

THEORETICAL DEVELOPMENT

Dole's Approach

Dole's theory is based on the assumption that since the Earth and Venus are similar in mass and size the only differences between them must be fundamentally due to the amount of solar radiation received by each. Hence, an evolutionary theory of the origin of the Earth's atmosphere expressed by conservation equations of atmospheric constituents may be looked at by describing the effects of placing Earth in Venus' orbit some 3 or 4 billion years ago. Briefly, the results are that due to the increased surface temperature no surface water could exist. The water vapor would be subject to a

---

*One m-atm of a gas is the mass contained in a tube 1 m long and with a 1-cm^2 cross-sectional area, when the gas is at standard pressure and temperature.

higher rate of dissociation due to increased radiation, and the result would be a dry planet. In the absence of liquid water, CO_2 produced by volcanic action would not go into solid carbonates or sea water. Atmospheric turbulence would be very high, wind erosion would be increased, and, coupled with a higher surface temperature and normal isostasy, surface oxidation would be very great. Together with the oxidation of CO produced by volcanic action, surface oxidation would remove most of the O_2 from the atmosphere. The balance of N_2 would be only slightly affected. Therefore, the net result is a dry atmosphere of CO_2 and N_2. This enables a quantitative estimate of these constituents.

Under the assumption of static equilibrium with no centrifugal force, and considering a spherical coordinate system fixed to a planet, the hydrostatic differential equation may be shown to be of complete generality as

$$dp = - g\rho dr \tag{1}$$

Now consider an atmosphere of constant composition consisting of "i" perfect gases in over-all hydrostatic equilibrium; also, consider the acceleration of gravity to be constant through the depth of the atmosphere. By integrating the mass of the atmosphere through its depth above a unit surface area using Eq. (1) and perfect gas relations, it may be shown that

$$\left(\begin{array}{c}\text{mass of species i in the atmosphere}\\ \text{per unit surface area}\end{array}\right) = \frac{1}{g_s}\,\frac{M_i}{M}\,p_{i_s}$$

or

$$p_{i_s} = \left(\frac{m_i}{A_s}\right)\frac{M}{M_i}\,g_s \tag{2}$$

Alternatively, since

$$m_i = n_i M_i$$

$$p_{i_s} = \left(\frac{n_i}{A_s}\right) M\, g_s \qquad (3)$$

Therefore, if the mass of species i in the total atmosphere is known, and if the composition percentages are known along with the physical size of the planet, the partial pressure of species i at the surface may be found. Note that this equation requires that each species in a constant-composition atmosphere be not in hydrostatic equilibrium with itself, and that the surface partial pressure of a particular species be not generally equal to the weight per unit area of the gas above the surface as was reported by Dole. This is therefore a refinement in Dole's findings. It is known that for perfect gases partial-pressure ratios represent ratios of percentage by volume, not by weight. Therefore, it would be impossible to have the surface partial pressure of a particular species generally equal to the weight per unit area of this species above the surface of the planet. This refinement will decrease the fraction of CO_2 reported by Dole by approximately 4 per cent.

The method of computation then becomes

1. Consistent with the original assumption, the acceleration of gravity on Earth is assumed to be a constant with altitude. From the air composition data on p. 4 and from Eq. (2), the mass of N_2 in Earth's atmosphere per unit surface area is calculated.

$$\left(\frac{m_{N_2}}{A_s}\right)_E = \frac{p_{N2_E}\, M_{N_2}}{M_{Air}\, g_{s_E}} = 780.11 \text{ gm/cm}^2$$

2. From the data on p. 5 concerning the CO_2 and from step (1) above, the composition by weight of CO_2 and N_2 is found. Under Dole's theory, and neglecting the trace of argon, this comprises the atmosphere of Venus.

$$(\%\ CO_2 \text{ by weight}) = 100 \times \left(\frac{m_{CO_2}}{A_s}\right)_E \Bigg/ \left[\left(\frac{m_{CO_2}}{A_s}\right)_E + \left(\frac{m_{N_2}}{A_s}\right)_E\right]$$

$$(\%\ N_2 \text{ by weight}) = 100 \times \left(\frac{m_{N_2}}{A_s}\right)_E \Bigg/ \left[\left(\frac{m_{N_2}}{A_s}\right)_E + \left(\frac{m_{CO_2}}{A_s}\right)_E\right]$$

3. From step (2) above, and the molecular-weight data previously mentioned, the composition by volume is found.

$$(\%\ CO_2 \text{ by volume}) = \frac{(\%\ CO_2 \text{ by weight})\left(\dfrac{M_{N_2}}{M_{CO_2}}\right)}{1 + \dfrac{(\%\ CO_2 \text{ by weight})}{100}\left(\dfrac{M_{N_2}}{M_{CO_2}} - 1\right)}$$

$$(\%\ N_2 \text{ by volume}) = \frac{(\%\ N_2 \text{ by weight})\left(\dfrac{M_{CO_2}}{M_{N_2}}\right)}{1 + \dfrac{(\%\ N_2 \text{ by weight})}{100}\left(\dfrac{M_{CO_2}}{M_{N_2}} - 1\right)}$$

4. From Eq. (2), the molecular weight and planetary data, step (3), and the assumption that the mass of N_2 in the atmosphere is proportional to surface area, the surface partial pressure of N_2 is found for Venus. Essentially the mass of N_2 per unit surface area is assumed to be the same for Earth and Venus.

$$M = \left(\frac{\%\ CO_2 \text{ by volume}}{100}\right) M_{CO_2} + \left(\frac{\%\ N_2 \text{ by volume}}{100}\right) M_{N_2}$$

$$p_{N_{2_{s_V}}} = \left(\frac{m_{N_2}}{A_s}\right)_E \frac{M}{M_{N_2}} g_{s_V}$$

5. From steps (3) and (4) the surface partial pressure of CO_2 is found.

$$p_{CO_{2_{s_V}}} = p_{N_{2_{s_V}}} \left(\frac{\% \; CO_2 \text{ by volume}}{\% \; N_2 \text{ by volume}} \right)$$

6. From steps (4) and (5) the total surface pressure is found.

$$p_{s_V} = p_{N_{2_{s_V}}} + p_{CO_{2_{s_V}}}$$

The results of this computation are presented in Table 1. It should not be construed, however, that the significant figures shown are indicative of the precision of the theory.

Second Approach

For an atmosphere in adiabatic equilibrium the following relation must hold

$$S_a = S_b \tag{4a}$$

where a and b denote any two positions in the atmosphere. Under our original assumptions and with the above-mentioned data, this relation must hold below the layer at 300°K, above which there are 1000 m-atm of CO_2. In particular, it must hold between the points where $T_1 = 300°K$ and $T_s = 600°K$. Using the data and methods of Ref. 10, the temperatures T_1 and T_s, and Eq. (4a), a relation among p_s, p_1, and the composition is easily obtained.

$$n_{N_2} \; R \ln \frac{p_1}{p_s} + (\bar{\phi}_s - \bar{\phi}_1)_{N_2} \, n_{N_2} + n_{CO_2} \; R \ln \frac{p_1}{p_s} + (\bar{\phi}_s - \bar{\phi}_1)_{CO_2} \, n_{CO_2} = 0$$

where $\bar{\phi} = \int \frac{C_p}{T} \, dT + \text{constant}$

Since 1000 m-atm of CO_2 = 4.461 g-mole/cm^2 of CO_2, the partial pressure of the CO_2 at point 1 may be found by Eq. (3).

$$p_{CO_{2_1}} = \left(\frac{n_{CO_{2_1}}}{A_s}\right) M\, g_s$$

Then from the law of partial pressures, the total pressure at point 1 may be found as a function of the composition.

$$p_1 = p_{CO_{2_1}} + p_{N_{2_1}} = p_{CO_{2_1}} \left(1 + \frac{n_{N_2}}{n_{CO_2}}\right) = \left(\frac{n_{CO_{2_1}}}{A_s}\right) M\, g_s \left(1 + \frac{n_{N_2}}{n_{CO_2}}\right)$$

The mass of N_2 in the atmosphere of Venus obtained in step (4) of Dole's approach is also assumed to hold here:

$$\left(\frac{n}{A_S}\right)_{N_{2_V}} = 27.845 \text{ g-mole/cm}^2$$

Now, from the law of partial pressures, Eq. (3), and the amount of N_2, the total surface pressure p_s may be found as a function of composition.

$$p_{N_{2_s}} = \left(\frac{n_{N_2}}{A_s}\right) M\, g_s$$

$$p_s = p_{N_{2_s}} + p_{CO_{2_s}} = p_{N_{2_s}} \left(1 + \frac{n_{CO_2}}{n_{N_2}}\right) = \left(\frac{n_{N_2}}{A_s}\right) M\, g_s \left(1 + \frac{n_{CO_2}}{n_{N_2}}\right)$$

These three relations yield a relation for determining the composition.

$$\frac{p_1}{p_s} = \frac{\left(n_{CO_{2_1}}/A_s\right)}{\left(n_{N_2}/A_s\right)} \quad \frac{n_{N_2}/\left(n_{N_2} + n_{CO_2}\right)}{n_{CO_2}/\left(n_{N_2} + n_{CO_2}\right)} = \frac{n_{CO_{2_1}}}{n_{CO_2}}$$

$$A_s\left(\frac{n_{N_2}}{A_s}\right)\left[R \ln\left(\frac{n_{CO_{2_1}}}{n_{CO_2}}\right) + \left(\Phi_s - \Phi_1\right)_{N_2}\right] + n_{CO_2}\left[R \ln\left(\frac{n_{CO_{2_1}}}{n_{CO_2}}\right) + \left(\Phi_s - \Phi_1\right)_{CO_2}\right] = 0$$

which must be solved for n_{CO_2} by trial. Carrying out the computation gives the following composition

$$CO_2 = 81.6 \text{ per cent}$$

$$N_2 = 18.4 \text{ per cent}$$

compared to the average values obtained by Dole's approach

$$CO_2 = 87.3 \text{ per cent}$$

$$N_2 = 12.7 \text{ per cent}$$

Thus it is apparent that both theories give quantitative results in close agreement with each other.

MODEL OF THE VENUS ATMOSPHERE

Assuming therefore that these two theories do give good quantitative estimates of the atmosphere of Venus, the remaining problem is that of adopting a tentative composition for our model Venus atmosphere. Rather than investigate the probable effects of experimental uncertainty in the data, nonuniform gravitation, trace elements, imperfect gases, etc., which would

in fact invalidate all of the original assumptions and require more accuracy than is obviously contained in this model, we make a fundamental assumption: that the temperature lapse rate with altitude is slightly less than dry adiabatic. The experimental data and all of the original assumptions are retained except that of a dry adiabatic lapse rate below T_1. As an alternative to Eq. (4a), the well-known relation

$$\frac{p_a}{p_b} = \left(\frac{T_a}{T_b}\right)^{\gamma/\gamma-1} \tag{4b}$$

could have been written for an adiabatic atmosphere of perfect gases. It was not used because γ has a strong variation with temperature for this mixture, and a "proper" average γ would have had to be chosen as in the "C" data on p. 5. If a polytropic atmosphere is assumed where an adiabatic atmosphere was previously assumed, the following equation holds by definition

$$\frac{p_a}{p_b} = \left(\frac{T_a}{T_b}\right)^{q/q-1} \tag{5}$$

For an adiabatic atmosphere, $q = \gamma$; for an isothermal atmosphere, $q = 1$; therefore, we will choose $1 < q < \gamma$. Using this criterion and Eq. (5) in place of Eq. (4a), and repeating the computations of the second approach, it is found that the composition must contain more than 81.6 per cent CO_2 by volume. This tends to reduce the discrepancy between the two approaches. The atmosphere of Venus is now arbitrarily chosen to consist of 85 per cent CO_2 and 15 per cent N_2 by volume.

With a composition assumed, the atmosphere is modeled as follows:

1. From the known composition, amount of N_2, and Eq. (3), the total surface pressure is found.

2. From the known composition, amount of CO_2 above point 1, T_s, T_1, and Eqs. (3) and (5), the exponent q is found.

3. This polytropic atmosphere is assumed to hold true until point 2 is reached, where $T_2 = 235^{\circ}K$, the assumed "cloud top."

4. The atmosphere will be considered isothermal above point 2, where $T = T_2 = 235^{\circ}K$ and $q = 1$. Now it is highly improbable that this situation precisely prevails, but it should represent a reasonable assumption over altitudes of aerodynamic interest. From the standpoint of radiative equilibrium, the temperature probably drops to about $190^{\circ}K$ at 55 km. There may also be a slight increase in temperature above this level due to O_3 heating. This will be much more suppressed, however, than the case on Earth because of the absence of much O_2 at these altitudes (provided, of course, that there is no appreciable amount of O_2 in the atmosphere of Venus). Effects of this kind are neglected in this model, however, because they are inconsistent with the accuracy possible through use of the other assumptions of the model.

5. With the above information, Eq. (5), and the perfect gas law, Eq. (1) can be integrated. This yields a complete pressure-density-temperature-altitude relation consistent with the assumptions and data. This relation is presented below, and it is represented in Table 2 and in Fig. 1.

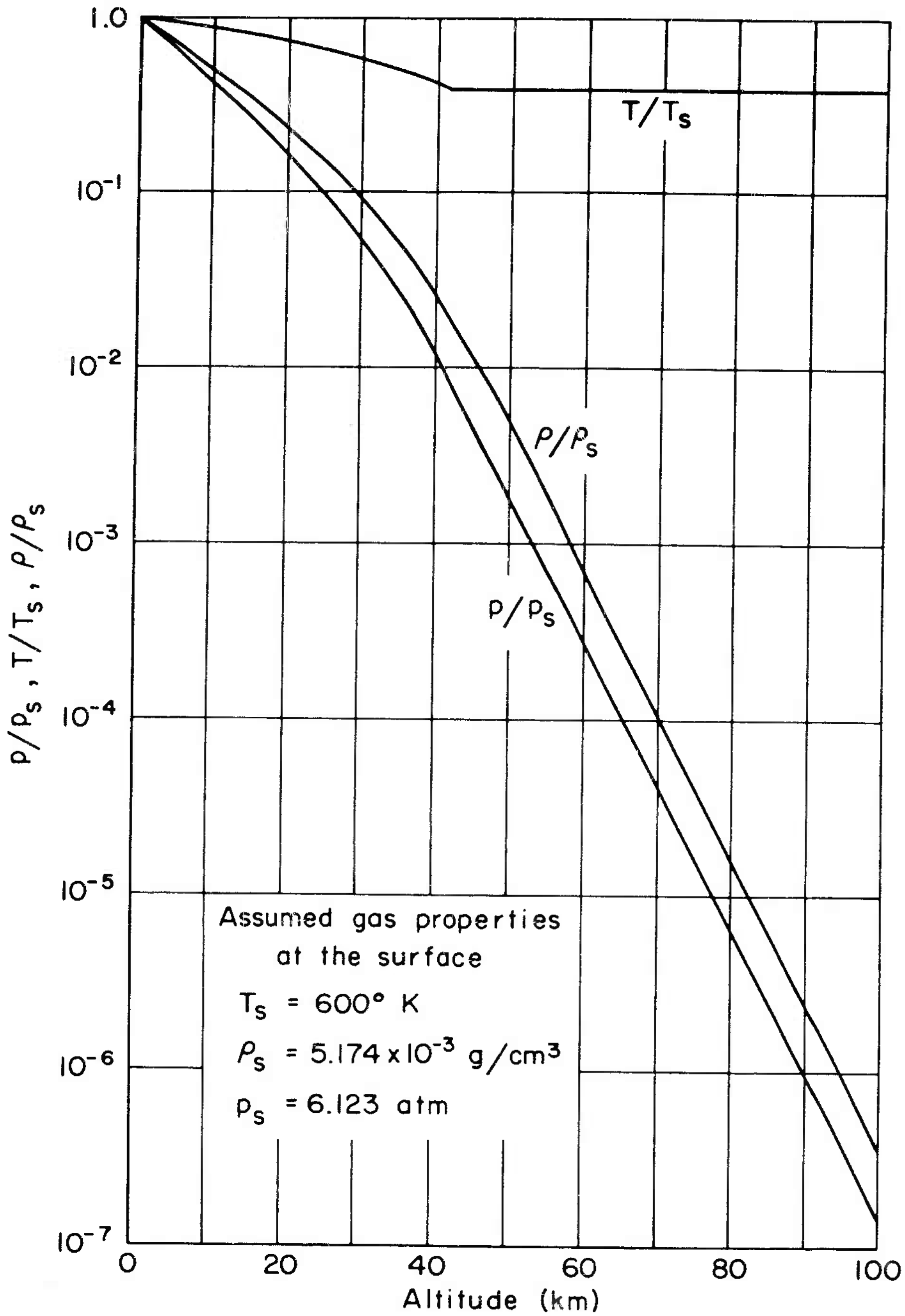

Fig. 1 — Tentative atmosphere of Venus

For $0 \le (r - r_s) \le 42.16$ km, the cloud "top" altitude,

$$\frac{p}{p_s} = \left[1 - \frac{M}{R}\frac{(q-1)}{q}\frac{g_s}{T_s}(r - r_s)\right]^{q/q-1} \tag{6}$$

$$\frac{T}{T_s} = 1 - \frac{M}{R}\frac{(q-1)}{q}\frac{g_s}{T_s}(r - r_s) = \left(\frac{p}{p_s}\right)^{q-1/q} \tag{7}$$

$$\frac{\rho}{\rho_s} = \left[1 - \frac{M}{R}\frac{(q-1)}{q}\frac{g_s}{T_s}(r - r_s)\right]^{1/q-1} = \left(\frac{p}{p_s}\right)^{(1/q)} \tag{8}$$

For $42.16 \le (r - r_s)$

$$T = T_2 = 235^\circ K$$

$$\frac{p}{p_s} = \left(\frac{p_2}{p_s}\right) \exp\left[-\frac{Mg_s}{RT_2}(r - r_2)\right] \tag{9}$$

$$\frac{\rho}{\rho_s} = \left(\frac{\rho_2}{\rho_s}\right) \exp\left[-\frac{Mg_s}{RT_2}(r - r_2)\right] \tag{10}$$

where consistent with the assumptions and derivation of the model

$T_s = 600^\circ K$

$p_s = 6.784$ atm

$\rho_s = 5.734 \times 10^{-3}$ g/cm^3

$r_s = 6052.45$ km

$p_2 = 5.464 \times 10^{-2}$ atm

$$\rho_2 = 1.179 \times 10^{-4} \text{ g/cm}^3$$

$$g_s = 889.9 \text{ cm/sec}^2$$

$$\frac{q}{q-1} = 5.1443$$

$$M = 41.612 \text{ g/g-mole}$$

$$r_2 = r_s + 42.16 \text{ km}$$

$$R = 8.31433 \times 10^7 \text{ erg/g-mole } ^\circ K$$

DISCUSSION

It is necessary at this point to review exactly what has been done in order to see what assumptions are basic to this atmospheric model. In analogy to the Earth, it is immediately evident that the assumptions of uniform gravitation, constant composition, perfect gases, and hydrostatic equilibrium with no centrifugal force are not the major sources of uncertainty. It is in the statements that followed that great uncertainty was introduced. In essence, Dole's theory was assumed correct at the outset, and was investigated as to compatibility with some experimental observations. It was necessary at the start to assume that CO_2 and N_2 are the only major constituents in the atmosphere and additionally to assume the total amount (not proportion) of N_2 in the atmosphere. Then it was necessary to assume accuracy in some experimental data that are known to contain a high degree of uncertainty. Further, it was necessary to speculate on the nature of the cloud layer surrounding the planet so that the nature of the temperature lapse rate with altitude could be specified. At this point it would appear that the entire problem had been assumed away. However, there are indications that this may not be the case.

Consider first that Dole's approach is accepted and that the question is one of compatibility with some experimental measurements. In dealing with the second approach, it is found first of all that any uncertainty in the amount of N_2 chosen greatly affects the derived composition. Uncertainties of 1 per cent in this amount affect the resulting fraction of N_2 by approximately 1 - 2 per cent. It is also found that uncertainties in the data concerning the amount of CO_2 above the "reflecting surface" greatly affect the derived composition. For instance, if there were only 500 m-atm of CO_2 above this surface instead of the chosen figure of 1000 m-atm, the derived composition would contain approximately 30 per cent N_2 by volume. The results are also highly dependent upon the temperatures chosen and upon the nature of temperature lapse rate below the "reflecting surface." In other words, there are no chosen parameters that tend to suppress uncertainty effects or that cause less uncertainty in the results for N_2 composition than is contained in the chosen parameter. It is then apparent that the close agreement of the two approaches must either be a remarkable coincidence or have some basis in fact. However, this model is inconsistent with the measurements of Ref. 7, and consequently with the results of Ref. 8.

It must also be noted that the amount of CO_2 reported by Dole is approximately one-half that which would result if the figures for the amount of Earth CO_2 from Ref. 14 were used. Attention must also be called to Ref. 15 in which a method similar to the second approach here is used to derive a composition of approximately 75 per cent CO_2 and 25 per cent N_2.

All that is claimed here is that under the assumptions a tentative atmosphere of Venus has been derived. Now if the assumptions involved ultimately prove reasonable and the experimental data, and consequently the

conclusions derived therefrom, are reasonably correct, then the close agreement of the two approaches indicates that the chosen composition may be representative of the Venus atmosphere. Further, the pressure-temperature distribution below the cloud layer may be reasonably correct. The difficulties in accepting an isothermal atmosphere above the cloud layer have been discussed previously. Above 100 km, photodissociation and ionization will surely become appreciable, and in going to these higher altitudes the assumption of a uniform gravitational field becomes poorer. The cutoff at 100 km was chosen because the density at this point roughly corresponds to that density in the Earth's atmosphere (at approximately 300,000 ft) at which incipient aerodynamic effects associated with re-entry nose cones are no longer negligible.

One immediate objection to the acceptance of this model concerns the arbitrary choice of the temperature lapse rate below the cloud layer. In reality, the real justification for choosing a lapse rate slightly less than an adiabatic lapse rate is that this choice reduces the discrepancy in atmospheric composition between the two approaches. However, it may be partially justified by other arguments. For instance, if the clouds are composed of water and ice crystals, the lapse rate in the cloud layer must be less than the dry adiabatic lapse rate because of the release of the heats of vaporization and fusion as altitude increases. The chosen lapse rate may then be considered an average between the surface and the top of the cloud layer. Yet another possibility may be considered. If the surface temperature is slightly greater than $600^{\circ}K$, as may well be possible considering the uncertainty in the data, Eq. (4a) requires that the surface pressure be higher than that originally derived. Assuming that the amount of N_2 is fixed, Eq. (2)

requires that there be more CO_2. The chosen lapse rate may then be considered as a correction device to fix the surface temperature at $600^\circ K$, but still be consistent with the amount of CO_2 in the atmosphere. Of course this argument works in reverse if the surface temperature is less than $600^\circ K$. It does not seem profitable to investigate all of these minor effects in view of the uncertainties already introduced. This lapse rate was chosen simply because it serves to reduce the discrepancy between the two approaches and appears to be as good as any other assumption at this time.

It is interesting to note that if the clouds surrounding Venus are assumed to consist of ice crystals,(5,6) according to the present model the vapor pressure above ice at $T_2 = 235^\circ K$ indicates that water vapor comprises 0.29 per cent by volume of the Venus atmosphere above the cloud layer (assuming a constant mixing ratio above this point). This is larger by a factor of approximately 40 than that which would exist in this model according to the recent measurements of the Moore-Ross balloon flight.(16) It must be cautioned, however, that these measurements contained a high degree of uncertainty.

In view of the above-mentioned difficulties, this model is proposed only as a first approximation with which aerodynamic entry problems concerning Venus may be studied. It may be used as a mean to which perturbations may be applied; this mean may be bracketed by other existing theories until more experimental data are accumulated. The significant figures presented for this model are obviously not indicative of the precision of the knowledge of the Venus atmosphere, but are consistent with the proposed model if the experimental data and assumptions involved are taken as "exact."

III. THE THERMODYNAMIC PROPERTIES OF 15 PER CENT N_2 AND 85 PER CENT CO_2 BY VOLUME

CONDITIONS AND ASSUMPTIONS

The thermodynamic properties of a mixture of 85 per cent CO_2 and 15 per cent N_2 by volume will be presented on the premise that they may be useful regardless of specific application to this tentative Venus atmosphere. In this light, the calculations of this section will be carried out for exactly the stated composition and will contain far less computational uncertainty than does Section II concerning the constituency of the atmosphere of Venus.

The gas mixture constituents are assumed to obey the perfect gas law, $pM/R\rho T = 1$. Investigation of the critical constants of the constituents shows that this is a good assumption over the selected temperature range of from $1000^{\circ}K$ to $24{,}000^{\circ}K$. CO_2 deviates most from the perfect gas law (the effects of compressibility for this constituent have been discussed by Raymond).[17] Since N_2 is better-behaved in this respect than CO_2, the compressibility at $1000^{\circ}K$ and 10^2 atm for this mixture is slightly depressed from the value of 1.026 quoted by Raymond for pure CO_2. However, this assumption becomes poorer at temperatures below $1000^{\circ}K$ and at the higher pressures. The justification for neglecting the effects of intermolecular forces at these lower temperatures is that the thermodynamic states of interest with respect to the atmosphere of Venus do not occur where large effects of intermolecular forces are apparent. When the pressure is nearest the critical pressure (for CO_2) the temperature is high; where the temperature approaches and falls below the critical temperature, the pressure is low. Again, the presence of N_2 will generally tend to influence the mixture to behave more like a perfect gas than will pure CO_2.

The mixture will be assumed to be in thermodynamic equilibrium. From the standpoint of the use of these properties, this assumes that for any particular state to which these properties are to be applied, e.g., aft of a shock wave, the time required for relaxation phenomena to take place is much shorter than that in which the gas changes appreciably in state. The equilibrium composition of the gas mixture is then computed by the method of Ref. 18 under the criteria that the Gibbs Free Energy is a minimum for a selected particular temperature and pressure.

Below $1000^{\circ}K$ the mixture is assumed to consist solely of molecular CO_2 and N_2. This assumption is justified by noting the calculated equilibrium composition at $T = 1000^{\circ}K$ and $p = 10^{-4}$ atm. Using perfect gas relations, the thermodynamic properties of the mixture can be calculated from the basic data in Ref. 10. However, a slight correction must be applied to these data in order that they may become consistent with the data above $1000^{\circ}K$; the method of correction will be described later.

METHOD OF CALCULATION

$T \geq 1000^{\circ}K$

Under the criteria of significantly contributing to the thermodynamic properties of the mixture it was first assumed that the mixture could consist of the following possible species: CO_2, N_2, O_2, NO_2, CO, NO, O_3, C, N, O, C^+, N^+, O^+, O_2^-, O^-, CO^+, NO^+, N_2^+, O_2^+, C^{++}, N^{++}, O^{++}, and e^-. Using the basic referenced data in Tables 3 - 6, and the method of Ref. 18, the equilibrium composition was calculated over the temperature range $1000^{\circ}K \leq T \leq 24,000^{\circ}K$. Constituents present in amounts smaller than 10^{-4} g-mole per original "cold" g-mole of mixture were then considered negligible and not listed.

Thus, thermodynamic properties are presented for the following significant constituents in the temperature ranges specified below:

$1000^\circ K \leq T \leq 4000^\circ K$

CO_2, N_2, O_2, CO, NO, C, N, and O

$4000^\circ K < T \leq 24,000^\circ K$

CO_2, N_2, O_2, CO, NO, C, N, O, C^+, N^+, O^+,

O^-, CO^+, NO^+, O_2^+, C^{++}, N^{++}, O^{++}, and e^-

The equilibrium composition is presented on the basis of one g-mole of the "cold" mixture in Figs. 2 and 3 and Tables 7 and 8 over a temperature range of $1000^\circ K$ to $24,000^\circ K$ and a pressure range of 10^2 atm to 10^{-4} atm.

Since the thermodynamic data are presented on the basis of one g-mole of the "cold" gas mixture, i.e., 41.612 g, the following relation applies

$$M = M_o \frac{n_o}{\sum_i n_i} = \frac{M_o}{n} \qquad (11)$$

since $n_o = 1$ and $\sum_i n_i = n$. Thus, n_i/n represents the mole fraction of species i. The datum density, ρ_o, is chosen to correspond to $p_o = 1$ atm (on the surface of the earth) and $T_o = 273.16^\circ K$ for the original "cold" mixture. Thus

$$\rho_o = \frac{p_o M_o}{RT_o} = 1.85647 \times 10^{-3} \text{ gm/cm}^3$$

Then

$$\frac{\rho}{\rho_o} = \frac{(p/p_o)(M/M_o)}{T/T_o} \qquad (12)$$

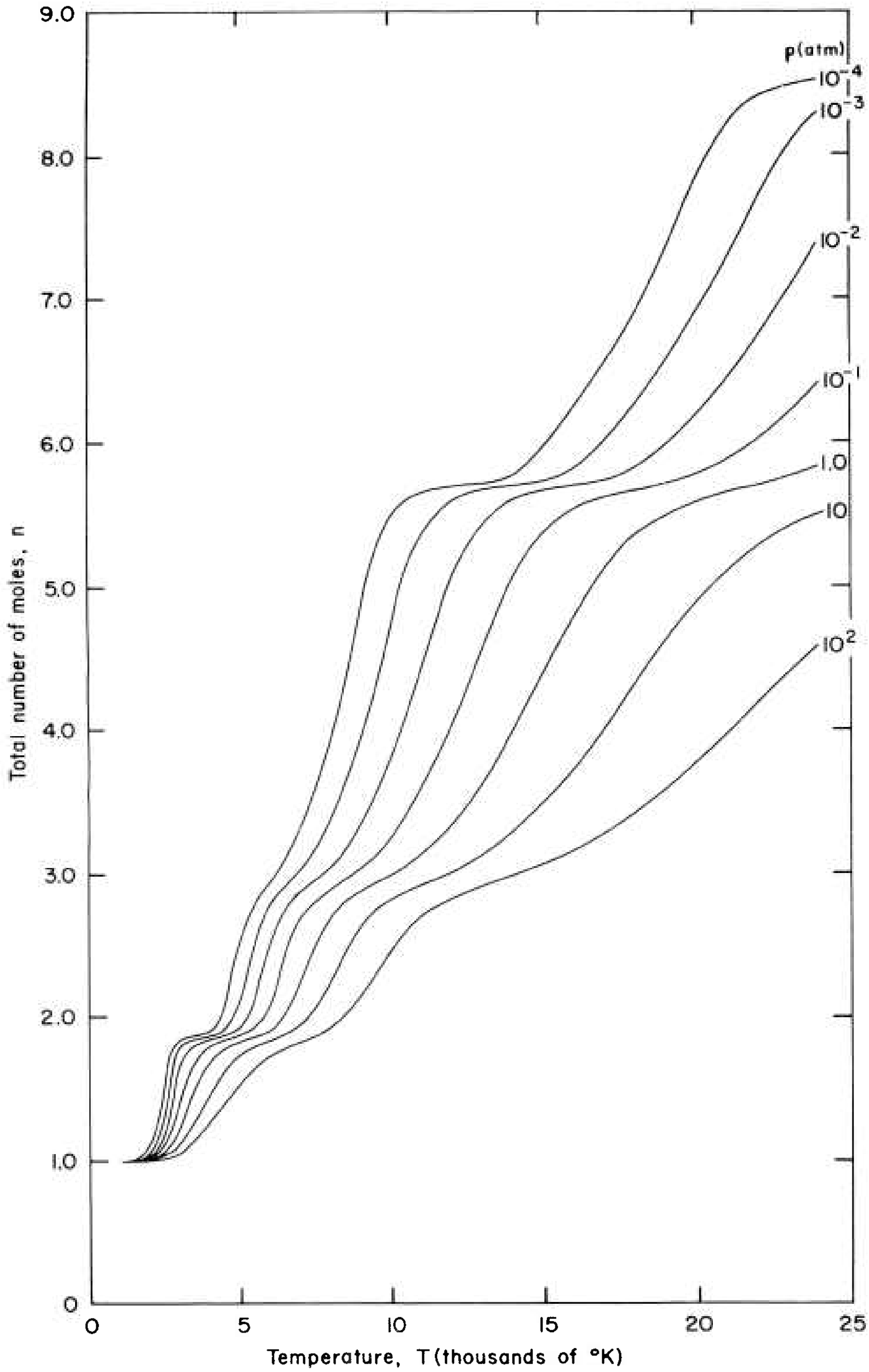

Fig. 2 — Total number of moles as a function of temperature

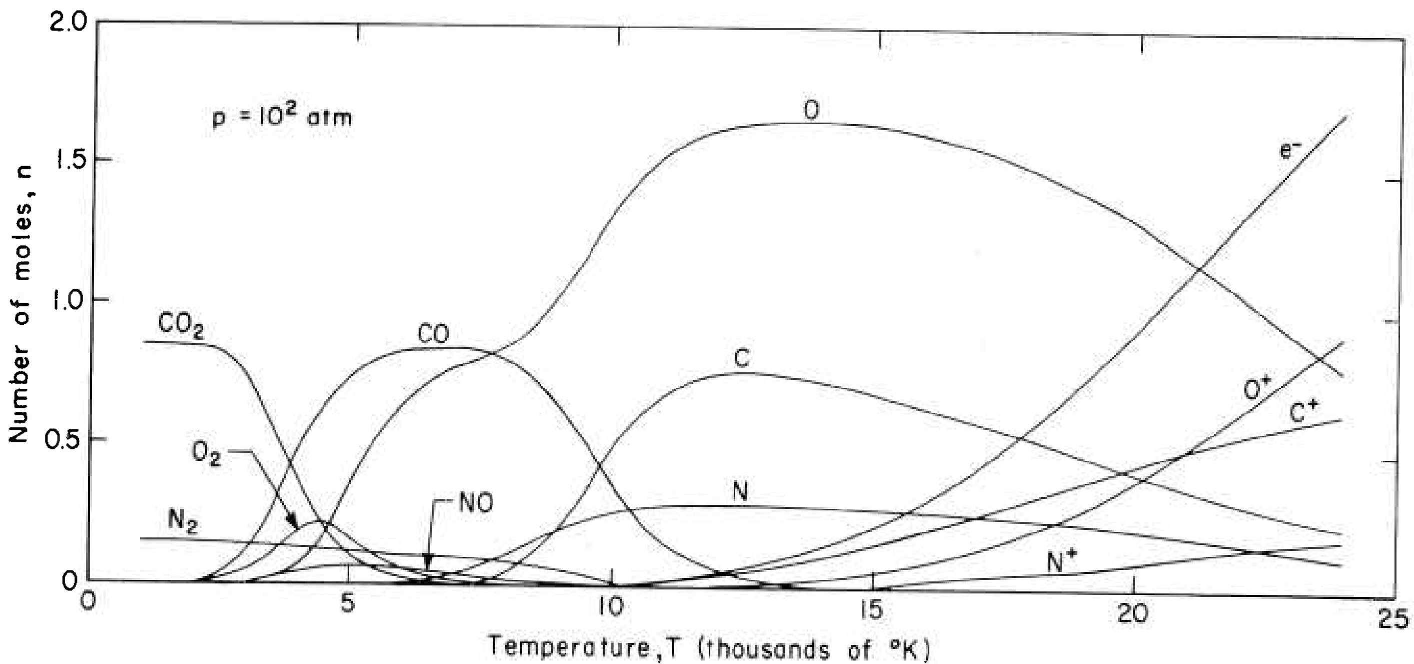

Fig. 3a — Molar composition

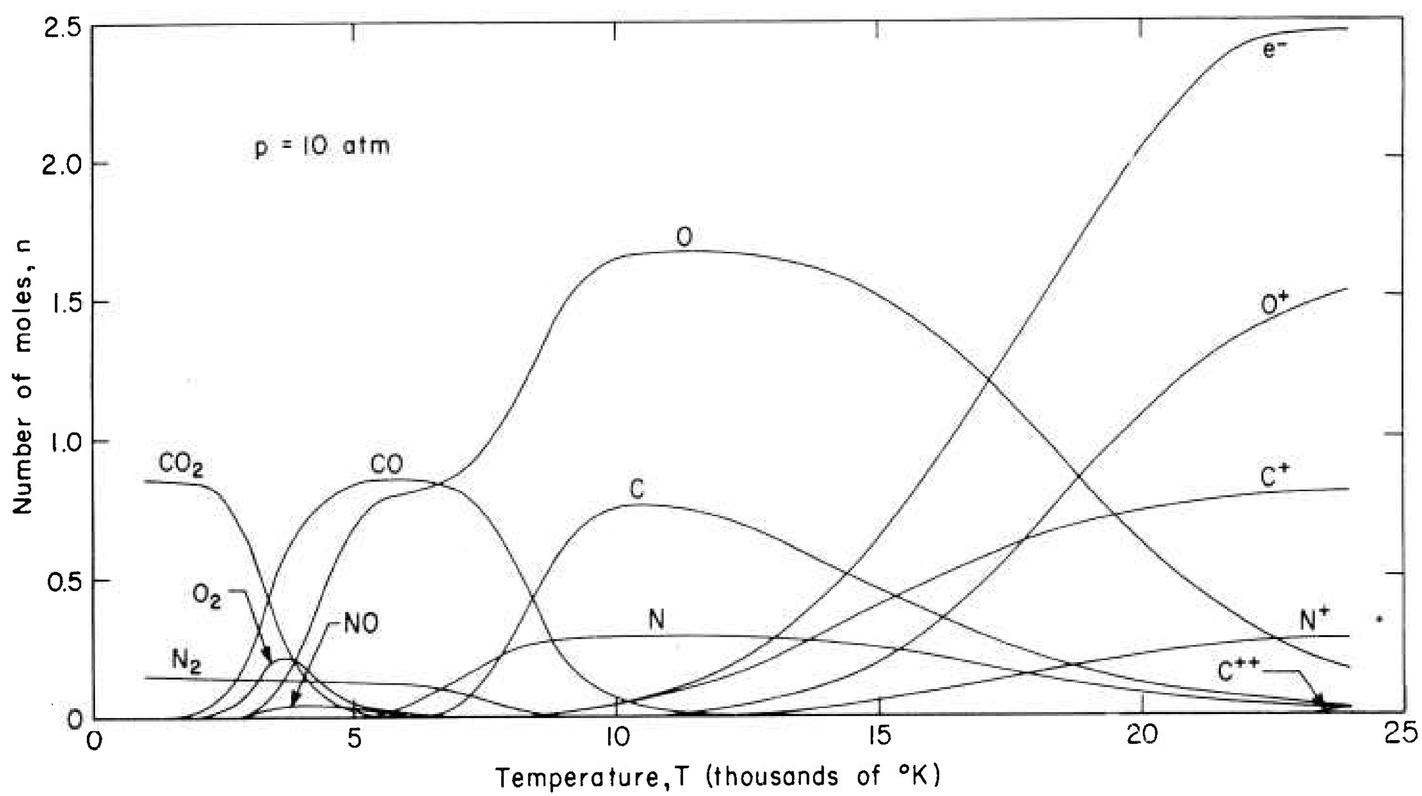

Fig. 3b — Molar composition

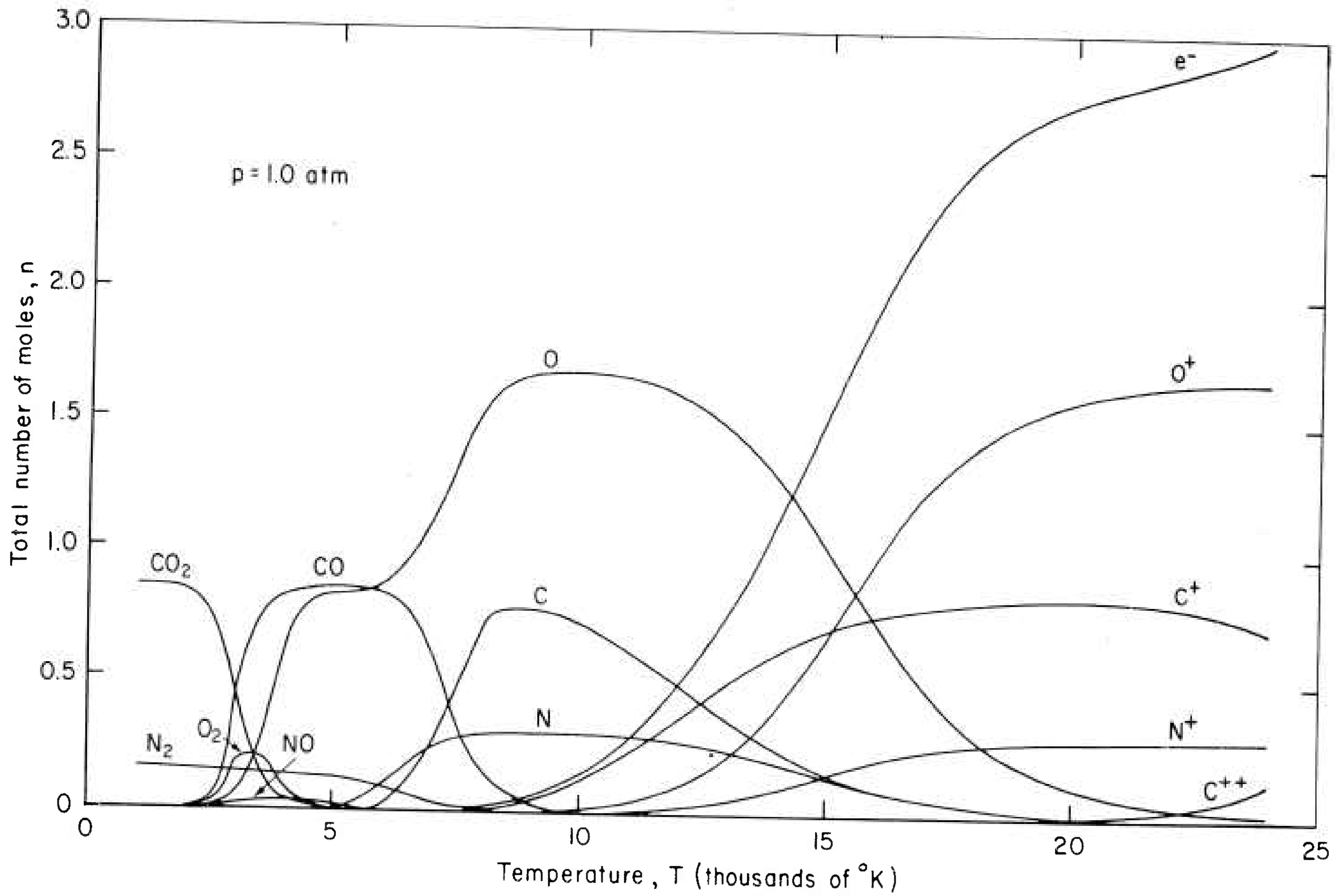

Fig. 3c—Molar composition

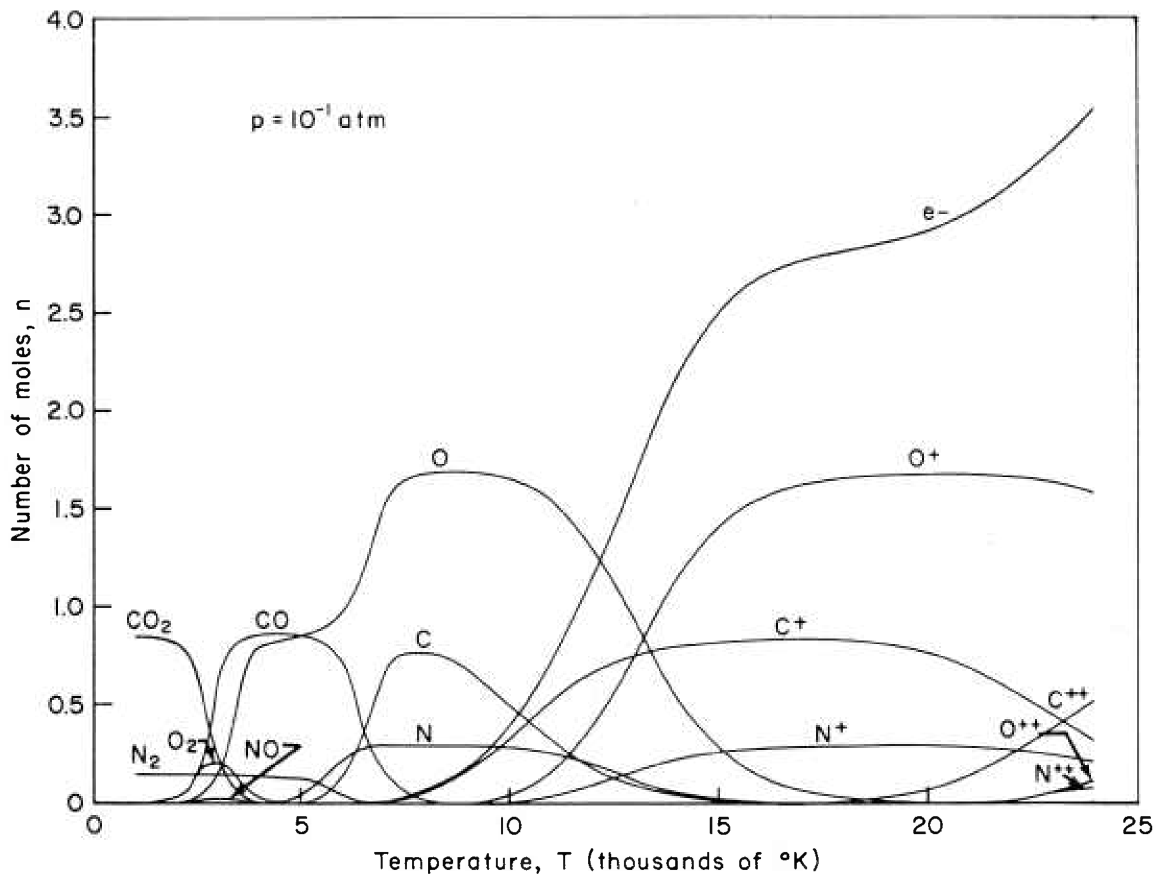

Fig. 3d — Molar composition

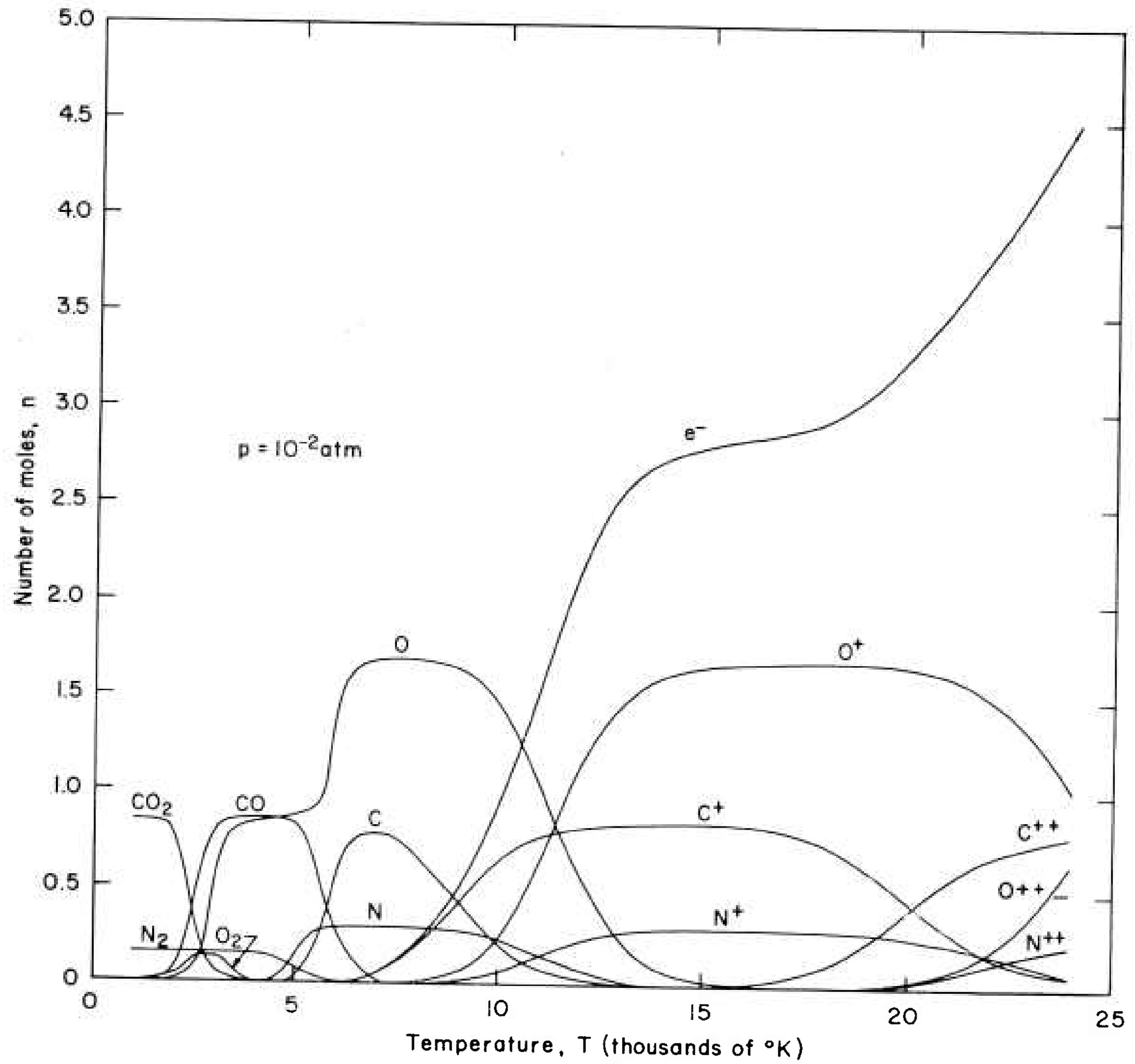

Fig. 3e — Molar composition

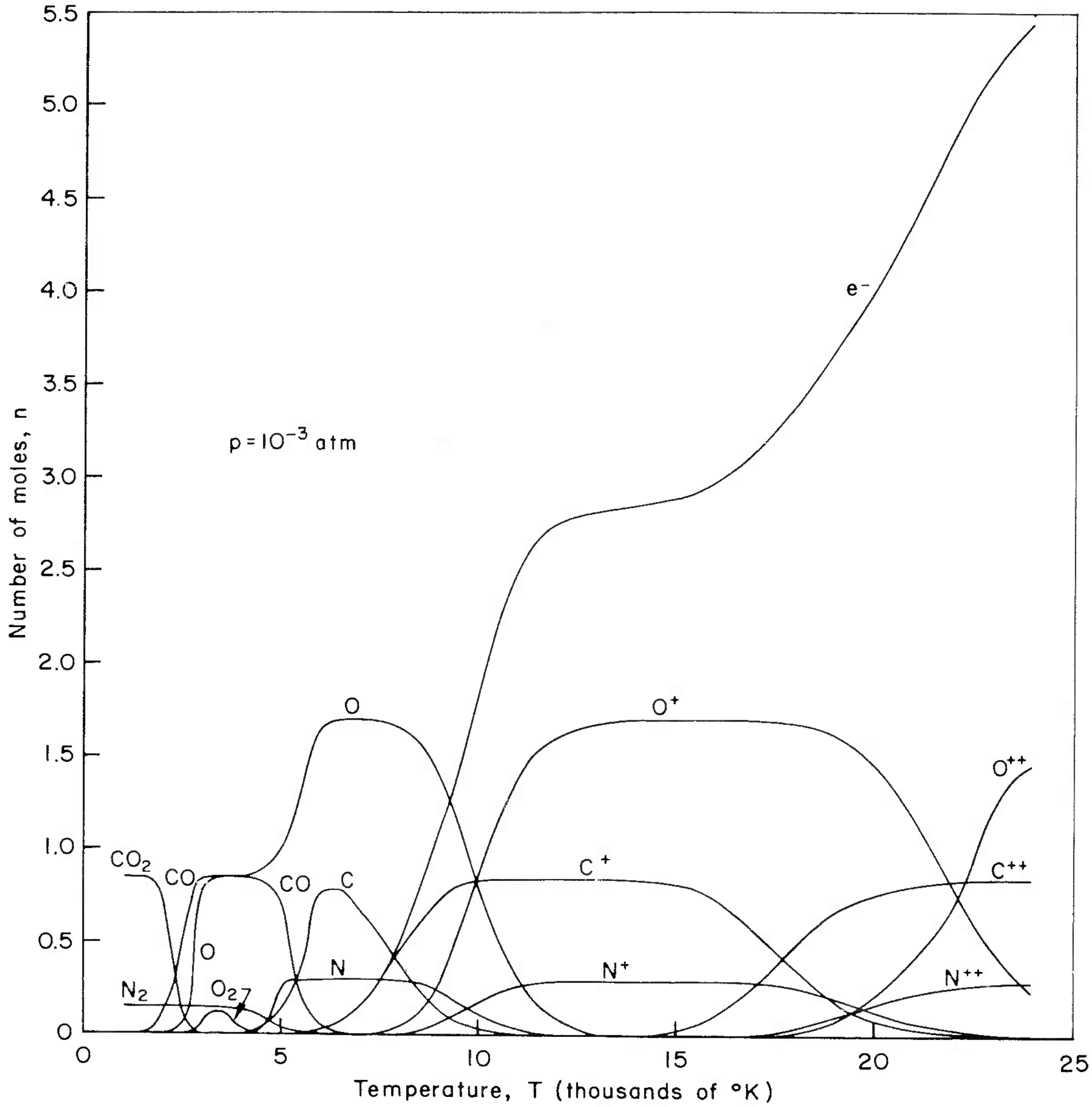

Fig.3f — Molar composition

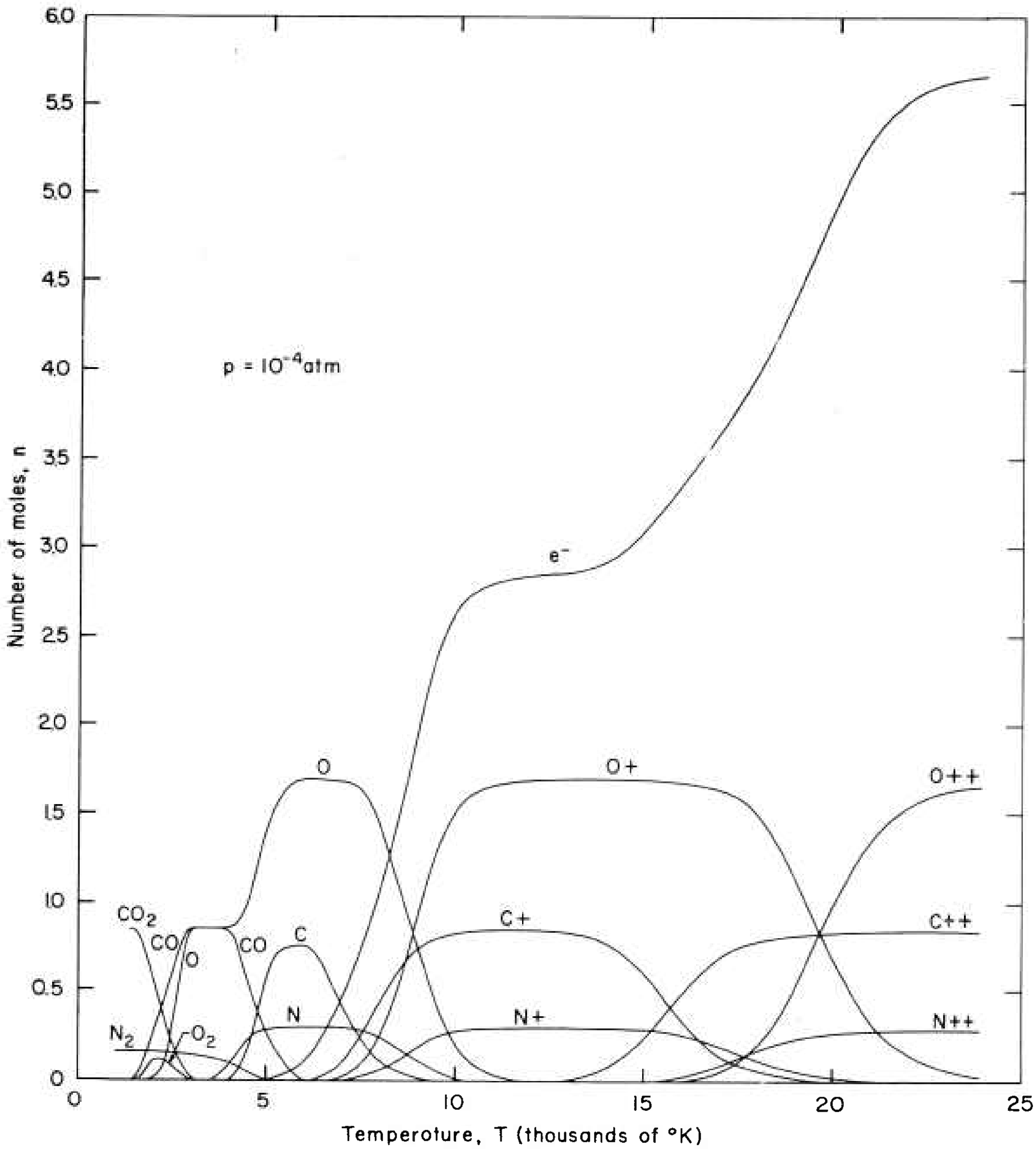

Fig. 3g — Molar composition

The molecular weights and densities are shown in Tables 9 and 10 and Figs. 4 and 5.

The datum state chosen for the internal energy equal to 0 is where carbon (graphite), gaseous molecular oxygen, and gaseous molecular nitrogen exist at a temperature of $0^{\circ}K$ and zero pressure. Then the internal energy per "cold" g-mole of the mixture may be calculated as follows:

$$E = \sum_i n_i E_i \tag{13}$$

where

$$E_i = (E^{\circ} - E_o^{\circ})_i + E_{o_i}^{\circ} \tag{14}$$

and $E_{o_i}^{\circ}$ is the heat of formation of species i from the ground state mentioned above. In dimensionless form, the computing equation becomes

$$\frac{E}{RT_o} = \frac{T}{T_o} \sum_i n_i \left[\left(\frac{E^{\circ} - E_o^{\circ}}{RT}\right)_i + \left(\frac{E_o^{\circ}}{RT}\right)_i \right] \tag{15}$$

The basic data are taken from the previously mentioned tables.

Since the enthalpy is given by

$$H_i = E_i + p_i V = E_i + n_i RT \tag{16}$$

the computing equation is

$$\frac{H}{RT_o} = \frac{T}{T_o} \sum_i n_i \left[\left(\frac{E - E_o^{\circ}}{RT}\right)_i + \left(\frac{E_o^{\circ}}{RT}\right)_i + 1 \right] \tag{17}$$

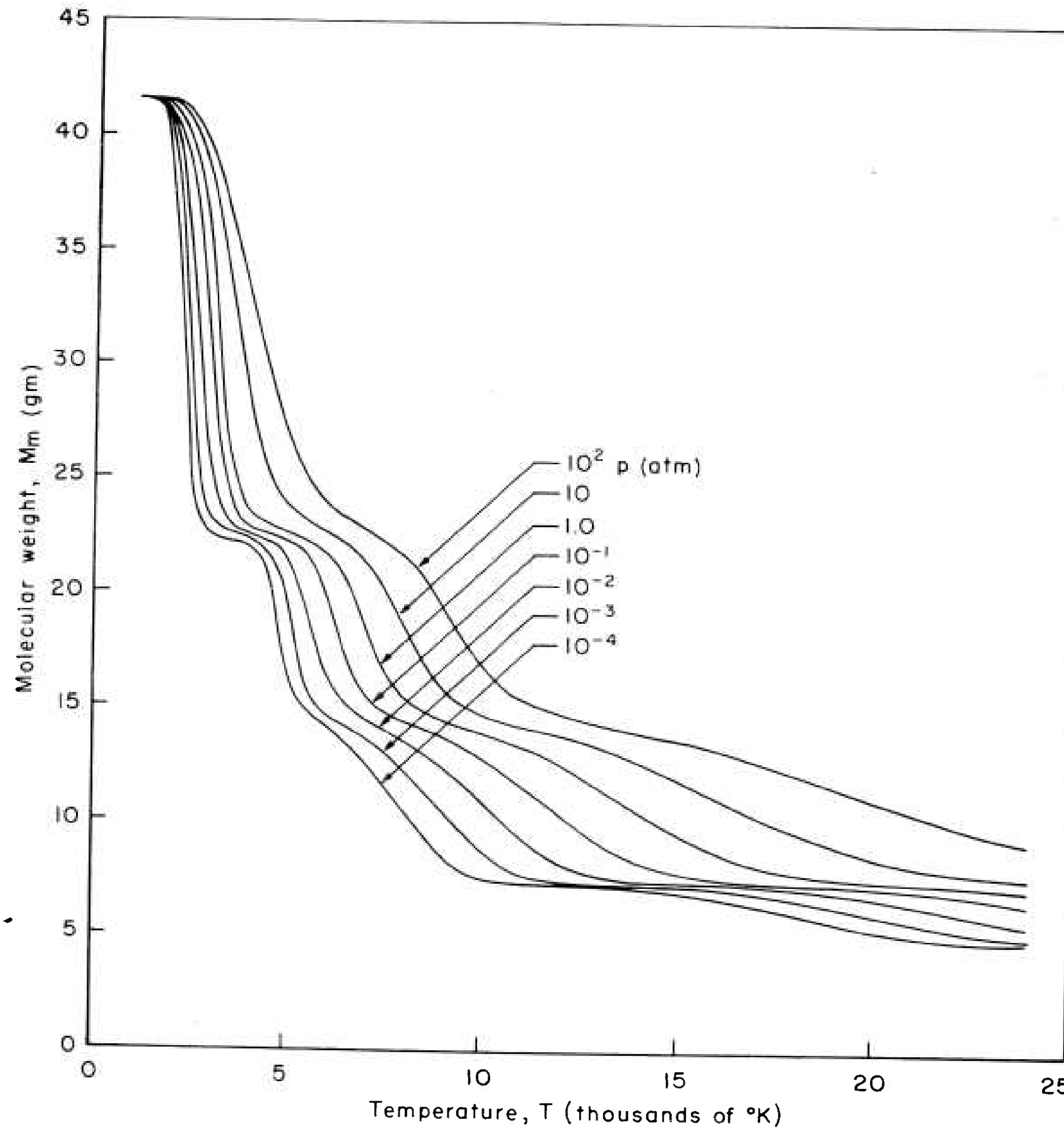

Fig. 4 — Molecular weight versus temperature

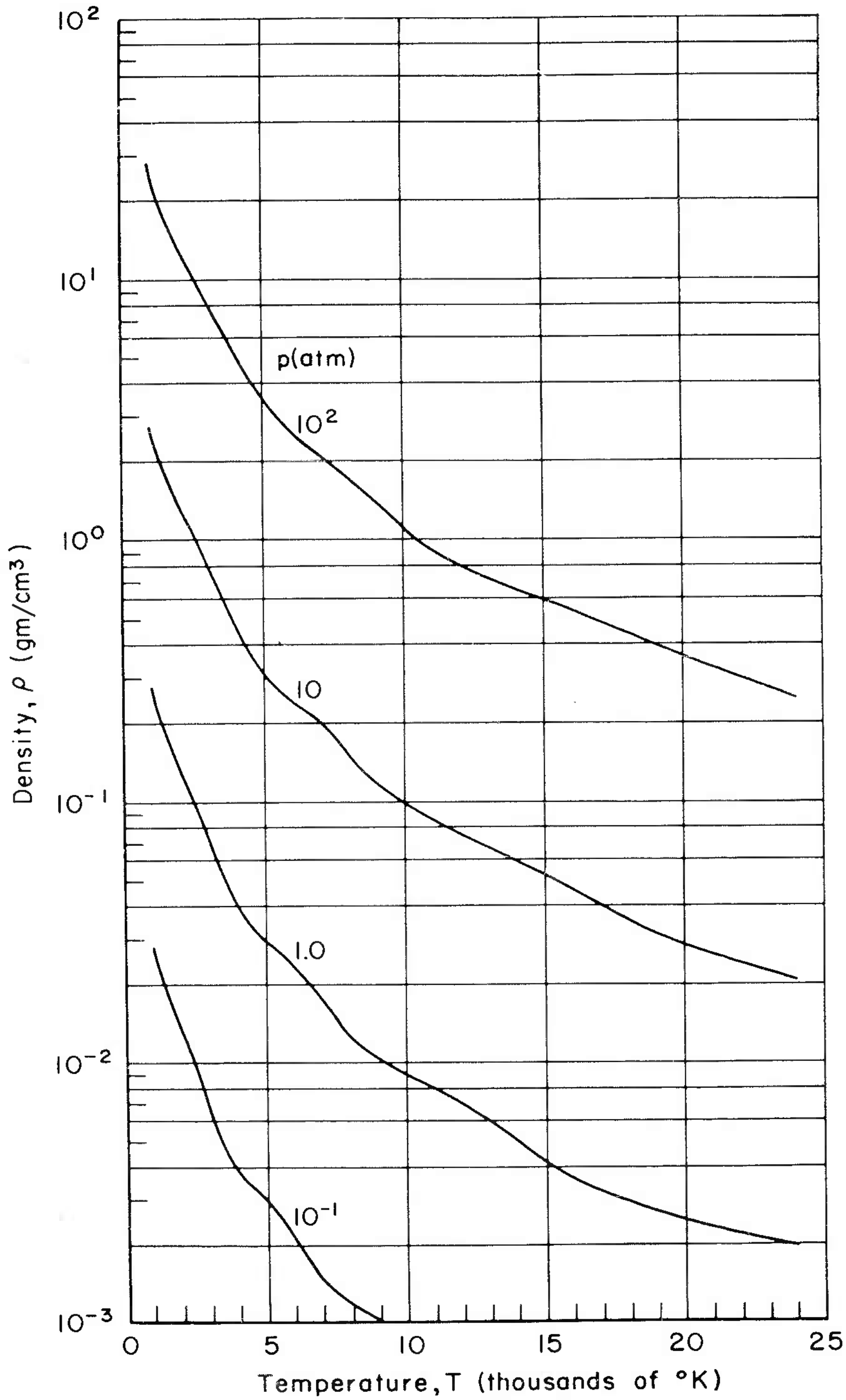

Fig. 5a — Density versus temperature

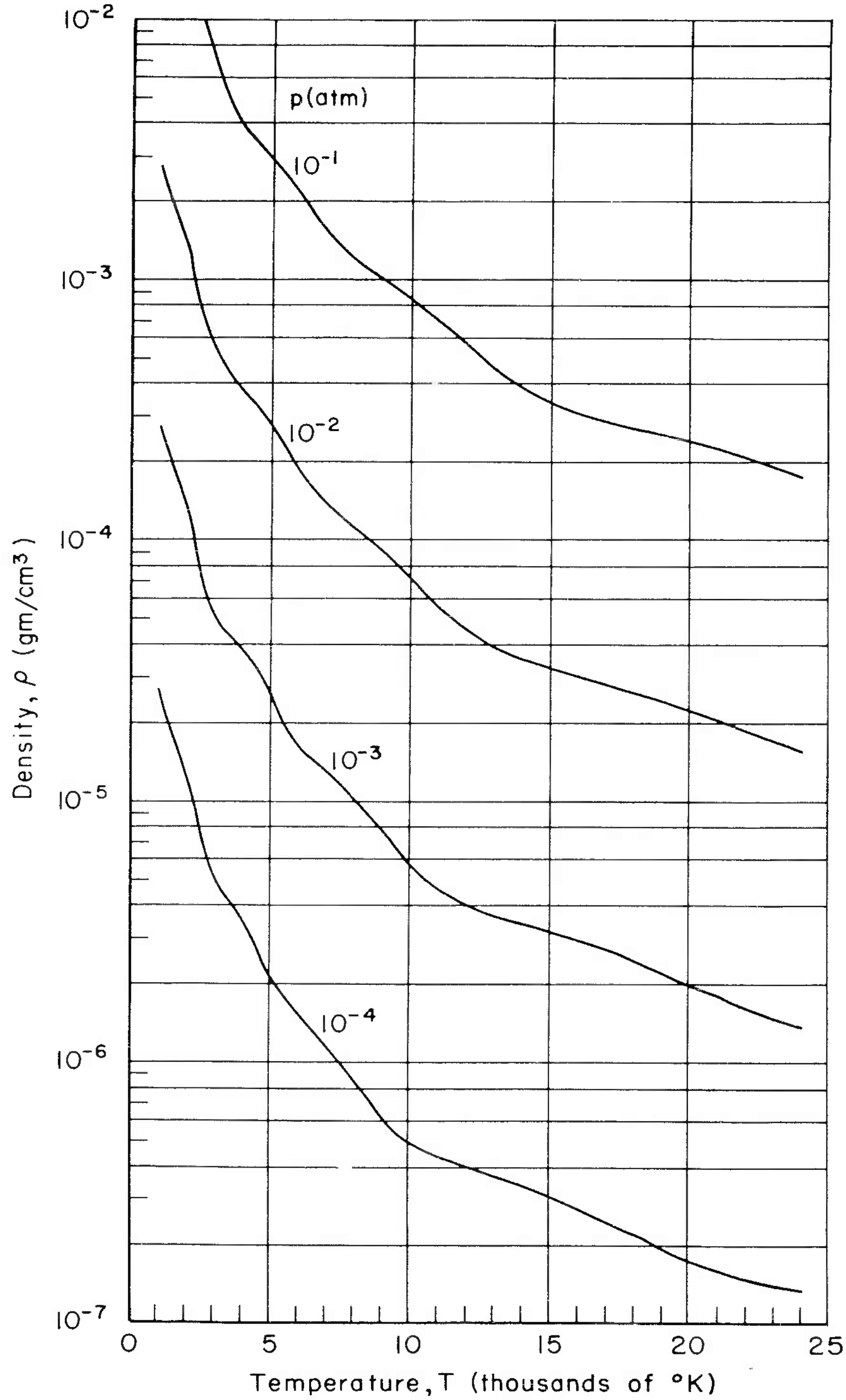

Fig. 5b — Density versus temperature

The Gibbs Free Energy is given by

$$F_i = H_i - TS_i \tag{18}$$

Also

$$F_i = F_i^o + RT \ln p_i \tag{19}$$

Then

$$\frac{S_i}{R} = \frac{E_i - F_i^o}{RT} - \ln p_i + 1 \tag{20}$$

or

$$\frac{S_i}{R} = \left(\frac{E^o - E_o^o}{RT}\right)_i - \left(\frac{F^o - E_o^o}{RT}\right)_i - \ln p_i + 1 \tag{21}$$

Since

$$p_i = \frac{n_i}{n} p \tag{22}$$

and

$$\frac{S}{R} = \sum_i n_i \left(\frac{S}{R}\right)_i \tag{23}$$

the computing equation is

$$\frac{S}{R} = \sum_i n_i \left[\left(\frac{E^o - E_o^o}{RT}\right)_i - \left(\frac{F^o - E_o^o}{RT}\right)_i - \ln \left(\frac{n_i}{n} p\right) + 1 \right] \tag{24}$$

Again, the basic energy data are taken from the previously mentioned tables.

The values for internal energy, enthalpy, and entropy are shown in Tables 11 - 13 and Figs. 6 - 8, respectively. High-temperature Mollier charts are presented in Figs. 9 and 10.

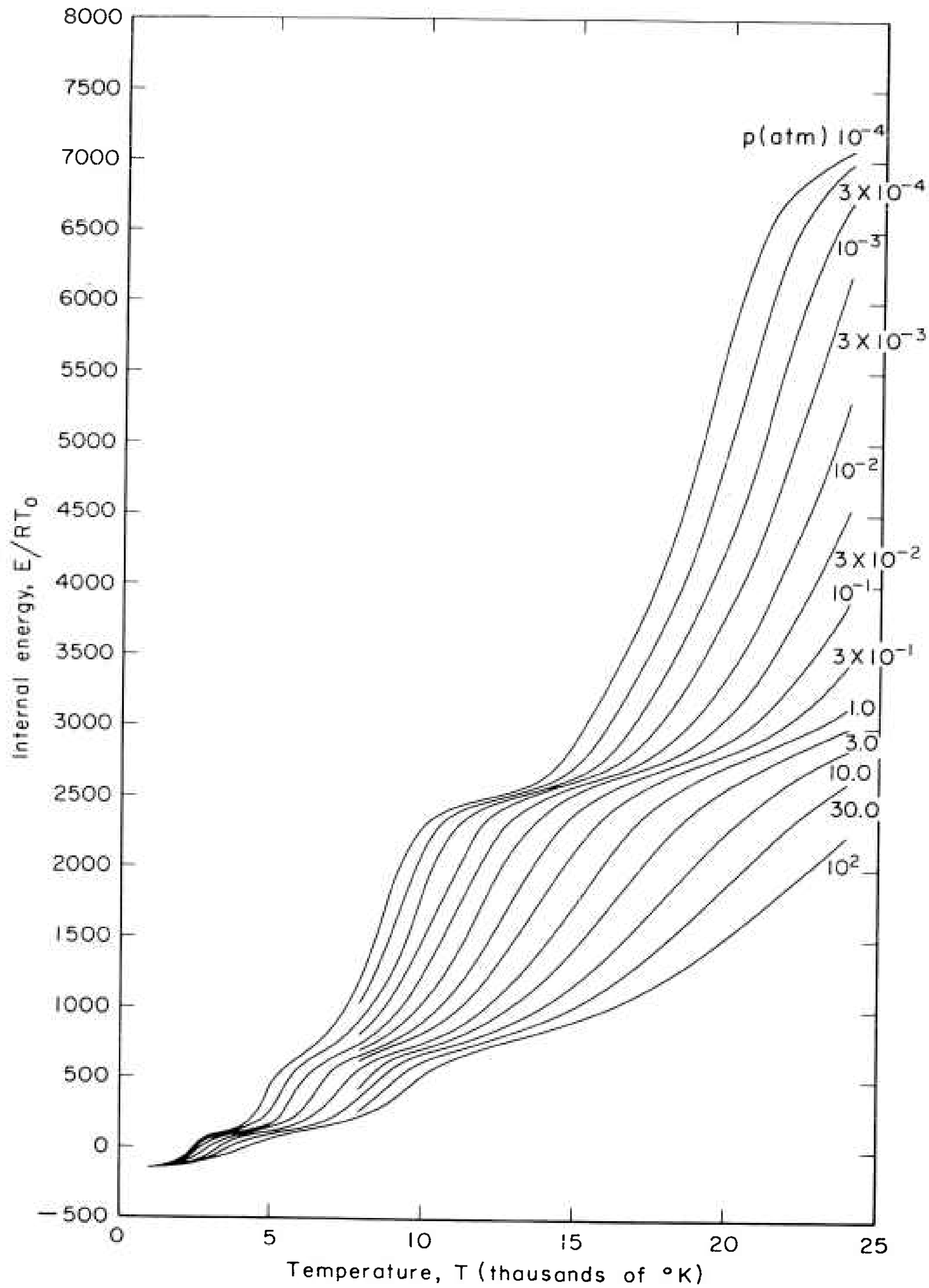

Fig. 6 — Internal energy, E/RT_0, versus temperature

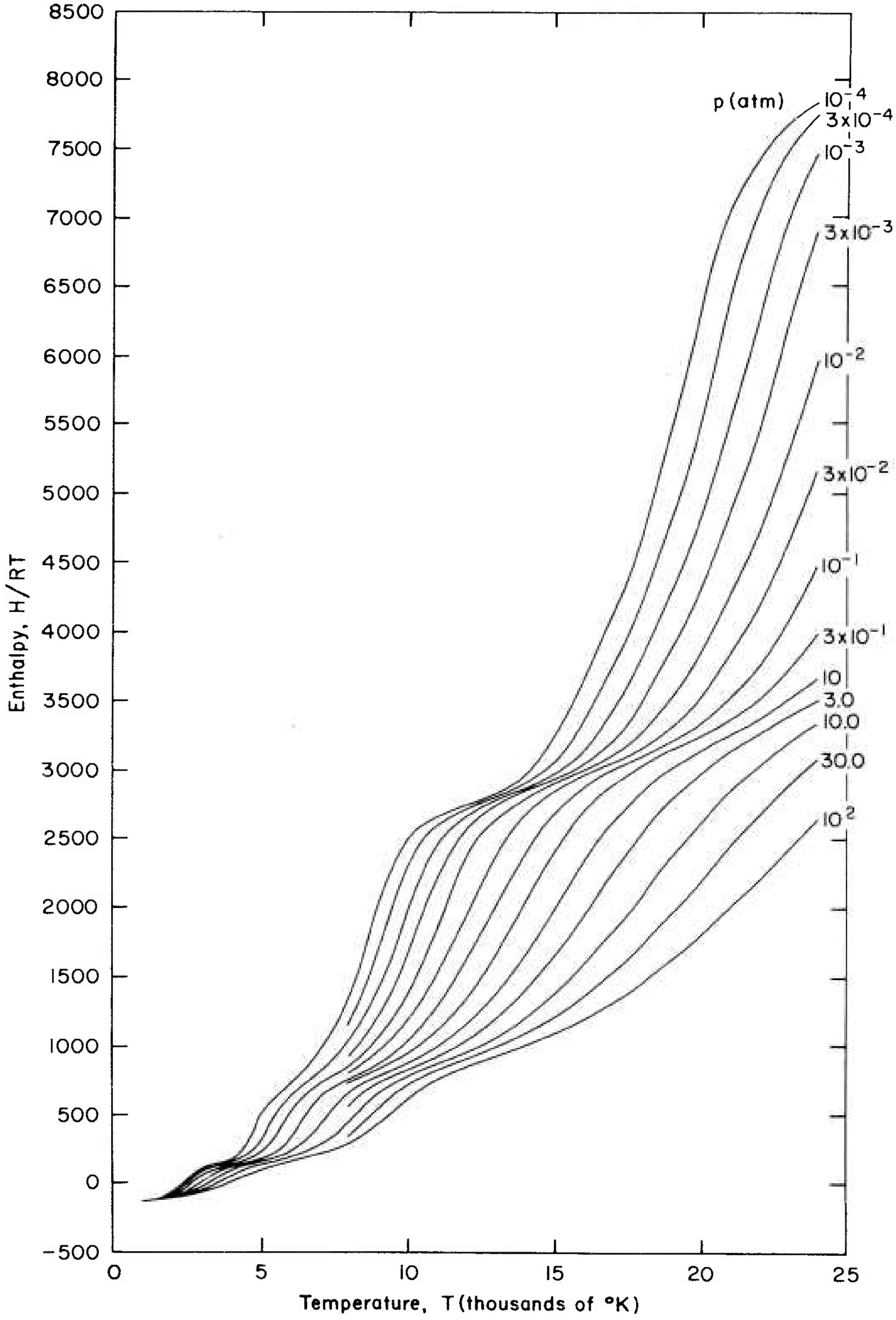

Fig. 7 — Enthalpy, H/RT_0, versus temperature

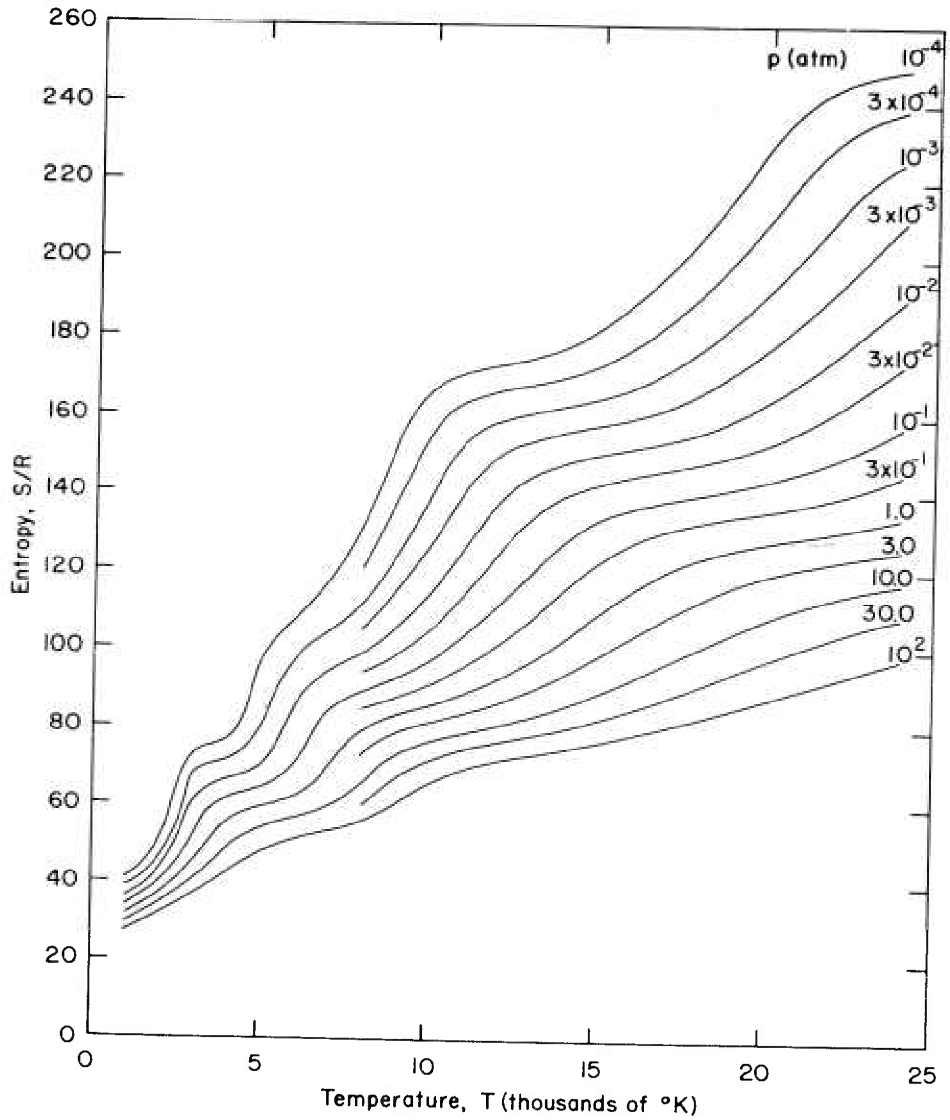

Fig. 8 — Entropy, S/R, versus temperature

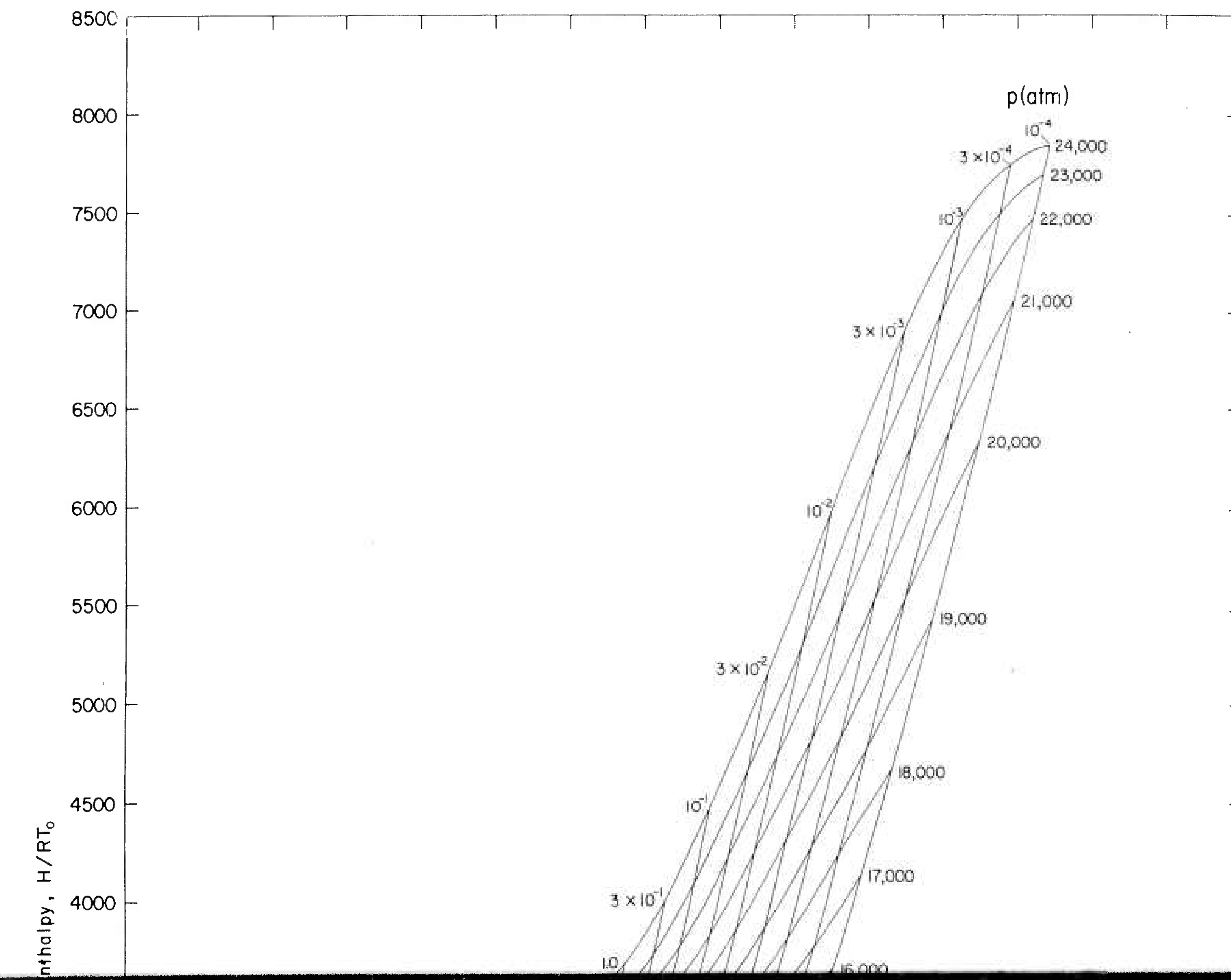

nthalpy, H/RT$_0$
8500
8000
7500
7000
6500
6000
5500
5000
4500
4000
p(atm)
10^{-4}
3×10^{-4}
10^{-3}
3×10^{-3}
10^{-2}
3×10^{-2}
10^{-1}
3×10^{-1}
1.0
24,000
23,000
22,000
21,000
20,000
19,000
18,000
17,000

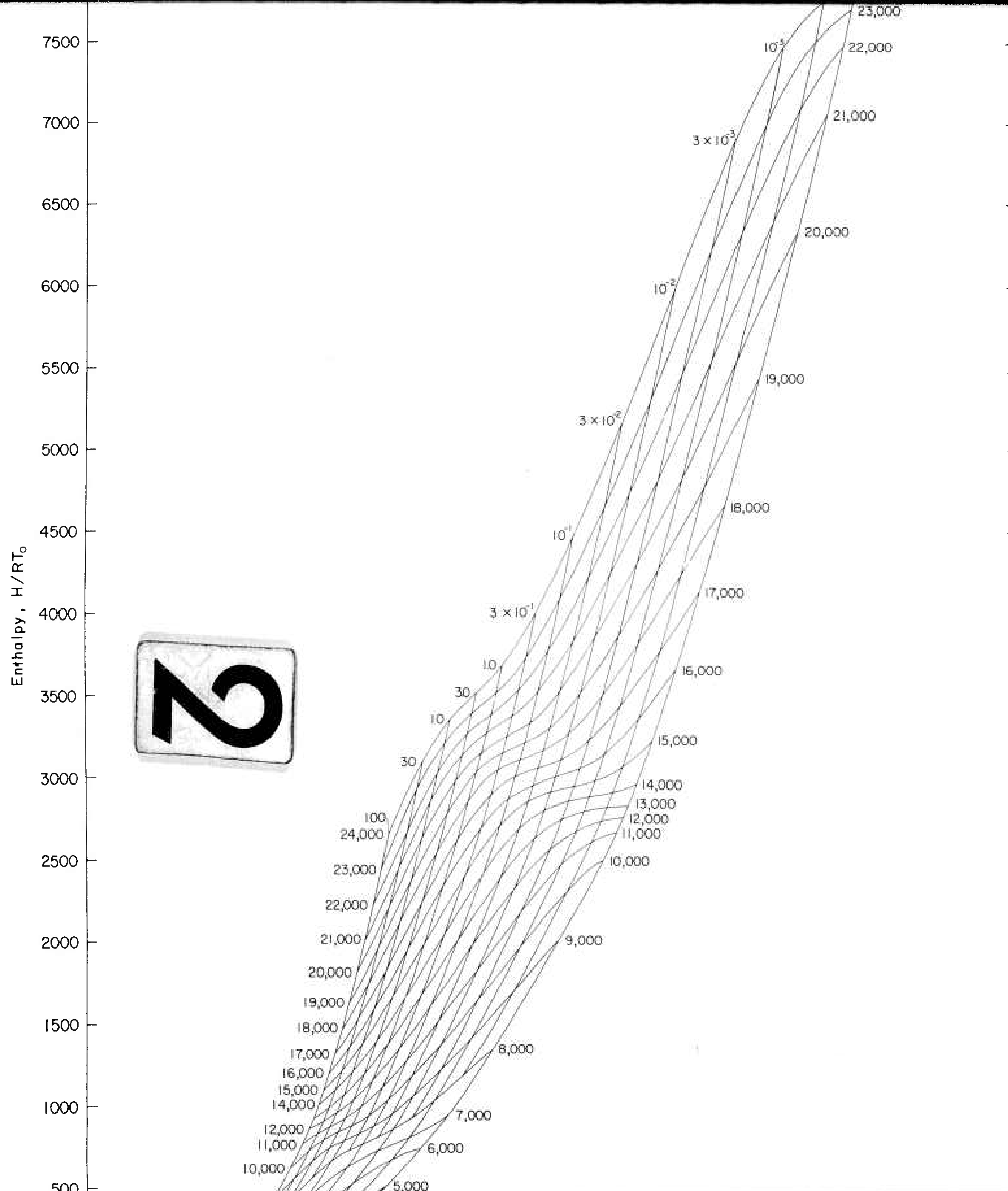
Enthalpy, H/RT_0
7500
7000
6500
6000
5500
5000
4500
4000
3500
3000
2500
2000
1500
1000
500
23,000
22,000
21,000
20,000
19,000
18,000
17,000
16,000
15,000
14,000
13,000
12,000
11,000
10,000
9,000
8,000
7,000
6,000
5,000
10^{-3}
3×10^{-3}
10^{-2}
3×10^{-2}
10^{-1}
3×10^{-1}
1.0
3.0
10
30
100
24,000
23,000
22,000
21,000
20,000
19,000
18,000
17,000
16,000
15,000
14,000
12,000
11,000
10,000
2

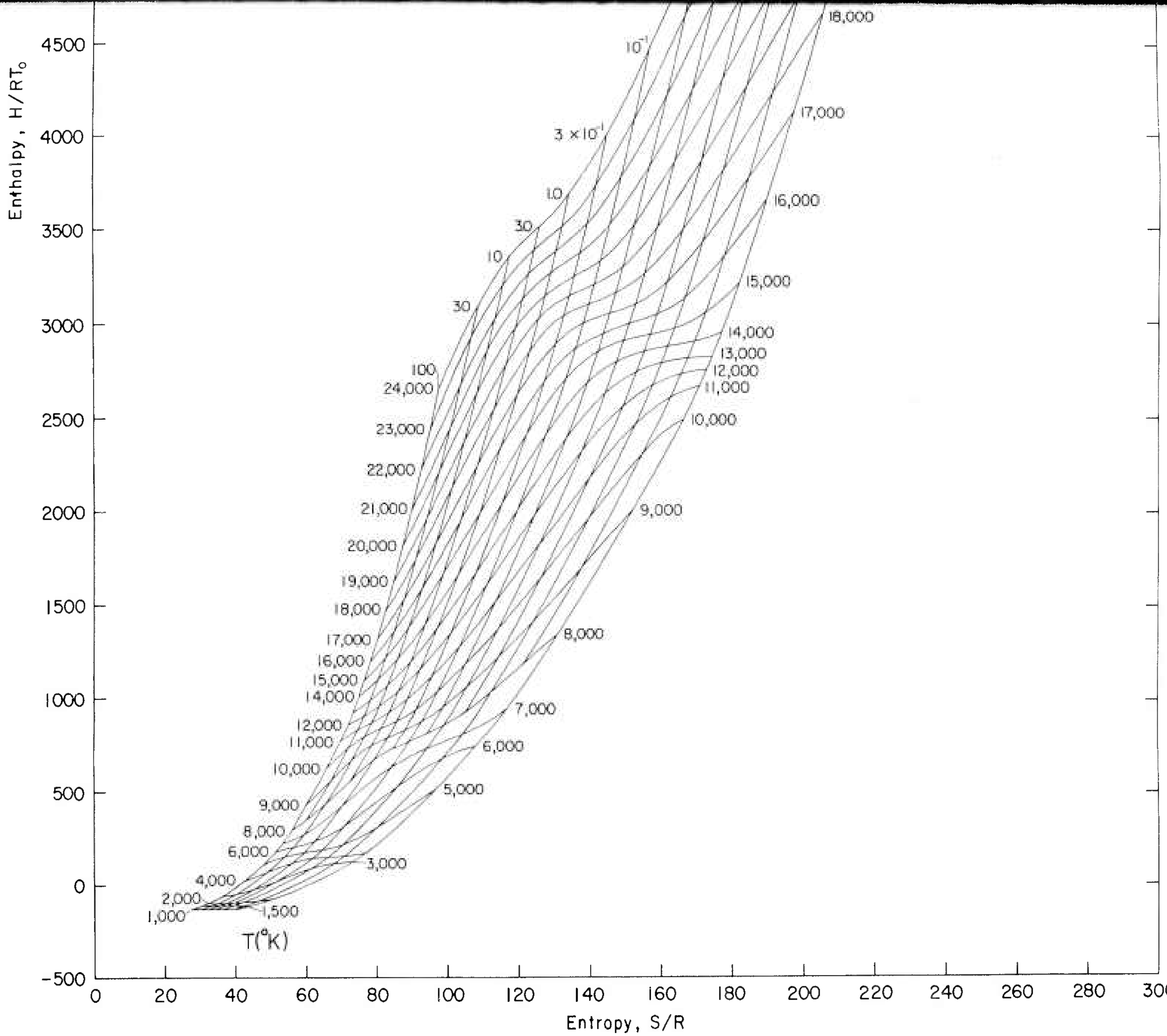

Fig. 9 — Mollier chart to 24,000 °K for a volumetric mixture of 85% CO_2 and 15% N_2

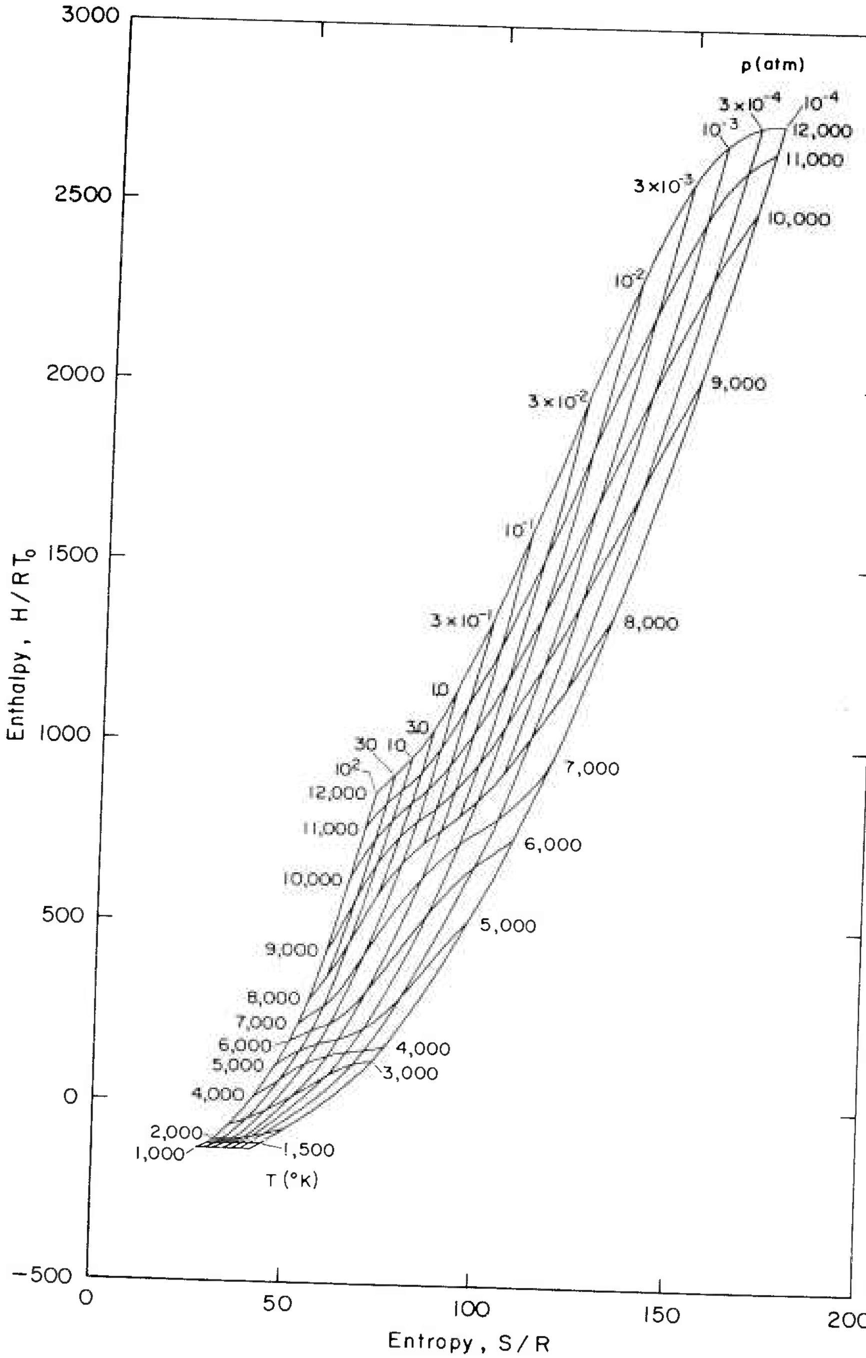

Fig. 10 — Mollier chart to 12,000 °K for a volumetric mixture of 85% CO_2 and 15% N_2

To convert the thermodynamic properties to the mass basis, it is merely necessary to divide the properties by the "cold" molecular weight. Thus

$$\frac{e}{RT_o} = \frac{1}{M_o} \frac{E}{RT_o} \tag{25}$$

$$\frac{h}{RT_o} = \frac{1}{M_o} \frac{H}{RT_o} \tag{26}$$

and

$$\frac{s}{RT_o} = \frac{1}{M_o} \frac{S}{R} \tag{27}$$

$\underline{T \leq 1000^{o}K}$

The thermodynamic properties in this range were computed from Tables 12 and 17 of Ref. 10 for a mixture of 0.85 g-mole of CO_2 and 0.15 g-mole of N_2. In this reference the zero for internal energy and enthalpy is taken at $0^{o}K$. It was necessary, therefore, to add the heat of formation of CO_2 to the enthalpy of CO_2 tabulated in Ref. 10. In order for these data also to match the computed properties at $1000^{o}K$ but still retain the zero at $0^{o}K$, it is necessary to multiply the enthalpy data in Ref. 10 by a factor only very slightly different from unity. In effect, this means that the specific heat at constant pressure is multiplied by this factor. The computing equation then becomes

$$\frac{H}{RT_o} = \frac{1}{RT_o} \left[0.85 \left(\frac{K_{CO_2} \bar{h}_{CO_2}}{1.8} - 173.1048 \right) + 0.15 \left(\frac{K_{N_2} \bar{h}_{N_2}}{1.8} \right) \right] \tag{28}$$

where the K's are the multiplying factors to match the data at $1000^{o}K$ and

$$K_{CO_2} = 1.000324$$

$$K_{N_2} = 1.0004675$$

Now the entropy function $\overline{\Phi}$, tabulated in Ref. 10, represents the following:

$$\overline{\Phi} = S^{o} = E^{o} - F^{o} + R \tag{29}$$

Also

$$\overline{\Phi} = \int \frac{c_p}{T} dT + \text{constant} \tag{30}$$

Thus, the same multiplying factor must be applied to this function as is applied to the enthalpy above. The final matching of these data with the computed data at 1000°K is then taken care of by the additive constant in Eq. (30). Thus, the computing equation is

$$\frac{S}{R} = 0.85\left[\frac{K_{CO_2}\overline{\Phi}_{CO_2}}{R} + B_{CO_2} - \ln(0.85p)\right] + 0.15\left[\frac{K_{N_2}\overline{\Phi}_{N_2}}{R} + B_{N_2} - \ln(0.14p)\right] \tag{31}$$

where

$$B_{CO_2} = 0.0114$$

$$B_{N_2} = -0.0008$$

The values for the enthalpy, internal energy, and entropy over the range of 150°K to 800°K and 10^2 to 10^{-4} atm are shown in Figs. 6 - 8 and Tables 11 - 13. In Table 2, values are also included for the entropy at the particular pressure-temperature combinations that occur in the model of the Venus atmosphere selected in Section II.

DISCUSSION

Since much of the basic data were taken from Gilmore's paper,[9] the reader is referred to Ref. 9 for an adequate discussion of the accuracy of the basic data. Constituents having a large error in the basic data (due

to a summation over too few energy levels in the internal partition function) are present in such small amounts at the temperatures and pressures when the error is quite significant that the error introduced in the thermodynamic functions may be considered very slight. It should also be mentioned that the data are significantly in error near the liquefaction points of the CO_2.

For more accurate results in this region, better data for CO_2 should be used.[19]

Selected cases were calculated over the complete pressure range at temperatures of 5000°K and 12,000°K for a mixture of 84.7 per cent CO_2, 15 per cent N_2, and 0.3 per cent H_2O vapor by volume. This was done to investigate the effect of water vapor on these properties in the event that a substantial amount of water vapor actually exists in the atmosphere of Venus. The additional constituents considered were H_2O, H_2, OH, H, H^+, H_2^+, OH^+, H^-, and OH^-. Table 8H shows the effect of this addition on the composition and thermodynamic properties of the mixture. It may be stated that the thermodynamic properties are not affected by more than the order of percentage addition of H_2O.

The three most important differences between this case and that of pure CO_2[17] are the reduction in internal degrees of freedom at low temperatures, since N_2 is present; the appearance of NO at moderate temperatures; and the reduction in electron concentration at high temperatures due to the high ionization potential of N_2. Since NO forms quite readily around 5000°K, more energy goes toward dissociation at this level than in the pure-CO_2 case. Since NO ionizes quite readily, the electron concentration at this temperature level is higher than that for pure CO_2. All effects mentioned are generally of the order of the percentage of N_2 addition to pure CO_2.

IV. NORMAL-SHOCK-WAVE CHARACTERISTICS OF A TENTATIVE VENUS ATMOSPHERE

CONDITIONS AND ASSUMPTIONS

The gasdynamic properties of the atmosphere of Venus depend upon the gas mixture assumed and the thermodynamic properties at the high temperature and pressure ratios usually expected through a normal shock at high entry speeds. Therefore, it should be recalled that the gas mixture assumed is 85 per cent CO_2 and 15 per cent N_2 by volume (Section II), and that the calculations of the thermodynamic properties are based upon the assumption of thermodynamic equilibrium (Section III).

In addition, it must be assumed that aerodynamics of continuum flow apply; that is, that the shock thickness must be very much smaller than the characteristic length of the object causing the shock. This is necessary in order that the conservation equations may be applied across a very thin flow discontinuity. Since the highest altitude (and lowest density) chosen corresponds to the altitude in Earth's atmosphere where this assumption still generally applies, the assumption does not impose an appreciable limitation. However, it must be cautioned that the mean free path at 100 km is of the order of 10 cm.

METHOD OF COMPUTATION

Several methods of calculating shock-wave characteristics were investigated;[9,20,21] however, because the upstream state must be specified and because of the desirability of a rapid convergence of the iteration procedure, the method of Ref. 20 was selected, since it appeared to be well-suited to the solution of the problem. Applying conservation of mass, momentum, and energy across a flow discontinuity

$$\text{Continuity:} \qquad \rho_1 u_1 = \rho_2 u_2 \qquad (32)$$

$$\text{Momentum:} \qquad p_1 + \rho_1 u_1^2 = p_2 + \rho_2 u_2^2 \tag{33}$$

$$\text{Energy:} \qquad h_1 + \frac{1}{2} u_1^2 = h_2 + \frac{1}{2} u_2^2 \tag{34}$$

Substituting Eq. (32) in Eq. (33) and manipulating, the pressure ratio becomes

$$\frac{p_2}{p_o} = \frac{p_1}{p_o} + \frac{\rho_1}{\rho_o} \frac{M_o}{RT_o} u_1^2 \left(1 - \frac{u_2}{u_1}\right) \tag{35}$$

Rearranging and manipulating Eq. (34), the enthalpy becomes

$$\frac{H_2}{RT_o} = \frac{H_1}{RT_o} + \frac{M_o}{RT_o} \frac{u_1^2}{2} \left[1 - \left(\frac{u_2}{u_1}\right)^2\right] \tag{36}$$

From Section III the equation of state is presented in Tables 10 and 12 in the form

$$\frac{H_2}{RT_o} = f\,(T_2,\ p_2/p_o) \tag{37a}$$

$$\frac{\rho_2}{\rho_o} = f\,(T_2,\ p_2/p_o) \tag{37b}$$

Finally, from Eq. (32)

$$\frac{\rho_1/\rho_o}{\rho_2/\rho_o} = \frac{u_2}{u_1} \tag{38}$$

With the equations above, the machine iteration procedure follows this pattern:

1. Pick an upstream thermodynamic state and velocity u_1, and enter all known quantities.

2. Assume $u_2/u_1 = 0$. Calculate p_2/p_o from Eq. (35) and H_2/RT_o from Eq. (36).

3. Enter these values in the tabular relations (Eq. (37)) and find ρ_2/ρ_o.

4. Calculate u_2/u_1 from Eq. (38) and enter this into Eqs. (35) and (36).

5. Repeat this procedure until u_2/u_1 obtained in step (4) above differs from that used in the previous iteration by less than 0.0001.

6. Print out p_2/p_1, T_2/T_1, ρ_2/ρ_1, u_2/u_1.

The results of these computations are presented as a function of altitude in the adopted model of the Venus atmosphere in Figs. 11a - 11d and Tables 14a - 14d over a flight-speed range of 2,000 to 40,000 ft/sec. A typical sound speed is 910 ft/sec (at an altitude of 34.65 km in this model) so that the free-stream Mach number range is roughly 2.2 to 44.

DISCUSSION

It is interesting to note that to a good approximation at low Mach numbers, air may be treated as a perfect gas with constant specific heats as far as shock-wave relations are concerned; however, this atmosphere cannot be so treated because of the marked variation with temperature of the specific heats of CO_2 in the normal temperature range of interest. It may be shown through an error analysis that the iteration procedure can be cut off when two successive values of u_2/u_1 differ by less than 0.0001 and yet generally yield errors in the thermodynamic-state variables of the order of 0.01 per cent.

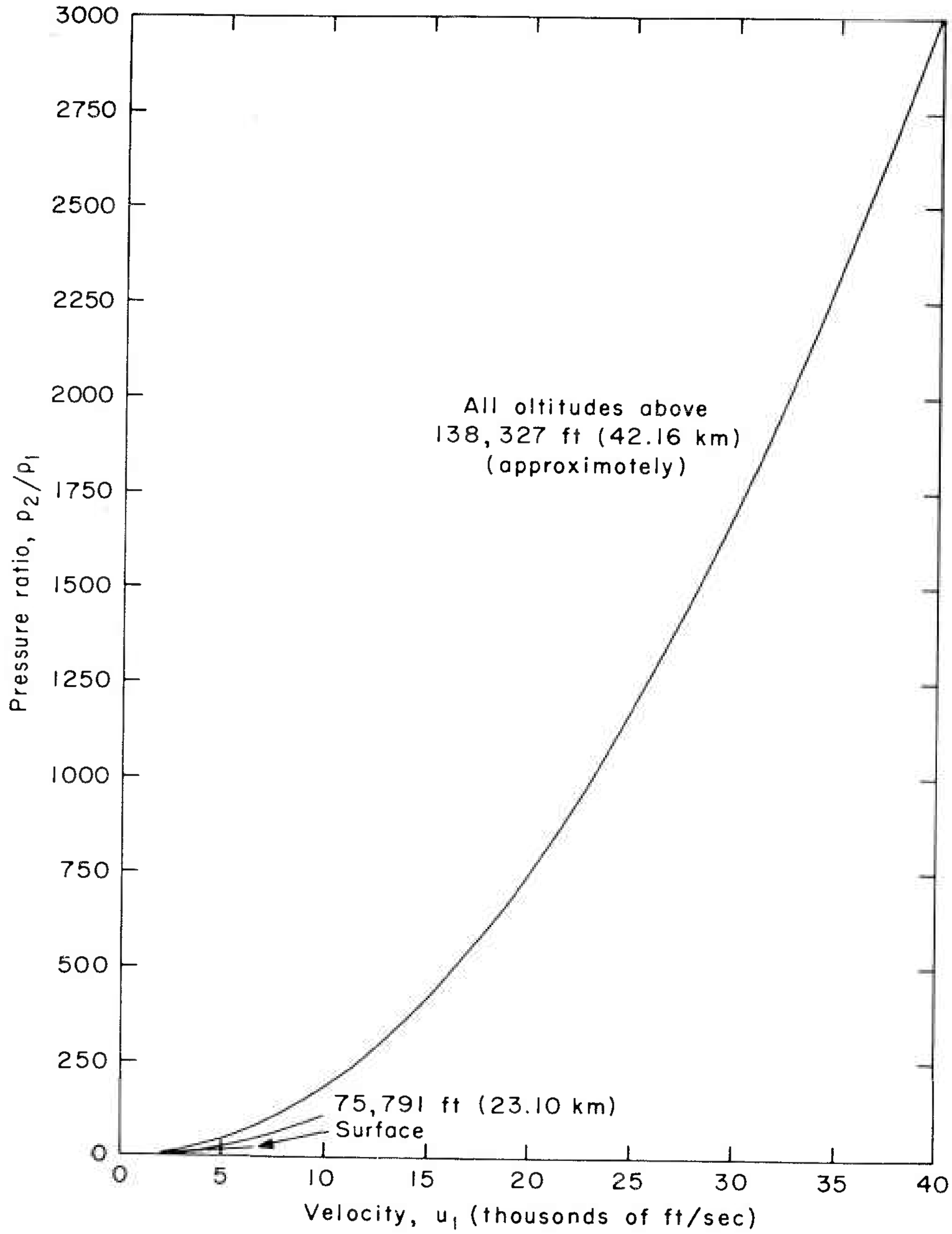

Fig. IIa-1 — Normal-shock-wave characteristics of a tentative Venus atmosphere (pressure ratio, p_2/p_1)

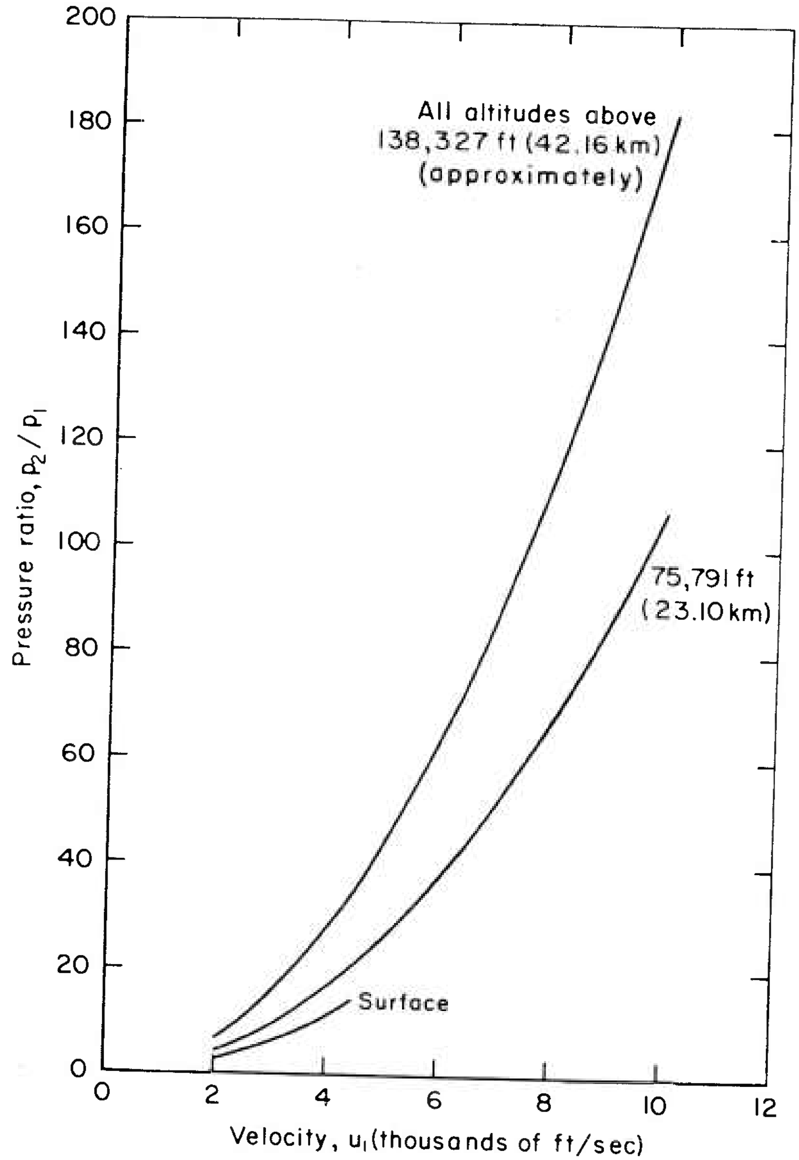

Fig. IIa-2—Normal-shock-wave characteristics of a tentative Venus atmosphere (pressure ratio, p_2/p_1)

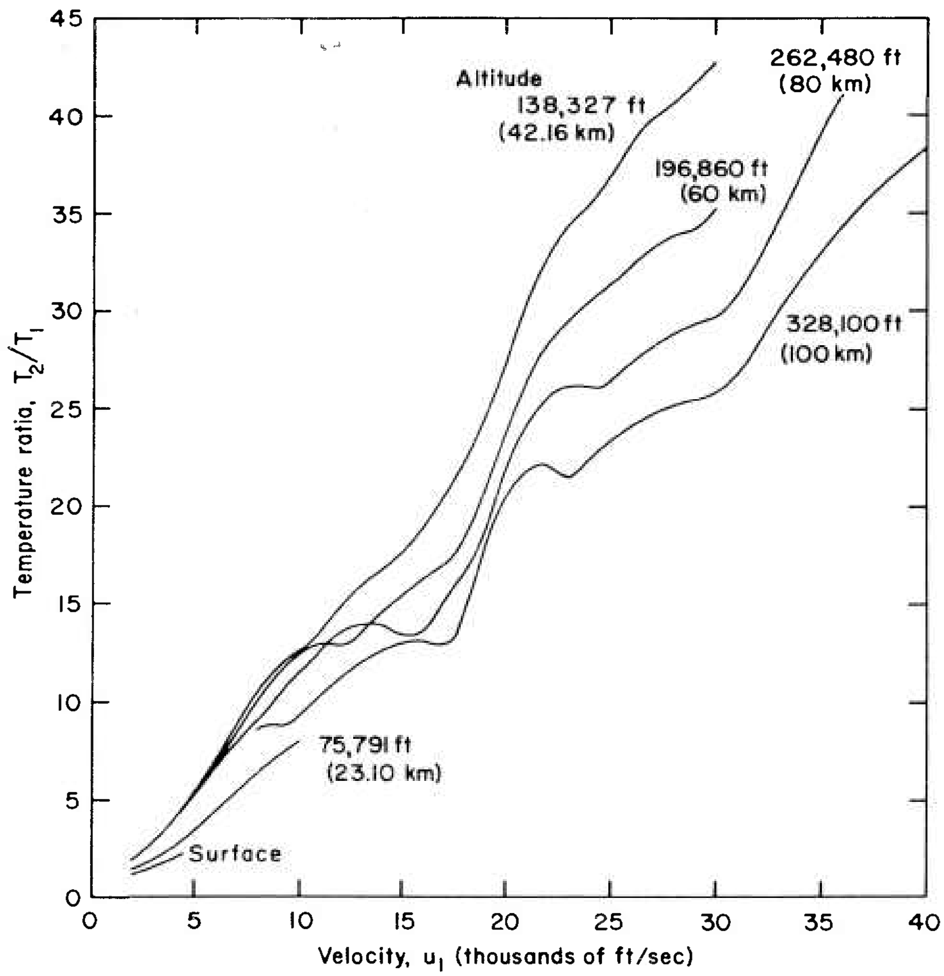

Fig. 11b — Normal-shock-wave characteristics of a tentative Venus atmosphere
(temperature ratio, T_2/T_1)

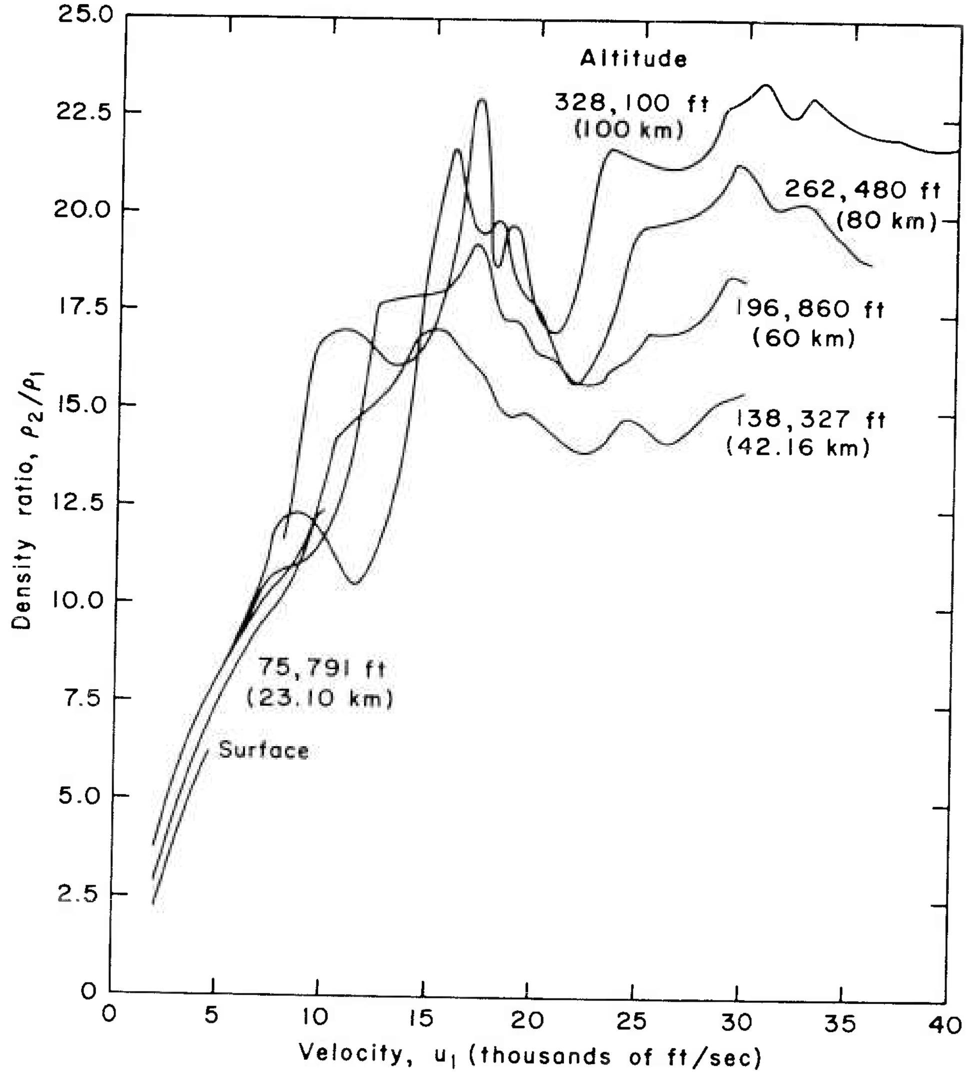

Fig. 11c — Normal-shock-wave characteristics of a tentative Venus atmosphere (density ratio, ρ_2/ρ_1)

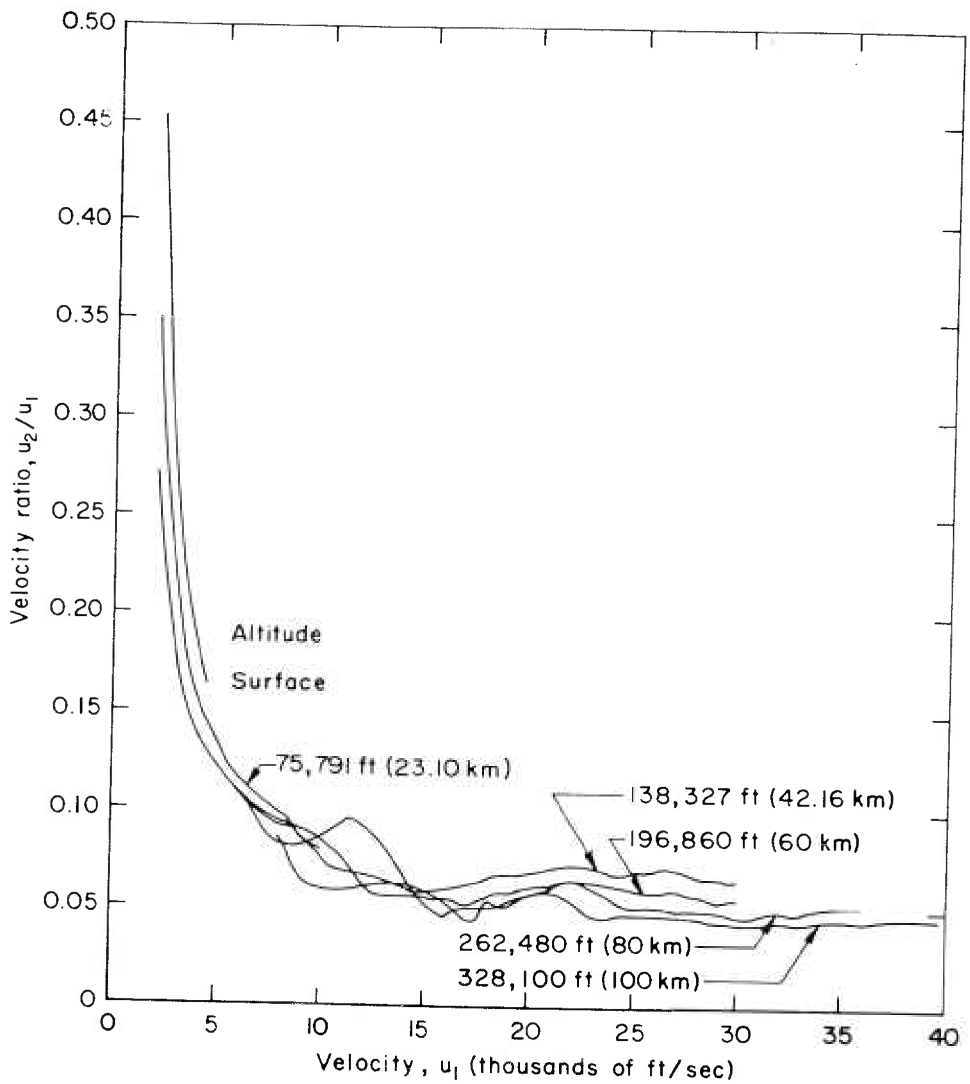

Fig. 11d-1 — Normal-shock-wave characteristics of a tentative Venus atmosphere (velocity ratio, u_2/u_1 ; u_1, from 0 to 40,000 fps)

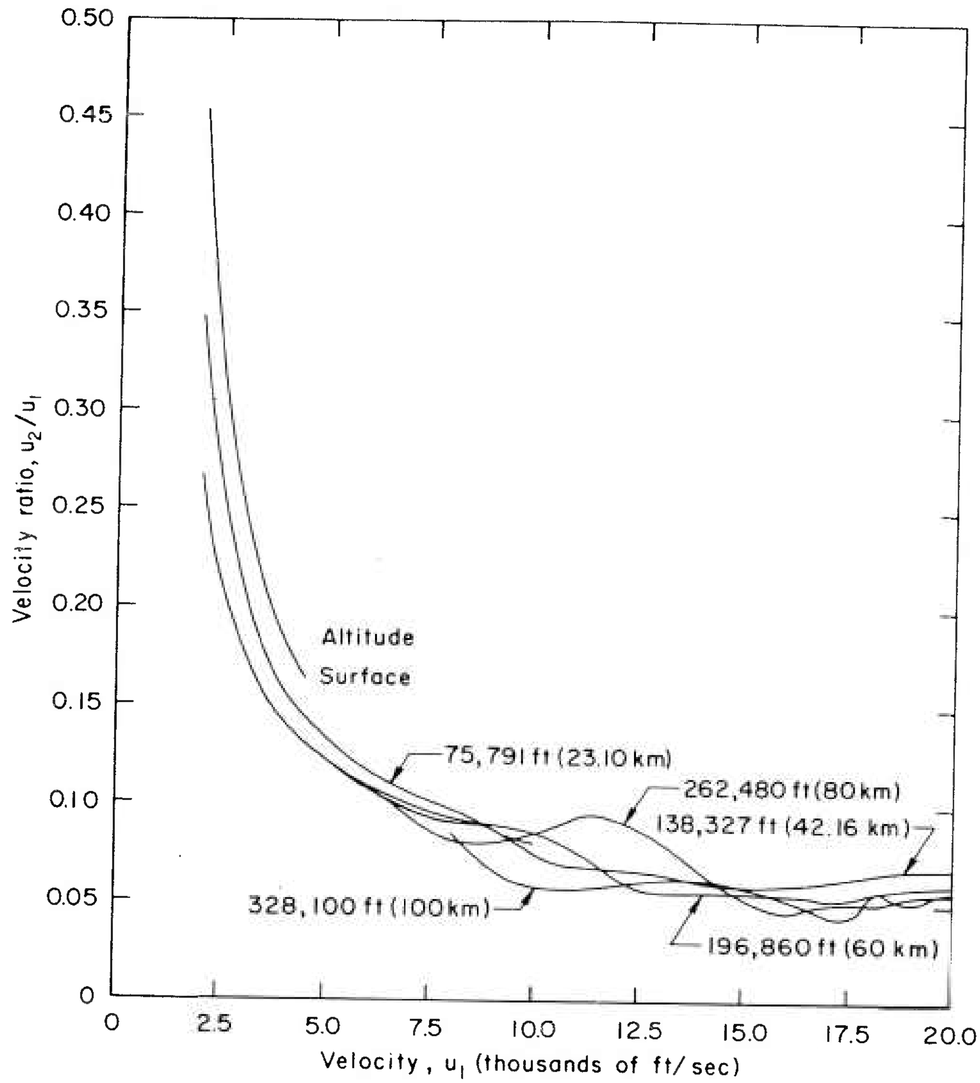

Fig. 11d-2—Normal-shock-wave characteristics of a tentative Venus atmosphere (velocity ratio, u_2/u_1 ; u_1, from 0 to 20,000 fps)

APPENDIX A
TABLES

Table 1

ESTIMATION OF COMPOSITION OF ATMOSPHERE OF VENUS BY DOLE

Constituent	Case L=low CO_2 H=high CO_2	Partial Pressures at Surface		Per Cent Composition (at all altitudes)	
		Atmospheres	mm Hg	By weight	By volume
CO_2	L	6.0171	4573.0	90.261	85.507
	H	8.1390	6185.6	92.528	88.742
	Average	7.0754	5377.3	91.544	87.327
N_2	L	1.0199	775.1	9.739	14.493
	H	1.0325	784.7	7.472	11.258
	Average	1.0268	780.4	8.456	12.673
Totals	L	7.0370	5348.1	100.000	100.000
	H	9.1715	6970.3	100.000	100.000
	Average	8.1022	6157.7	100.000	100.000

Table 2

A TENTATIVE ATMOSPHERE OF VENUS

Altitude (km)	Temperature (°K)	T/T_s	Pressure (atm)	p/p_s	Density (g/cm^3)	ρ/ρ_s	E/RT_o	H/RT_o	S/R
0	600	1.0000	6.784	1.000	5.734^{-3}	1.000	-139.84	-137.65	27.191
11.55	500	0.8333	2.655	3.914^{-1}	2.693^{-3}	4.696^{-1}	-141.40	-139.57	27.173
23.10	400	0.6667	8.428^{-1}	1.242^{-1}	1.068^{-3}	1.863^{-1}	-142.83	-141.37	27.222
34.65	300	0.5000	1.918^{-1}	2.827^{-2}	3.242^{-4}	5.655^{-2}	-144.13	-143.03	27.395
42.16	235	0.3917	5.464^{-2}	8.054^{-3}	1.179^{-4}	2.056^{-2}	-144.89	-144.03	27.636
50	235	0.3917	1.236^{-2}	1.822^{-3}	2.667^{-5}	4.652^{-3}	-144.89	-144.03	29.376
60	235	0.3917	1.857^{-3}	2.738^{-4}	4.008^{-6}	6.990^{-4}	-144.89	-144.03	31.247
70	235	0.3917	2.791^{-4}	4.115^{-5}	6.023^{-7}	1.051^{-4}	-144.89	-144.03	33.143
80	235	0.3917	4.195^{-5}	6.183^{-6}	9.051^{-8}	1.579^{-5}	-144.89	-144.03	35.038
90	235	0.3917	6.305^{-6}	9.294^{-7}	1.360^{-8}	2.373^{-6}	-144.89	-144.03	36.933
100	235	0.3917	9.474^{-7}	1.397^{-7}	2.044^{-9}	3.565^{-7}	-144.89	-144.03	38.828

For $0 \leq r - r_s \leq 42.16$ Km

$$p/p_s = \left[1 - 1.44297 \times 10^{-2} (r - r_s)\right]^{5.1444}$$

$$T/T_s = (p/p_s)^{1/5.1444}$$

$$\rho/\rho_s = (p/p_s)(T/T_s)$$

For $42.16 \leq r - r_s$

$$p/p_s = 8.0535 \times 10^{-3} e^{-0.18953 (r - r_s - 42.158)}$$

$$T/T_s = 0.39167$$

$$\rho/\rho_s = \frac{2.0561}{8.0535} \times 10\ p/p_s$$

Table 3

BASIC PHYSICAL CONSTANTS AND CONVERSION FACTORS

Universal Gas Constant (chemical scale)

$$R = 8.31433 \times 10^7 \text{ erg/g-mole } {}^{\circ}K$$
$$= 1.98717 \text{ cal/g-mole } {}^{\circ}K$$
$$= 82.0561 \text{ atm cm}^3\text{/g-mole } {}^{\circ}K$$

Avogadro's Number (chemical scale)

$$L = 6.02306 \times 10^{23}\text{/g-mole}$$

Energy Conversion Factors (chemical scale)

$$1 \text{ cal/g-mole} = 4.33605 \times 10^{-5} \text{ ev}$$
$$1 \text{ thermochemical calorie} = 4.18400 \times 10^7 \text{ erg}$$

Pressure Conversion Factor

$$1 \text{ standard atmosphere} = 1.01325 \times 10^6 \text{ dyne/cm}^2$$

Ratio of Physical to Chemical Scales

$$M_{phys}/M_{chem} = L_{phys}/L_{chem} = 1.000275$$

Table 4

ENERGIES OF FORMATION E_o^o

Constituent	E_o^o kcal/g-mole	All obtained from Ref. 9 by method indicated below
CO_2	-93.9639	Direct
N_2	0	Definition
O_2	0	Definition
CO	-27.1992	Direct
NO	21.479	Direct
C(g)	169.99	Direct
N	112.535	Computed
O	58.985	Computed
C^+	429.832	Computed
N^+	448.051	Computed
O^+	373.033	Computed
O_2^+	277.9	Computed
CO^+	295.981	Computed
NO^+	234.879	Computed
C^{++}	992.125	Computed
N^{++}	1130.969	Computed
O^{++}	1183.77	Computed
O^-	25.485	Computed
e^-	0	Definition

Table 5

INTERNAL ENERGIES $(E - E_0^0)/RT$

	Constituent																		
$T(^\circ K \times 10^{-3})$	CO_2	N_2	O_2	CO	NO	C	N	O	C^+	N^+	O^+	O_2^+	CO^+	NO^+	C^{++}	N^{++}	O^{++}	O^-	e^-
1	4.1434	2.6239	2.7749	2.6515	2.7787	1.5432	1.5	1.6122	1.5619	1.6281	1.5				1.5	1.6669	1.7993	1.5	1.5
1.5	4.6988	(2.7773)	2.9520	2.8102	(2.9240)	1.5291	1.5	1.5748	1.5412	1.5854	1.5				1.5	1.6113	1.6995	1.5	1.5
2	5.0621	2.8976	3.0819	2.9337	3.0330	1.5243	1.5	1.5562	1.5309	1.5641	1.5				1.5	1.5835	1.6496	1.5	1.5
3	5.5033	3.0656	3.2808	3.0979	3.1790	1.5350	1.5023	1.5396	1.5206	1.5454	1.5001	3.158	3.093	3.095	1.5	1.5556	1.6001	1.5	1.5
4	5.7650	3.1719	3.4378	3.2006	3.2721	1.5629	1.5176	1.5388	1.5155	1.5447	1.5016	3.255	3.207	3.197	1.5	1.5417	1.5778	1.5	1.5
5	5.9432	3.2463	3.5622	3.2721	3.3396	1.5950	1.5572	1.5492	1.5125	1.5559	1.5087	3.328	3.315	3.267	1.5	1.5334	1.5698	1.5	1.5
6	(6.10)	3.3034	3.6709	3.3265	3.3933	1.6244	1.6217	1.5661	1.5110	1.5736	1.5267	3.397	3.433	3.323	1.5004	1.5278	1.5716	1.5	1.5
7	(6.23)	3.338	3.7250	3.369	3.414	1.6494	1.7030	1.5855	1.5114	1.5937	1.5581	3.478	3.571	3.376	1.5020	1.5240	1.5797	1.5	1.5
8	(6.34)	3.380	3.796	3.409	3.452	1.6707	1.7905	1.6048	1.5145	1.6137	1.6023	3.583	3.692	3.438	1.5068	1.5216	1.5914	1.5	1.5
9	(6.42)	(3.3945)	(3.871)	(3.470)	(3.482)	1.6898	1.9754	1.6227	1.5212	1.6323	1.6566	(3.730)	(3.815)	(3.511)	1.5173	1.5205	1.6049	1.5	1.5
10	(6.51)	(3.4415)	(3.960)	(3.552)	(3.523)	1.7084	1.9522	1.6387	1.5319	1.6493	1.7170	(3.888)	(3.937)	(3.617)	1.5359	1.5211	1.6188	1.5	1.5
11	(6.58)	(3.5205)	(4.055)	(3.657)	(3.573)	1.7290	2.0187	1.6528	1.5469	1.6646	1.7796	(4.051)	(4.038)	(3.746)	1.5646	1.5237	1.6325	1.5	1.5
12	(6.67)	3.635	4.159	3.792	3.628	1.7540	2.0751	1.6658	1.5659	1.6785	1.8413	4.211	4.122	3.894	1.6041	1.5285	1.6456	1.5	1.5
13		(3.776)	(4.269)	(3.952)	(3.688)	1.7856	2.1233	1.6786	1.5886	1.6910	1.8996	(4.365)	(4.190)	(4.035)	1.6544	1.5356	1.6576	1.5	1.5
14		(3.922)	(4.385)	(4.118)	(3.755)	1.8258	2.1664	1.6924	1.6144	1.7026	1.9529	(4.525)	(4.255)	(4.200)	1.7143	1.5452	1.6694	1.5	1.5
15		(4.063)	(4.505)	(4.340)	(3.823)	1.8762	2.2077	1.7089	1.6427	1.7133	2.0004	(4.675)	(4.305)	(4.376)	1.7822	1.5573	1.6801	1.5	1.5
16		(4.202)	(4.631)	(4.570)	(3.892)	1.9376	2.2506	1.7297	1.6730	1.7234	2.0419	(4.815)	(4.355)	(4.560)	1.8557	1.5717	1.6901	1.5	1.5
17		(4.341)	(4.955)	(4.802)	(3.959)	2.0101	2.2981	1.7565	1.7047	1.7332	2.0774	(4.940)	(4.390)	(4.655)	1.9326	1.5881	1.6994	1.5	1.5
18		4.471	4.883	5.025	4.022	2.0934	2.3528	1.7910	1.7372	1.7427	2.1074	5.043	4.425	4.923	2.0107	1.6063	1.7082	1.5	1.5
19		4.596	(5.001)	(5.211)	(4.0845)	2.1864	2.4165	1.8347	1.7703	1.7521	2.1322	(5.130)	(4.450)	(5.085)	2.0881	1.6262	1.7166	1.5	1.5
20		(4.725)	(5.118)	(5.385)	(4.149)	2.2876	2.4902	1.8888	1.8036	1.7616	2.1526	(5.200)	(4.475)	(5.230)	2.1632	1.6473	1.7245	1.5	1.5
21		(4.8505)	(5.222)	(5.534)	(4.2115)	2.3951	2.5743	1.9541	1.8368	1.7712	2.1691	(5.260)	(4.495)	(5.355)	2.2347	1.6695	1.7322	1.5	1.5
22		(4.9755)	(5.341)	(5.662)	(4.274)	2.5070	2.6680	2.0308	1.8700	1.7811	2.1823	(5.310)	(4.510)	(5.456)	2.3019	1.6925	1.7396	1.5	1.5
23		(5.105)	(5.445)	(5.765)	(4.3385)	2.6211	2.7703	2.1188	1.9029	1.7914	2.1927	(5.360)	(4.524)	(5.540)	2.3642	1.7160	1.7469	1.5	1.5
24		5.230	5.547	5.845	4.401	2.7355	2.8794	2.2172	1.9356	1.8022	2.2009	5.401	4.543	5.607	2.4214	1.7399	1.7540	1.5	1.5
Reference	17	9	17	17	9	17	a	17	17	a	17	9	9	9	17	a	17	a	17

( ) denotes extrapolation or interpolation

[a] Also from F. R. Gilmore, unpublished thermodynamic properties from statistical mechanics calculations.

Table 6

FREE ENERGIES $-(F^{o} - E_{o}^{o})/RT$

	Constituent																		
$T(^{o}K \times 10^{-3})$	CO_2	N_2	O_2	CO	NO	C	N	O	C^+	N^+	O^+	O_2^+	CO^+	NO^+	C^{++}	N^{++}	O^{++}	O^-	e^-
1	27.233	23.800	25.512	24.544	26.100	19.4871	18.9500	19.8481	19.0628	19.6328	19.1494			24.64	17.3329	19.1884	19.6610	19.5550	3.0352
1.5	(29.432)	(25.274)	27.078	26.055	(27.635)	20.5151	19.9637	20.8992	20.0971	20.6892	20.1631				18.3465	20.2577	20.7744	20.5696	4.0489
2	31.124	26.402	28.234	27.169	28.805	21.2418	20.6829	21.6371	20.8266	21.4297	20.8823			27.27	19.0657	21.0048	21.5435	21.2878	4.7681
3	33.675	28.017	29.928	28.798	30.470	22.2666	21.6968	22.6698	21.8506	22.4651	21.8959	29.933	29.457	28.90	20.0794	22.0462	22.6071	22.3015	5.7818
4	35.584	29.202	31.183	29.992	31.686	22.9995	22.4183	23.3999	22.5750	23.1969	22.6153	31.142	30.650	30.09	20.7986	22.7794	23.3516	23.0207	6.5010
5	37.114	30.141	32.186	30.938	32.647	23.5748	22.9838	23.9674	23.1359	23.7658	23.1741	32.099	31.600	31.04	21.3565	23.3456	23.9257	23.5786	7.0588
6	(38.44)	30.920	33.028	31.722	33.443	24.0506	23.4554	24.4336	23.5938	24.2333	23.6329	32.893	32.396	31.82	21.8123	23.8069	24.3943	24.0344	7.5146
7	39.73	31.580	33.731	32.384	34.149	24.4571	23.8655	24.8306	23.9809	24.6315	24.0246	33.576	33.091	32.49	22.1978	24.1963	24.7913	24.4197	7.9000
8	40.84	32.162	34.365	32.969	34.679	24.8123	24.2321	25.1771	24.3164	24.9792	24.3689	34.179	33.705	33.08	22.5322	24.5332	25.1365	24.7536	8.2338
9	(41.64)	(32.626)	(34.91)	(33.49)	(35.159)	25.1280	24.5658	25.4850	24.6130	25.2881	24.6785	(34.701)	(34.190)	(33.62)	22.8282	24.8301	25.4425	25.0480	8.5283
10	(42.60)	(33.144)	(35.43)	(33.97)	(35.663)	25.4123	24.8728	25.7622	24.8791	25.5664	24.9615	(35.222)	(34.705)	(34.09)	23.0941	25.0957	25.7176	25.3114	8.7917
11	(43.58)	(33.607)	(35.90)	(34.40)	(36.124)	25.6714	25.1574	26.0143	25.1211	25.8196	25.2234	(35.710)	(35.226)	(34.51)	23.3371	25.3361	25.9679	25.5497	9.0300
12	(44.67)	33.980	36.36	34.81	36.51	25.9099	25.4225	26.2457	25.3435	26.0521	25.4679	36.14	35.69	34.94	23.5618	25.5558	26.1975	25.7672	9.2475
13		(34.338)	(36.78)	(35.20)	(36.851)	26.1315	25.6706	26.4596	25.5498	26.2670	25.6976	(36.54)	(36.10)	(35.35)	23.7722	25.7585	26.4098	25.9673	9.4476
14		(34.694)	(37.16)	(35.55)	(37.202)	26.3394	25.9037	26.6586	25.7425	26.4668	25.9145	(36.93)	(36.50)	(35.73)	23.9710	25.9467	26.6072	26.1526	9.6329
15		(35.026)	(37.54)	(35.92)	(37.540)	26.5360	26.1235	26.8449	25.9238	26.6536	26.1199	(37.33)	(36.87)	(36.09)	24.1606	26.1227	26.7917	26.3251	9.8054
16		(35.365)	(37.89)	(36.27)	(37.869)	26.7235	26.3319	27.0204	26.0954	26.8291	26.3149	(37.69)	(37.20)	(36.43)	24.3424	26.2882	26.9649	26.4864	9.9667
17		(35.694)	(38.21)	(36.61)	(38.180)	26.9037	26.5304	27.1866	26.2584	26.9945	26.5004	(38.03)	(37.53)	(36.78)	24.5179	26.4446	27.1284	26.6380	10.1183
18		35.99	38.53	36.97	38.45	27.0781	26.7204	27.3451	26.4139	27.1510	26.6772	38.40	37.82	37.11	24.6877	26.5931	27.2829	26.7809	10.2612
19		(36.267)	(38.82)	(37.29)	(38.694)	27.2478	26.9033	27.4972	26.5627	27.2995	26.8459	(38.70)	(38.12)	(37.43)	24.8526	26.7345	27.4296	26.9161	10.3963
20		(36.553)	(39.11)	(37.60)	(38.946)	27.4138	27.0804	27.6439	26.7057	27.4409	27.0070	(39.00)	(38.40)	(37.73)	25.0129	26.8697	27.5691	27.0443	10.5245
21		(36.830)	(39.40)	(37.92)	(39.190)	27.5768	27.2527	27.7864	26.8433	27.5759	27.1613	(39.30)	(38.67)	(38.03)	25.1690	26.9994	27.7022	27.1663	10.6465
22		(37.107)	(39.67)	(38.23)	(39.434)	27.7373	27.4211	27.9255	26.9760	27.7050	27.3090	(39.59)	(38.92)	(38.32)	25.3210	27.1241	27.8295	27.2826	10.7628
23		(37.393)	(39.93)	(38.54)	(39.686)	27.8957	27.5864	28.0621	27.1043	27.8289	27.4507	(39.87)	(39.17)	(38.62)	25.4692	27.2443	27.9514	27.3937	10.8740
24		37.67	40.20	38.83	39.93	28.0522	27.7491	28.1969	27.2286	27.9479	27.5868	40.14	39.39	38.91	25.6136	27.3604	28.0685	27.5001	10.9804
Reference	9	9	17	17	9	a	a	a	17	a	17	9	9	9	17	a	17	a	a

( ) denotes extrapolation or interpolation [a]Also from F. R. Gilmore, unpublished thermodynamic properties from statistical mechanics calculations.

Table 7

TOTAL NUMBER OF G-MOLES n

$T(^{o}K) \times 10^{-3}$	Pressure (atm) 10^2	30	10	3	1	3×10^{-1}	10^{-1}	3×10^{-2}	10^{-2}	3×10^{-3}	10^{-3}	3×10^{-4}	10^{-4}
1	1.0000		1.0000		1.0000		1.0000		1.0000		1.0000		1.0000
1.5	1.0000		1.0001		1.0002		1.0004		1.0008		1.0016		1.0045
2	1.0015		1.0032		1.0068		1.0144		1.0309		1.0656		1.1370
3	1.0567		1.1160		1.2258		1.4060		1.6486		1.8098		1.8479
4	1.2272		1.4704		1.7013		1.8233		1.8502		1.8629		1.8924
5	1.5511		1.7580		1.8406		1.8734		1.9343		2.1279		2.5608
6	1.7396		1.8454		1.9126		2.0950		2.5310		2.8286		2.9399
7	1.8298		1.9427		2.2356		2.6906		2.8842		3.0154		3.2938
8	1.9308	2.0595	2.2509	2.5118	2.7085	2.8324	2.8978	2.9640	3.0482	3.1885	3.3698	3.6163	3.8861
9	2.1610	2.4191	2.6445	2.8024	2.8818	2.9512	3.0319	3.1664	3.3472	3.6099	3.9120	4.3488	4.8317
10	2.4827	2.7106	2.8328	2.9141	2.9855	3.0972	3.2529	3.4985	3.7963	4.2227	4.7042	5.2045	5.4925
11	2.7173	2.8490	2.9254	3.0128	3.1291	3.3249	3.5829	3.9646	4.4145	4.9606	5.3527	5.5772	5.6569
12	2.8388	2.9300	3.0147	3.1494	3.3392	3.6449	4.0263	4.5538	5.0497	5.4328	5.5998	5.6693	5.6919
13	2.9145	3.0106	3.1323	3.3399	3.6239	4.0572	4.5536	5.0969	5.4365	5.6111	5.6706	5.6972	5.7104
14	2.9847	3.1113	3.2894	3.5897	3.9811	4.5276	5.0371	5.4282	5.5987	5.6707	5.7013	5.7209	5.7672
15	3.0645	3.2404	3.4909	3.8969	4.3871	4.9633	5.3606	5.5822	5.6621	5.7045	5.7289	5.7994	5.9433
16	3.1626	3.4022	3.7366	4.2459	4.7851	5.2800	5.5336	5.6503	5.6949	5.7370	5.8137	5.9920	6.2383
17	3.2822	3.5974	4.0194	4.6021	5.1116	5.4711	5.6200	5.6886	5.7344	5.8258	5.9971	6.2749	6.5372
18	3.4247	3.8229	4.3223	4.9214	5.3400	5.5775	5.6688	5.7294	5.8127	5.9980	6.2572	6.5654	6.8593
19	3.5898	4.0707	4.6202	5.1733	5.4847	5.6399	5.7105	5.7997	5.9576	6.2390	6.5382	6.8920	7.2996
20	3.7748	4.3280	4.8871	5.3534	5.5747	5.6866	5.7678	5.9225	6.1678	6.5088	6.8532	7.3201	7.8129
21	3.9749	4.5785	5.1063	5.4760	5.6360	5.7382	5.8609	6.1039	6.4170	6.8116	7.2468	7.7952	8.1977
22	4.1826	4.8068	5.2750	5.5604	5.6881	5.8119	6.0017	6.3290	6.6964	7.1762	7.6863	8.1602	8.3969
23	4.3890	5.0028	5.4002	5.6242	5.7466	5.9212	6.1889	6.5864	7.0211	7.5827	8.0557	8.3653	8.4836
24	4.5864	5.1641	5.4939	5.6818	5.8240	6.0700	6.4108	6.8784	7.3875	7.9472	8.2912	8.4633	8.5201

Table 8A

MOLAR COMPOSITION n_1 (PRESSURE = 10^2 ATM)

$T(^\circ K \times 10^{-3})$	Constituent																		
	CO_2	N_2	C_2	CO	NO	C	N	O	C^+	N^+	O^+	O_2^+	CO^+	NO^+	C^{++}	N^{++}	O^{++}	O^-	e^-
1	.8500	.1500	0	0	0	0	0	0	0	0	0	0	0	0	0	0	0	0	0
1.5	.8499	.1500	0	.0001	0														
2	.8470	.1499	.0014	.0030	.0003			0											
3	.7383	.1448	.0499	.1118	.0104		0	.0026											
4	.3668	.1271	.1831	.4833	.0456		.0001	.0713											
5	.0998	.1144	.1647	.7502	.0696	0	.0139	.3508						0					0
6	.0235	.1145	.0621	.8263	.0604	.0002	.0105	.6418						.0001					.0001
7	.0065	.1068	.0187	.8391	.0425	.0044	.0436	.7676	0		0		0	.0003					.0003
8	.0025	.0797	.0071	.8024	.0255	.0450	.1146	.8524	.0002	0	.0001		.0002	.0006				0	.0009
9	.0010	.0390	.0039	.6314	.0149	.2152	.2063	1.0422	.0020	.0001	.0003		.0006	.0007				.0001	.0035
10	.0004	.0142	.0028	.3511	.0084	.4890	.2623	1.3312	.0086	.0004	.0012		.0009	.0005				.0003	.0114
11	.0001	.0049	.0019	.1472	.0045	.6794	.2843	1.5389	.0222	.0010	.0033		.0011	.0004				.0005	.0275
12	0	.0018	.0013	.0581	.0024	.7478	.2914	1.6268	.0430	.0023	.0078		.0010	.0003				.0008	.0538
13		.0007	.0009	.0242	.0013	.7532	.2921	1.6543	.0717	.0048	.0161	0	.0009	.0003				.0009	.0929
14		.0003	.0006	.0107	.0008	.7302	.2893	1.6551	.1087	.0090	.0303	.0001	.0008	.0002				.0011	.1480
15		.0002	.0004	.0052	.0005	.6905	.2834	1.6384	.1536	.0156	.0528	.0001	.0007	.0002				.0012	.2218
16		.0001	.0003	.0027	.0003	.6413	.2743	1.6075	.2055	.0251	.0867	.0001	.0006	.0002				.0013	.3168
17		0	.0002	.0014	.0002	.5856	.2617	1.5609	.2625	.0379	.1350	.0001	.0005	.0002				.0013	.4348
18			.0002	.0008	.0001	.5265	.2455	1.4962	.3224	.0542	.2005	.0001	.0004	.0001				.0013	.5764
19			.0001	.0004	.0001	.4665	.2261	1.4123	.3827	.0737	.2852	.0001	.0003	.0001	0			.0012	.7409
20			.0001	.0002	.0001	.4080	.2040	1.3090	.4415	.0958	.3889	.0001	.0002	.0001	.0001			.0011	.9257
21			.0001	.0001	0	.3526	.1805	1.1889	.4969	.1194	.5094	.0001	.0002	.0001	.0002			.0010	1.1255
22			0	.0001		.3017	.1567	1.0569	.5477	.1432	.6418	.0001	.0001	.0001	.0004			.0008	1.3330
23				0		.2566	.1336	.9198	.5925	.1662	.7792	.0001	.0001	0	.0008	0		.0007	1.5392
24						.2160	.1125	.7854	.6325	.1874	.9138	.0001	.0001		.0015	.0001		.0005	1.7366

Table 8B

MOLAR COMPOSITION n_i (PRESSURE = 10 ATM)

$T(^{\circ}K \times 10^{-3})$	Constituent																	
	CO_2	N_2	O_2	CO	NO	C	N	O	C^+	N^+	O^+	O_2^+	CO^+	NO^+	C^{++}	N^{++}	O^{++}	O^-	e^-
1	.8500	.1500	0	0	0	0	0	0	0	0	0	0	0	0	0	0	0	0	0
1.5	.8499	.1500	.0001	.0002	0														
2	.8436	.1498	.0030	.0064	.0004			0											
3	.6290	.1428	.0977	.2210	.0144		0	.0117											
4	.1598	.1264	.1963	.6902	.0470		.0002	.2504											
5	.0189	.1265	.0546	.8311	.0421	0	.0049	.6799						0					0
6	.0028	.1204	.0092	.8455	.0239	.0017	.0352	.8063	0				0	.0002					.0002
7	.0007	.0814	.0023	.8097	.0129	.0398	.1239	.8711	.0001	0	0		.0001	.0004					.0007
8	.0002	.0289	.0011	.5661	.0059	.2805	.2359	1.1244	.0029	.0001	.0003		.0004	.0004				0	.0040
9	0	.0061	.0006	.2123	.0024	.6227	.2848	1.4818	.0145	.0003	.0012		.0005	.0003				.0001	.0168
10		.0016	.0004	.0582	.0010	.7527	.2945	1.6351	.0387	.0011	.0042		.0004	.0002				.0001	.0446
11		.0005	.0002	.0165	.0005	.7551	.2952	1.6708	.0784	.0032	.0011		.0004	.0001				.0002	.0934
12		.0002	.0001	.0053	.0002	.7081	.2916	1.6668	.1362	.0078	.0267		.0003	.0001				.0002	.1710
13		.0001	.0001	.0019	.0001	.6357	.2832	1.6411	.2122	.0164	.0561		.0002	.0001				.0003	.2848
14		0	0	.0007	.0001	.5475	.2687	1.4908	.3017	.0311	.1078		.0002	.0001				.0003	.4406
15				0	0	.4529	.2465	1.5077	.3967	.0534	.1914		.0001	.0001				.0003	.6415
16						.3613	.2165	1.3844	.4885	.0835	.3150		.0001	0	0			.0003	.8869
17						.2795	.1808	1.2195	.5704	.1191	.4801		.0001		.0001			.0002	1.1695
18						.2111	.1435	1.0226	.6387	.1564	.6771		0		.0001			.0002	1.4724
19						.1568	.1089	.8142	.6928	.1911	.8856				.0004			.0001	1.7702
20						.1153	.0797	.6187	.7338	.2202	1.0812				.0009	0		.0001	2.0370
21						.0846	.0573	.4538	.7655	.2426	1.2460				.0019	.0001	0	.0001	2.2563
22						.0623	.0408	.3263	.7837	.2589	1.3735				.0040	.0002	.0002	0	2.4250
23						.0464	.0292	.2331	.7957	.2702	1.4664				.0079	.0005	.0005		2.5502
24						.0347	.0212	.1673	.8005	.2777	1.5314				.0147	.0011	.0013		2.6439

Table 8c

MOLAR COMPOSITION n_i (PRESSURE = 1.0 ATM)

$T(^{\circ}K \times 10^{-3})$	Constituent: CO_2	N_2	O_2	CO	NO	C	N	O	C^+	N^+	O^+	O_2^+	CO^+	NO^+	C^{++}	N^{++}	O^{++}	O^-	e^-
1	.8500	.1500	0	0	0	0	0	0	0	0	0	0	0	0	0	0	0	0	0
1.5	.8497	.1500	.0002	.0003	0			0											
2	.8364	.1497	.0065	.0136	.0006			.0001											
3	.4489	.1407	.1660	.4011	.0186		0	.0506											
4	.0383	.1329	.0942	.8118	.0334	0	.0008	.5900						0					0
5	.0022	.1337	.0075	.8476	.0161	.0002	.0163	.8169						.0001					.0001
6	.0003	.0958	.0010	.8331	.0070	.0165	.1011	.8571	0		0		0	.0003					.0003
7	.0001	.0271	.0003	.5867	.0028	.2606	.2429	1.1092	.0025	0	.0002		.0002	.0002					.0031
8	0	.0037	.0002	.1556	.0008	.6766	.2915	1.5418	.0176	.0002	.0010		.0003	.0001					.0192
9		.0006	.0001	.0271	.0003	.7682	.2974	1.6680	.0545	.0011	.0043		.0002	.0001					.0601
10		.0002	0	.0054	.0001	.7213	.2957	1.6798	.1231	.0038	.0143		.0001	.0001				0	.1415
11		0		.0013	0	.6197	.2886	1.6581	.2289	.0112	.0403		.0001	0				.0001	.2806
12				.0003		.4872	.2719	1.6003	.3624	.0280	.0992		.0001					.0001	.4897
13				.0001		.3511	.2406	1.4838	.4988	.0593	.2159		0					.0001	.7741
14				0		.2363	.1941	1.2883	.6137	.1059	.4112							.0005	1.1311
15						.1519	.1404	1.0204	.6980	.1596	.6795				0			0	1.5372
16						.0951	.0919	.7279	.7548	.2081	.9721				.0001				1.9352
17						.0589	.0563	.4737	.7906	.2437	1.2263				.0005				2.2616
18						.0367	.0335	.2912	.8119	.2665	1.4088				.0013	0	0		2.4900
19						.0234	.0200	.1757	.8232	.2799	1.5242				.0035	.0002	.0001		2.6347
20						.0152	.0122	.1069	.8265	.2874	1.5928				.0083	.0004	.0003		2.7247
21						.0102	.0077	.0665	.8214	.2912	1.6326				.0184	.0011	.0009		2.7860
22						.0069	.0050	.0427	.8053	.2924	1.6550				.0378	.0025	.0023		2.8381
23						.0048	.0034	.0283	.7733	.2911	1.6660				.0719	.0055	.0057		2.8966
24						.0033	.0023	.0193	.7216	.2866	1.6678				.1251	.0111	.0129		2.9740

Table 8D

MOLAR COMPOSITION n_1 (PRESSURE = 10^{-1} ATM)

$T(^{\circ}K \times 10^{-3})$	Constituent																		
	CO_2	N_2	O_2	CO	NO	C	N	O	C^+	N^+	O^+	O_2^+	CO^+	NO^+	C^{++}	N^{++}	O^{++}	O^-	e^-
1	.8500	.1500	0	0	0	0	0	0	0	0	0	0	0	0	0	0	0	0	0
1.5	.8493	.1500	.0003	.0007	0			0											
2	.8212	.1496	.0140	.0290	.0009			.0002											
3	.2284	.1397	.2053	.6216	.0206		0	.1904											
4	.0050	.1415	.0161	.8450	.0143	0	.0028	.7987						0					0
5	.0002	.1225	.0008	.8479	.0050	.0019	.0499	.8450	0		0		0	.0001					.0001
6	0	.0404	.0001	.7138	.0016	.1352	.2174	.9840	.0009	0	.0001		.0001	.0002					.0012
7		.0033	.0001	.1711	.0004	.6640	.2929	1.5277	.0148	.0001	.0005		.0001	.0001					.0156
8		.0004	0	.0180	.0001	.7702	.2985	1.6787	.0620	.0007	.0033		.0001	0					.0661
9		.0001		.0023	0	.6817	.2962	1.6828	.1659	.0036	.0148		.0001						.1844
10		0		.0003		.5142	.2858	1.6459	.3354	.0141	.0537		0						.4033
11				.0001		.3245	.2562	1.5361	.5254	.0438	.1638								.7330
12				0		.1795	.1978	1.2964	.6705	.1022	.4036								1.1763
13						.0933	.1246	.9285	.7567	.1754	.7715				0				1.7036
14						.0472	.0656	.5501	.8027	.2344	1.1499				.0001				2.1871
15						.0240	.0316	.2842	.8256	.2684	1.4158				.0004				2.5106
16						.0126	.0151	.1401	.8360	.2848	1.5599				.0013	0	0		2.6836
17						.0070	.0075	.0701	.8387	.2923	1.6298				.0044	.0001	.0001		2.7700
18						.0040	.0040	.0367	.8333	.2955	1.6631				.0127	.0005	.0003		2.8188
19						.0024	.0022	.0202	.8148	.2963	1.6789				.0328	.0015	.0009		2.8605
20						.0015	.0013	.0117	.7734	.2945	1.6853				.0751	.0042	.0030		2.9178
21						.0010	.0008	.0071	.6984	.2888	1.6842				.1507	.0104	.0086		3.0109
22						.0005	.0005	.0045	.5874	.2766	1.6731				.2620	.0229	.0224		3.1517
23						.0003	.0003	.0030	.4547	.2547	1.6445				.3950	.0450	.0525		3.3389
24						.0002	.0002	.0020	.3277	.2213	1.5856				.5222	.0785	.1124		3.5608

Table 8E

MOLAR COMPOSITION n_i (PRESSURE = 10^{-2} ATM)

$T(^{\circ}K \times 10^{-3})$	Constituent CO_2	N_2	O_2	CO	NO	C	N	O	C^+	N^+	O^+	O_2^+	CO^+	NO^+	C^{++}	N^{++}	O^{++}	O^-	e^-
1	.8500	.1500	0	0	0	0	0	0	0	0	0	0	0	0	0	0	0	0	0
1.5	.8485	.1500	.0007	.0015	0			0											
2	.7889	.1493	.0295	.0611	.0013			.0012											
3	.0662	.1418	.1272	.7839	.0164		0	.5132											
4	.0005	.1432	.0018	.8496	.0047	0	.0091	.8418	0					0					0
5	0	.0832	.0001	.8311	.0013	.0191	.1322	.8672	.0001		0		0	.0001					.0002
6		.0059	0	.3202	.0002	.5226	.2879	1.3793	.0007	0	.0001		.0001	.0001					.0007
7		.0003		.0205	0	.7770	.2990	1.6780	.0528	.0003	.0017		0	0					.0549
8		0		.0015		.6627	.2974	1.6870	.1858	.0025	.0114								.1998
9				.0001		.4257	.2857	1.6409	.4241	.0143	.0590								.4974
10				0		.2002	.2409	1.4626	.6497	.0591	.2374								.9463
11						.0821	.1511	1.0526	.7679	.1489	.6477								1.5645
12						.0326	.0672	.5505	.8174	.2328	1.1495				0				2.1997
13						.0131	.0249	.2256	.8368	.2752	1.4743				.0001				2.5865
14						.0056	.0092	.0872	.8436	.2908	1.6128				.0007	0			2.7487
15						.0026	.0037	.0354	.8440	.2963	1.6649				.0034	.0001	0		2.8121
16						.0013	.0016	.0156	.8358	.2981	1.6845				.0129	.0003	.0001		2.8449
17						.0007	.0008	.0074	.8080	.2978	1.6920				.0413	.0014	.0006		2.8844
18						.0004	.0004	.0038	.7396	.2948	1.6937				.1100	.0048	.0025		2.9627
19						.0002	.0002	.0021	.6129	.2856	1.6889				.2369	.0142	.0090		3.1076
20						.0001	.0001	.0012	.4443	.2643	1.6707				.4056	.0356	.0280		3.3178
21						0	0	.0007	.2838	.2252	1.6223				.5661	.0748	.0770		3.5670
22								.0005	.1674	.1708	1.5144				.6826	.1292	.1851		3.8464
23								.0003	.0956	.1151	1.3176				.7544	.1849	.3822		4.1711
24								.0001	.0552	.0713	1.0358				.7948	.2287	.6641		4.5375

Table 8F

MOLAR COMPOSITION n_i (PRESSURE = 10^{-3} ATM)

	Constituent																		
$T(^{\circ}K \times 10^{-3})$	CO_2	N_2	O_2	CO	NO	C	N	O	C^+	N^+	O^+	O_2^+	CO^+	NO^+	C^{++}	N^{++}	O^{++}	O^-	e^-
1	.8500	.1500	0	0	0	0	0	0	0	0	0	0	0	0	0	0	0	0	0
1.5	.8468	.1500	.0017	.0032	0			0											
2	.7235	.1491	.0599	.1265	.0019		0	.0053											
3	.0098	.1461	.0267	.8402	.0076	0	.0002	.7792											
4	0	.1355	.0002	.8499	.0015	.0003	.0280	.8482	0										0
5		.0264	0	.6965	.0003	.1525	.2469	1.0032	.0010	0	0								.0011
6		.0006		.0505	0	.7703	.2988	1.6490	.0292	.0001	.0005								.0298
7		0		.0018		.6879	.2989	1.6925	.1604	.0010	.0058								.1672
8				.0001		.3879	.2898	1.6523	.4620	.0102	.0476								.5199
9				0		.1317	.2356	1.4206	.7183	.0644	.2794								1.0620
10						.0395	.1175	.8389	.8107	.1825	.8611								1.8542
11						.0118	.0354	.3000	.8382	.2646	1.3999				0				2.5027
12						.0038	.0095	.0871	.8460	.2906	1.6129				.0002				2.7498
13						.0013	.0028	.0268	.8474	.2972	1.6735				.0013	0			2.8206
14						.0006	.0010	.0093	.8427	.2995	1.6951				.0073	.0001	0		2.8513
15						.0003	.0004	.0037	.8174	.2989	1.6963				.0325	.0007	.0002		2.8789
16						.0001	.0002	.0016	.7382	.2964	1.6978				.1117	.0034	.0011		2.9637
17						.0001	.0001	.0008	.5706	.2869	1.6936				.2793	.0130	.0057		3.1471
18						0	0	.0004	.3554	.2600	1.6765				.4946	.0399	.0231		3.4072
19								.0002	.1858	.2054	1.6201				.6642	.0946	.0797		3.6882
20								.0001	.0904	.1339	1.4723				.7596	.1661	.2276		4.0032
21								.0001	.0441	.0742	1.1848				.8059	.2258	.5152		4.3968
22								0	.0222	.0380	.8034				.8278	.2620	.8966		4.8363
23									.0116	.0190	.4637				.8384	.2810	1.2363		5.2057
24									.0063	.0097	.2429				.8438	.2903	1.4572		5.4412

Table 8C

MOLAR COMPOSITION n_i (PRESSURE = 10^{-4} ATM)

	Constituent																		
T(°K×10⁻³)	CO_2	N_2	O_2	CO	NO	C	N	O	C^+	N^+	O^+	O_2^+	CO^+	NO^+	C^{++}	N^{++}	O^{++}	O^-	e^-
1	.8500	.1500	0	0	0	0	0	0	0	0	0	0	0	0	0	0	0	0	0
1.5	.8469	.1500	.0037	.0067	.0001			0											
2	.5996	.1488	.1122	.2504	.0026		0	.0024											
3	.0011	.1483	.0031	.8490	.0026	0	.0007	.8461						0					
4	0	.1098	0	.8478	.0004	.0025	.0804	.8522	0		0			.0001					0
5		.0003		.2929	0	.5504	.2937	1.4070	.0068	0	.0001			0					.0069
6		.0001		.0049		.7522	.2997	1.6935	.0930	.0002	.0016								.0948
7		0		.0001		.4338	.2957	1.6764	.4161	.0043	.0235								.4439
8				0		.1077	.2491	1.4571	.7423	.0510	.2429								1.0361
9						.0229	.1068	.7385	.8271	.1932	.9615								1.9817
10						.0050	.0219	.1807	.8450	.2781	1.5193				0				2.6425
11						.0013	.0042	.0378	.8486	.2958	1.6622				.0002				2.8069
12						.0004	.0010	.0093	.8479	.2990	1.6916				.0017	0			2.8419
13						.0001	.0003	.0027	.8372	.2996	1.6980				.0126	.0002	0		2.8604
14						.0001	.0001	.0009	.7830	.2990	1.6990				.0670	.0012	.0002		2.9172
15						0	0	.0004	.6144	.2936	1.6978				.2356	.0067	.0018		3.0933
16								.0002	.3513	.2709	1.6891				.4987	.0291	.0107		3.3883
17								.0001	.1530	.2110	1.6486				.6970	.0890	.0513		3.6872
18								0	.0609	.1234	1.5063				.7891	.1766	.1936		4.0093
19									.0249	.0570	1.1683				.8251	.2430	.5316		4.4496
20									.0109	.0242	.7021				.8392	.2758	.9979		4.9629
21									.0050	.0102	.3370				.8450	.2898	1.3630		5.3477
22									.0023	.0045	.1462				.8476	.2955	1.5538		5.5469
23									.0012	.0021	.0631				.8488	.2979	1.6369		5.6336
24									.0006	.0010	.0283				.8494	.2990	1.6717		5.6701

Table 8H

COMPOSITION FOR ATMOSPHERE OF 0.3 PER CENT H_2O, 84.7 PER CENT CO_2, AND 15 PER CENT N_2

Pressure (atm)	Constituent CO_2	H_2O	N_2	O_2	H_2	CO	NO	OH	C	N	O	H	C^+	N^+	O^+	H^+	O_2^+	CO^+	NO^+	H_2^+	OH^+	C^{++}	N^{++}	O^{++}	O^-	H^-	OH^-	e^-
T = 5000°K																												
10^{-4}	0	0	0.0031	0	0	0.2915	0	0	0.5487	0.2938	1.4054	0.0060	0.0068	0	0.0001	0	0	0	0	0	0	0	0	0	0	0	0	0.0068
10^{-3}			0.0236	0		0.6938	0.0003		0.1522	0.2470	1.0028	0.0060	0.0010		0				0.0001									0.0011
10^{-2}	0		0.0832	0.0001		0.8280	0.0013		0.0191	0.1323	0.8673	0.0060	0.0001						0.0001									0.0002
10^{-1}	0.0002		0.1225	0.0008		0.8449	0.0050	0	0.0019	0.0500	0.8450	0.0060	0						0.0001									0.0001
10^{0}	0.0022		0.1338	0.0075		0.8446	0.0161	0.0001	0.0002	0.0164	0.8168	0.0059							0.0001									0.0001
10^{1}	0.0188		0.1265	0.0544		0.8282	0.0421	0.0009	0	0.0049	0.6794	0.0051							0									0
10^{2}	0.0992	0	0.1145	0.1639	0	0.7478	0.0695	0.0030	0	0.0014	0.3501	0.0029	0	0	0	0	0	0	0	0	0	0	0	0	0	0	0	0
T = 12000°K																												
10^{-4}	0	0	0	0	0	0	0	0	0.0004	0.0010	0.0093	0																
10^{-3}									0.0038	0.0095	0.0869	0.0003	0.8449	0.2990	1.6877	0.0060	0	0	0	0	0	0.0017	0	0	0	0	0	2.8410
10^{-2}									0.0325	0.0671	0.5495	0.0018	0.8430	0.2906	1.6101	0.0057						0.0002						2.7497
10^{-1}					0	0			0.1788	0.1977	1.2939	0.0044	0.8145	0.2329	1.1475	0.0042						0						2.1191
10^{0}			0	0	0.0002	0.0003	0		0.4852	0.2719	1.5973	0.0052	0.6682	0.1023	0.4031	0.0015		0							0			1.1751
10^{1}			0.0002	0.0001	0.0012	0.0053	0.0002		0.7055	0.2915	1.6638	0.0036	0.3614	0.0280	0.0992	0.0004		0.0001	0						0.0001			0.4890
10^{2}	0	0	0.0018	0.0013	0.0022	0.0579	0.0024	0	0.7452	0.2914	1.6241	0.0015	0.1359	0.0078	0.0267	0.0001		0.0003	0.0001						0.0002			0.1707
													0.0429	0.0023	0.0078	0	0	0.0010	0.0003	0	0	0	0	0	0.0007	0	0	0.0537

Table 8I

THERMODYNAMIC PROPERTIES FOR ATMOSPHERE WITH 0.3 PER CENT WATER VAPOR

Pressure (atm)	Property				
	M	ρ/ρ_o	E/RT_o	H/RT_o	S/R
			T = 5000°K		
10^{-4}	16.211	2.1323^{-6}	459.25	506.15	96.563
10^{-3}	19.494	2.5642^{-5}	257.77	296.76	79.747
10^{-2}	21.438	2.8198^{-4}	170.54	206.00	70.147
10^{-1}	22.135	2.9115^{-3}	145.09	179.44	64.317
10^{0}	22.529	2.9634^{-2}	134.78	168.52	59.437
10^{1}	23.594	3.1035^{-1}	117.16	149.39	54.222
10^{2}	26.752	3.5189	74.32	102.74	47.842
			T = 12000°K		
10^{-4}	7.2981	3.9999^{-7}	2489.4	2739.4	172.87
10^{-3}	7.4171	4.0651^{-6}	2429.4	2675.4	158.38
10^{-2}	8.2261	4.5084^{-5}	2072.7	2294.5	137.31
10^{-1}	10.319	5.6554^{-4}	1420.0	1596.8	110.99
10^{0}	12.442	6.8188^{-3}	1006.8	1153.5	92.503
10^{1}	13.784	7.5544^{-2}	822.47	954.85	80.722
10^{2}	14.642	8.0246^{-1}	731.09	855.70	71.731

Table 9

MOLECULAR WEIGHT M

$T(^{o}K \times 10^{-3})$	Pressure (atm) 10^2	30	10	3	1	3×10^{-1}	10^{-1}	3×10^{-2}	10^{-2}	3×10^{-3}	10^{-3}	3×10^{-4}	10^{-4}
1	41.612		41.612		41.612		41.612		41.612		41.612		41.612
1.5	41.611		41.609		41.605		41.597		41.581		41.545		41.547
2	41.550		41.480		41.331		41.020		40.363		39.050		36.599
3	39.381		37.285		33.945		29.595		25.241		22.993		22.519
4	32.580		28.300		24.459		22.823		22.491		22.337		21.989
5	26.827		23.670		22.607		22.212		21.513		19.556		16.250
6	23.920		22.550		21.757		19.863		16.441		14.711		14.154
7	22.741		21.420		18.613		15.466		14.428		13.800		12.633
8	21.551	20.205	18.487	16.567	15.364	14.691	14.360	14.039	13.651	13.051	12.349	11.507	10.708
9	19.256	17.202	15.735	14.849	14.439	14.100	13.725	13.142	12.432	11.527	10.637	9.5687	8.6123
10	16.761	15.351	14.689	14.279	13.938	13.435	12.792	11.894	10.961	9.8544	8.8456	7.9953	7.5762
11	15.314	14.606	14.224	13.812	13.298	12.515	11.614	10.496	9.4263	8.3884	7.7740	7.4611	7.3560
12	14.659	14.202	13.803	13.212	12.462	11.417	10.335	9.1380	8.2405	7.6594	7.4309	7.3399	7.3107
13	14.278	13.822	13.285	12.459	11.483	10.256	9.1383	8.1641	7.6542	7.4161	7.3382	7.3039	7.2871
14	13.942	13.375	12.650	11.592	10.452	9.1908	8.2611	7.6658	7.4324	7.3381	7.2987	7.2737	7.2153
15	13.579	12.841	11.920	10.678	9.4850	8.3839	7.7626	7.4544	7.3492	7.2946	7.2636	7.1752	7.0014
16	13.158	12.231	11.136	9.8005	8.6961	7.8811	7.5199	7.3646	7.3069	7.2532	7.1575	6.9446	6.6704
17	12.678	11.567	10.353	9.0419	8.1407	7.6058	7.4043	7.3150	7.2566	7.1427	6.9387	6.6315	6.3655
18	12.151	10.885	9.6272	8.4553	7.7926	7.4607	7.3405	7.2628	7.1588	6.9377	6.6502	6.3381	6.0665
19	11.592	10.222	9.0066	8.0437	7.5870	7.3781	7.2870	7.1749	6.9847	6.6697	6.3645	6.0377	5.7006
20	11.024	9.6145	8.5148	7.7730	7.4644	7.3175	7.2145	7.0260	6.7466	6.3932	6.0719	5.6864	5.3261
21	10.469	9.0886	8.1492	7.5990	7.3833	7.2517	7.0999	6.8173	6.4846	6.1089	5.7421	5.3382	5.0760
22	9.9487	8.6569	7.8886	7.4837	7.3157	7.1598	6.9334	6.5748	6.2141	5.7986	5.4138	5.0994	4.9556
23	9.4811	8.3177	7.7056	7.3987	7.2411	7.0276	6.7237	6.3178	5.9267	5.4877	5.1655	4.9744	4.9050
24	9.0729	8.0579	7.5743	7.3237	7.1449	6.8554	6.4909	6.0497	5.6328	5.2361	5.0188	4.9176	4.8840

Table 8I

THERMODYNAMIC PROPERTIES FOR ATMOSPHERE WITH 0.3 PER CENT WATER VAPOR

Pressure (atm)	Property M	ρ/ρ_o	E/RT_o	H/RT_o	S/R
		$T = 5000^oK$			
10^{-4}	16.211	2.1323^{-6}	459.25	506.15	96.563
10^{-3}	19.494	2.5642^{-5}	257.77	296.76	79.747
10^{-2}	21.438	2.8198^{-4}	170.54	206.00	70.147
10^{-1}	22.135	2.9115^{-3}	145.09	179.44	64.317
10^{0}	22.529	2.9634^{-2}	134.78	168.52	59.437
10^{1}	23.594	3.1035^{-1}	117.16	149.39	54.222
10^{2}	26.752	3.5189	74.32	102.74	47.842
		$T = 12000^oK$			
10^{-4}	7.2981	3.9999^{-7}	2489.4	2739.4	172.87
10^{-3}	7.4171	4.0651^{-6}	2429.4	2675.4	158.38
10^{-2}	8.2261	4.5084^{-5}	2072.7	2294.5	137.31
10^{-1}	10.319	5.6554^{-4}	1420.0	1596.8	110.99
10^{0}	12.442	6.8188^{-3}	1006.8	1153.5	92.503
10^{1}	13.784	7.5544^{-2}	822.47	954.85	80.722
10^{2}	14.642	8.0246^{-1}	731.09	855.70	71.731

Table 9

MOLECULAR WEIGHT M

	Pressure (atm)												
T(^{o}K x 10^{-3})	10^2	30	10	3	1	$3x10^{-1}$	10^{-1}	$3x10^{-2}$	10^{-2}	$3x10^{-3}$	10^{-3}	$3x10^{-4}$	10^{-4}
1	41.612		41.612		41.612		41.612		41.612		41.612		41.612
1.5	41.611		41.609		41.605		41.597		41.581		41.545		41.547
2	41.550		41.480		41.331		41.020		40.363		39.050		36.599
3	39.381		37.285		33.945		29.595		25.241		22.993		22.519
4	32.580		28.300		24.459		22.823		22.491		22.337		21.989
5	26.827		23.670		22.607		22.212		21.513		19.556		16.250
6	23.920		22.550		21.757		19.863		16.441		14.711		14.154
7	22.741		21.420		18.613		15.466		14.428		13.800		12.633
8	21.551	20.205	18.487	16.567	15.364	14.691	14.360	14.039	13.651	13.051	12.349	11.507	10.708
9	19.256	17.202	15.735	14.849	14.439	14.100	13.725	13.142	12.432	11.527	10.637	9.5687	8.6123
10	16.761	15.351	14.689	14.279	13.938	13.435	12.792	11.894	10.961	9.8544	8.8456	7.9953	7.5762
11	15.314	14.606	14.224	13.812	13.298	12.515	11.614	10.496	9.4263	8.3884	7.7740	7.4611	7.3560
12	14.659	14.202	13.803	13.212	12.462	11.417	10.335	9.1380	8.2405	7.6594	7.4309	7.3399	7.3107
13	14.278	13.822	13.285	12.459	11.483	10.256	9.1383	8.1641	7.6542	7.4161	7.3382	7.3039	7.2871
14	13.942	13.375	12.650	11.592	10.452	9.1908	8.2611	7.6658	7.4324	7.3381	7.2987	7.2737	7.2153
15	13.579	12.841	11.920	10.678	9.4850	8.3839	7.7626	7.4544	7.3492	7.2946	7.2636	7.1752	7.0014
16	13.158	12.231	11.136	9.8005	8.6961	7.8811	7.5199	7.3646	7.3069	7.2532	7.1575	6.9446	6.6704
17	12.678	11.567	10.353	9.0419	8.1407	7.6058	7.4043	7.3150	7.2566	7.1427	6.9387	6.6315	6.3655
18	12.151	10.885	9.6272	8.4553	7.7926	7.4607	7.3405	7.2628	7.1588	6.9377	6.6502	6.3381	6.0665
19	11.592	10.222	9.0066	8.0437	7.5870	7.3781	7.2870	7.1749	6.9847	6.6697	6.3645	6.0377	5.7006
20	11.024	9.6145	8.5148	7.7730	7.4644	7.3175	7.2145	7.0260	6.7466	6.3932	6.0719	5.6864	5.3261
21	10.469	9.0886	8.1492	7.5990	7.3833	7.2517	7.0999	6.8173	6.4846	6.1089	5.7421	5.3382	5.0760
22	9.9487	8.6569	7.8886	7.4837	7.3157	7.1598	6.9334	6.5748	6.2141	5.7986	5.4138	5.0994	4.9556
23	9.4811	8.3177	7.7056	7.3987	7.2411	7.0276	6.7237	6.3178	5.9267	5.4877	5.1655	4.9744	4.9050
24	9.0729	8.0579	7.5743	7.3237	7.1449	6.8554	6.4909	6.0497	5.6328	5.2361	5.0188	4.9176	4.8840

Table 10

DENSITY ρ/ρ_o

Pressure (atm)

$T(^{\circ}K \times 10^{-3})$	10^2	3×10	10	3	1	3×10^{-1}	10^{-1}	3×10^{-2}	10^{-2}	3×10^{-3}	10^{-3}	3×10^{-4}	10^{-4}
1	2.7316^{+1}		2.7316		2.7316^{-1}		2.7316^{-2}		2.7316^{-3}		2.7316^{-4}		2.7316^{-5}
1.5	1.8210^{+1}		1.8209		1.8208^{-1}		1.8204^{-2}		1.8197^{-3}		1.8181^{-4}		1.8182^{-5}
2	1.3638^{+1}		1.3615		1.3566^{-1}		1.3464^{-2}		1.3248^{-3}		1.2817^{-4}		1.2012^{-5}
3	8.6172		8.1586^{-1}		7.4278^{-2}		6.4759^{-3}		5.5231^{-4}		5.0311^{-5}		4.9275^{-6}
4	5.3467		4.6444^{-1}		4.0140^{-2}		3.7454^{-3}		3.6910^{-4}		3.6658^{-5}		3.6087^{-6}
5	3.5221		3.1077^{-1}		2.9681^{-2}		2.9162^{-3}		2.8244^{-4}		2.5674^{-5}		2.1334^{-6}
6	2.6170		2.4671^{-1}		2.3804^{-2}		2.1731^{-3}		1.7988^{-4}		1.6905^{-5}		1.5486^{-6}
7	2.1326		2.0087^{-1}		1.7455^{-2}		1.4503^{-3}		1.3530^{-4}		1.2941^{-5}		1.1847^{-6}
8	1.7684	4.9735^{-1}	1.5169^{-1}	4.0781^{-2}	1.2607^{-2}	3.6165^{-3}	1.1783^{-3}	3.4560^{-4}	1.1202^{-4}	3.2125^{-5}	1.0133^{-5}	2.8326^{-6}	8.7864^{-7}
9	1.4040	3.7639^{-1}	1.1477^{-1}	3.2492^{-2}	1.0532^{-2}	3.0854^{-3}	1.0011^{-3}	2.8754^{-4}	9.0676^{-5}	2.5224^{-5}	7.7584^{-6}	2.0938^{-6}	6.2816^{-7}
10	1.1003	3.0232^{-1}	9.6428^{-2}	2.8121^{-2}	9.1494^{-3}	2.6458^{-3}	8.3975^{-4}	2.3423^{-4}	7.1955^{-5}	1.9407^{-5}	5.8067^{-6}	1.5745^{-6}	4.9734^{-7}
11	9.1381^{-1}	2.6149^{-1}	8.4894^{-2}	2.4727^{-2}	7.9361^{-3}	2.2406^{-3}	6.9309^{-4}	1.8791^{-4}	5.6253^{-5}	1.5018^{-5}	4.6393^{-6}	1.3358^{-6}	4.3898^{-7}
12	8.0185^{-1}	2.3337^{-1}	7.5508^{-2}	2.1683^{-2}	6.8169^{-3}	1.8736^{-3}	5.6537^{-4}	1.4996^{-4}	4.5079^{-5}	1.2570^{-5}	4.0650^{-6}	1.2046^{-6}	3.9998^{-7}
13	7.2172^{-1}	2.0938^{-1}	6.7084^{-2}	1.8874^{-2}	5.7982^{-3}	1.5537^{-3}	4.6144^{-4}	1.2368^{-4}	3.8650^{-5}	1.1234^{-5}	3.7057^{-6}	1.1064^{-6}	3.6801^{-7}
14	6.5388^{-1}	1.8814^{-1}	5.9315^{-2}	1.6306^{-2}	4.9011^{-3}	1.2928^{-3}	3.8735^{-4}	1.0783^{-4}	3.4850^{-5}	1.0322^{-5}	3.4251^{-6}	1.0232^{-6}	3.3831^{-7}
15	5.9426^{-1}	1.6839^{-1}	5.2166^{-2}	1.4019^{-2}	4.1509^{-3}	1.1007^{-3}	3.3971^{-4}	9.7868^{-5}	3.2164^{-5}	9.5770^{-6}	3.1786^{-6}	9.4202^{-7}	3.0639^{-7}
16	5.3983^{-1}	1.5034^{-1}	4.5690^{-2}	1.2063^{-2}	3.5678^{-3}	9.7003^{-4}	3.0853^{-4}	9.0646^{-5}	2.9979^{-5}	8.9275^{-6}	2.9363^{-6}	8.5477^{-7}	2.7367^{-7}
17	4.8956^{-1}	1.3400^{-1}	3.9977^{-2}	1.0474^{-2}	3.1435^{-3}	8.8108^{-4}	2.8591^{-4}	8.4739^{-5}	2.8021^{-5}	8.2743^{-6}	2.6793^{-6}	7.6821^{-7}	2.4580^{-7}
18	4.4312^{-1}	1.1909^{-1}	3.5110^{-2}	9.2507^{-3}	2.8419^{-3}	8.1626^{-4}	2.6770^{-4}	7.9461^{-5}	2.6107^{-5}	7.5903^{-6}	2.4253^{-6}	6.9343^{-7}	2.2124^{-7}
19	4.0049^{-1}	1.0595^{-1}	3.1118^{-2}	8.3372^{-3}	2.6213^{-3}	7.6473^{-4}	2.5176^{-4}	7.4367^{-5}	2.4132^{-5}	6.9130^{-6}	2.1989^{-6}	6.2580^{-7}	1.9695^{-7}
20	3.6182^{-1}	9.4671^{-2}	2.7948^{-2}	7.6538^{-3}	2.4500^{-3}	7.2053^{-4}	2.3680^{-4}	6.9183^{-5}	2.2144^{-5}	6.2951^{-6}	1.9929^{-6}	5.5974^{-7}	1.7481^{-7}
21	3.2724^{-1}	8.5231^{-2}	2.5474^{-2}	7.1262^{-3}	2.3080^{-3}	6.8005^{-4}	2.2194^{-4}	6.3931^{-5}	2.0270^{-5}	5.7288^{-6}	1.7950^{-6}	5.0060^{-7}	1.5867^{-7}
22	2.9685^{-1}	7.7492^{-2}	2.3538^{-2}	6.6990^{-3}	2.1829^{-3}	6.4091^{-4}	2.0688^{-4}	5.8854^{-5}	1.8542^{-5}	5.1907^{-6}	1.6154^{-6}	4.5647^{-7}	1.4787^{-7}
23	2.7060^{-1}	7.1219^{-2}	2.1993^{-2}	6.3350^{-3}	2.0667^{-3}	6.0173^{-4}	1.9190^{-4}	5.4095^{-5}	1.6916^{-5}	4.6988^{-6}	1.4743^{-6}	4.2592^{-7}	1.3999^{-7}
24	2.4816^{-1}	6.6120^{-2}	2.0717^{-2}	6.0095^{-3}	1.9543^{-3}	5.6252^{-4}	1.7754^{-4}	4.9641^{-5}	1.5407^{-5}	4.2965^{-6}	1.3727^{-6}	4.0345^{-7}	1.3359^{-7}

Below 1000°K this relation is given by $\rho/\rho_o = 273.16 \left(\frac{p}{T}\right)$ (p in atm, T in °K)

Table 11
INTERNAL ENERGY E/RT_0

$T(^{\circ}K \times 10^{-3})$	Pressure (atm) 10^2	30	10	3	1	3×10^{-1}	10^{-1}	3×10^{-2}	10^{-2}	3×10^{-3}	10^{-3}	3×10^{-4}	10^{-4}
.15	-145.76	Liquefaction of CO_2			-145.76	-145.76	-145.76	-145.76	-145.76	-145.76	-145.76	-145.76	-145.76
.2	-145.26			-145.26	-145.26	-145.26	-145.26	-145.26	-145.26	-145.26	-145.26	-145.26	-145.26
.235	-144.88		-144.88	-144.88	-144.88	-144.88	-144.88	-144.88	-144.88	-144.88	-144.88	-144.88	-144.88
.25	-144.72		-144.72	-144.72	-144.72	-144.72	-144.72	-144.72	-144.72	-144.72	-144.72	-144.72	-144.72
.3	-144.13	-144.13	-144.13	-144.13	-144.13	-144.13	-144.13	-144.13	-144.13	-144.13	-144.13	-144.13	-144.13
.4	-142.83	-142.83	-142.83	-142.83	-142.83	-142.83	-142.83	-142.83	-142.83	-142.83	-142.83	-142.83	-142.83
.5	-141.40	-141.40	-141.40	-141.40	-141.40	-141.40	-141.40	-141.40	-141.40	-141.40	-141.40	-141.40	-141.40
.6	-139.84	-139.84	-139.84	-139.84	-139.84	-139.84	-139.84	-139.84	-139.84	-139.84	-139.84	-139.84	-139.84
.7	-138.19	-138.19	-138.19	-138.19	-138.19	-138.19	-138.19	-138.19	-138.19	-138.19	-138.19	-138.19	-138.19
.8	-136.46	-136.46	-136.46	-136.46	-136.46	-136.46	-136.46	-136.46	-136.46	-136.46	-136.46	-136.46	-136.46
1.0	-132.80	-132.80	-132.80	-132.80	-132.80	-132.80	-132.80	-132.80	-132.80	-132.80	-132.80	-132.80	-132.80
1.5	-122.91		-122.90		-122.88		-122.83		-122.73		-122.53		-122.54
2	-112.08		-111.68		-110.81		-108.99		-105.06		-96.848		-80.071
3	-77.328		-63.624		-38.568		1.8227		54.976		89.722		97.824
4	-5.6133		36.361		85.414		110.88		116.85		121.29		133.34
5	73.880		116.57		134.08		144.38		169.77		257.21		459.32
6	132.77		156.09		180.10		261.23		463.70		603.88		658.74
7	173.92		213.76		345.64		557.58		649.94		716.98		862.14
8	231.56	286.47	373.14	493.74	585.62	644.38	676.49	710.52	754.63	828.81	925.99	1062.2	1219.5
9	354.66	471.77	576.10	650.20	688.81	724.38	767.16	839.36	937.93	1085.4	1263.4	1531.9	1834.3
10	523.19	628.04	685.59	726.00	763.67	824.21	909.87	1048.2	1222.4	1483.3	1785.8	2103.0	2286.0
11	653.03	714.83	753.22	800.15	864.41	974.61	1123.8	1353.4	1634.2	1981.7	2232.9	2377.1	2428.4
12	732.10	777.66	823.53	899.19	1008.0	1188.1	1421.3	1754.7	2073.6	2321.5	2429.9	2475.2	2490.4
13	792.52	844.30	913.34	1034.0	1203.4	1471.0	1787.5	2140.0	2361.9	2476.4	2515.8	2534.7	2547.2
14	853.92	925.88	1030.4	1211.0	1454.0	1804.2	2137.1	2395.0	2508.0	2556.4	2578.8	2599.7	2650.5
15	924.58	1028.1	1179.5	1432.1	1746.7	2125.0	2389.0	2537.2	2591.6	2623.5	2650.0	2728.4	2891.6
16	1009.6	1154.6	1362.6	1689.0	2043.5	2374.0	2544.8	2624.8	2659.0	2701.1	2787.1	2991.2	3277.4
17	1111.7	1307.2	1576.4	1958.7	2299.5	2542.8	2645.2	2696.7	2741.3	2844.2	3042.4	3370.0	3693.8
18	1232.4	1484.8	1810.3	2210.1	2493.8	2657.0	2723.7	2779.5	2872.6	3088.9	3398.4	3785.2	4189.4
19	1372.0	1682.5	2046.6	2420.4	2633.9	2744.4	2804.3	2901.3	3086.6	3425.9	3804.5	4293.6	4901.7
20	1529.2	1891.6	2266.5	2584.7	2739.3	2826.5	2909.3	3090.2	3387.7	3820.5	4294.7	4989.1	5748.1
21	1700.5	2100.1	2457.0	2711.8	2828.6	2921.9	3061.8	3357.1	3753.8	4292.0	4934.2	5776.6	6403.4
22	1880.4	2296.5	2614.9	2815.2	2917.8	3049.3	3278.2	3691.5	4185.5	4884.3	5664.2	6401.3	6771.4
23	2062.1	2472.9	2744.9	2908.7	3022.2	3225.7	3561.2	4088.0	4709.4	5560.3	6294.6	6778.8	6964.3
24	2239.6	2626.8	2855.5	3004.5	3155.4	3458.2	3902.8	4556.4	5317.2	6181.9	6719.7	6989.7	7078.8

Table 10

DENSITY ρ/ρ_0

$T(°K \times 10^{-3})$	Pressure (atm) 10^2	3×10	10	3	1	3×10^{-1}	10^{-1}	3×10^{-2}	10^{-2}	3×10^{-3}	10^{-3}	3×10^{-4}	10^{-4}
1	2.7316^{+1}		2.7316		2.7316^{-1}		2.7316^{-2}		2.7316^{-3}		2.7316^{-4}		2.7316^{-5}
1.5	1.8210^{+1}		1.8209		1.8208^{-1}		1.8204^{-2}		1.8197^{-3}		1.8181^{-4}		1.8182^{-5}
2	1.3638^{+1}		1.3615		1.3566^{-1}		1.3464^{-2}		1.3248^{-3}		1.2817^{-4}		1.2012^{-5}
3	8.6172		8.1586^{-1}		7.4278^{-2}		6.4759^{-3}		5.5231^{-4}		5.0311^{-5}		4.9275^{-6}
4	5.3467		4.6444^{-1}		4.0140^{-2}		3.7454^{-3}		3.6910^{-4}		3.6658^{-5}		3.6087^{-6}
5	3.5221		3.1077^{-1}		2.9681^{-2}		2.9162^{-3}		2.8244^{-4}		2.5674^{-5}		2.1334^{-6}
6	2.6170		2.4671^{-1}		2.3804^{-2}		2.1731^{-3}		1.7988^{-4}		1.6905^{-5}		1.5486^{-6}
7	2.1326		2.0087^{-1}		1.7455^{-2}		1.4503^{-3}		1.3530^{-4}		1.2941^{-5}		1.1847^{-6}
8	1.7684	4.9735^{-1}	1.5169^{-1}	4.0781^{-2}	1.2607^{-2}	3.6165^{-3}	1.1783^{-3}	3.4560^{-4}	1.1202^{-4}	3.2125^{-5}	1.0133^{-5}	2.8326^{-6}	8.7864^{-7}
9	1.4040	3.7639^{-1}	1.1477^{-1}	3.2492^{-2}	1.0532^{-2}	3.0854^{-3}	1.0011^{-3}	2.8754^{-4}	9.0676^{-5}	2.5224^{-5}	7.7584^{-6}	2.0938^{-6}	6.2816^{-7}
10	1.1003	3.0232^{-1}	9.6428^{-2}	2.8121^{-2}	9.1494^{-3}	2.6458^{-3}	8.3975^{-4}	2.3423^{-4}	7.1955^{-5}	1.9407^{-5}	5.8067^{-6}	1.5745^{-6}	4.9734^{-7}
11	9.1381^{-1}	2.6149^{-1}	8.4894^{-2}	2.4727^{-2}	7.9361^{-3}	2.2406^{-3}	6.9309^{-4}	1.8791^{-4}	5.6253^{-5}	1.5018^{-5}	4.6393^{-6}	1.3358^{-6}	4.3898^{-7}
12	8.0185^{-1}	2.3337^{-1}	7.3508^{-2}	2.1683^{-2}	6.8169^{-3}	1.8736^{-3}	5.6537^{-4}	1.4996^{-4}	4.5079^{-5}	1.2570^{-5}	4.0650^{-6}	1.2046^{-6}	3.9998^{-7}
13	7.2172^{-1}	2.0938^{-1}	6.7084^{-2}	1.8874^{-2}	5.7982^{-3}	1.5537^{-3}	4.6144^{-4}	1.2368^{-4}	3.8650^{-5}	1.1234^{-5}	3.7057^{-6}	1.1064^{-6}	3.6801^{-7}
14	6.5388^{-1}	1.8814^{-1}	5.9315^{-2}	1.6306^{-2}	4.9011^{-3}	1.2928^{-3}	3.8735^{-4}	1.0783^{-4}	3.4850^{-5}	1.0322^{-5}	3.4251^{-6}	1.0232^{-6}	3.3831^{-7}
15	5.9426^{-1}	1.6839^{-1}	5.2166^{-2}	1.4019^{-2}	4.1509^{-3}	1.1007^{-3}	3.3971^{-4}	9.7868^{-5}	3.2164^{-5}	9.5770^{-6}	3.1786^{-6}	9.4202^{-7}	3.0639^{-7}
16	5.3983^{-1}	1.5034^{-1}	4.5690^{-2}	1.2063^{-2}	3.5678^{-3}	9.7003^{-4}	3.0853^{-4}	9.0646^{-5}	2.9979^{-5}	8.9275^{-6}	2.9363^{-6}	8.5477^{-7}	2.7367^{-7}
17	4.8956^{-1}	1.3400^{-1}	3.9977^{-2}	1.0474^{-2}	3.1435^{-3}	8.8108^{-4}	2.8591^{-4}	8.4739^{-5}	2.8021^{-5}	8.2743^{-6}	2.6793^{-6}	7.6821^{-7}	2.4580^{-7}
18	4.4312^{-1}	1.1909^{-1}	3.5110^{-2}	9.2507^{-3}	2.8419^{-3}	8.1626^{-4}	2.6770^{-4}	7.9461^{-5}	2.6107^{-5}	7.5903^{-6}	2.4253^{-6}	6.9343^{-7}	2.2124^{-7}
19	4.0049^{-1}	1.0595^{-1}	3.1118^{-2}	8.3372^{-3}	2.6213^{-3}	7.6473^{-4}	2.5176^{-4}	7.4367^{-5}	2.4132^{-5}	6.9130^{-6}	2.1989^{-6}	6.2580^{-7}	1.9695^{-7}
20	3.6182^{-1}	9.4671^{-2}	2.7948^{-2}	7.6538^{-3}	2.4500^{-3}	7.2053^{-4}	2.3680^{-4}	6.9183^{-5}	2.2144^{-5}	6.2951^{-6}	1.9929^{-6}	5.5974^{-7}	1.7481^{-7}
21	3.2724^{-1}	8.5251^{-2}	2.5474^{-2}	7.1262^{-3}	2.3080^{-3}	6.8005^{-4}	2.2194^{-4}	6.3931^{-5}	2.0270^{-5}	5.7288^{-6}	1.7950^{-6}	5.0060^{-7}	1.5867^{-7}
22	2.9685^{-1}	7.7492^{-2}	2.3538^{-2}	6.6990^{-3}	2.1829^{-3}	6.4091^{-4}	2.0688^{-4}	5.8854^{-5}	1.8542^{-5}	5.1907^{-6}	1.6154^{-6}	4.5647^{-7}	1.4787^{-7}
23	2.7060^{-1}	7.1219^{-2}	2.1993^{-2}	6.3350^{-3}	2.0667^{-3}	6.0173^{-4}	1.9190^{-4}	5.4095^{-5}	1.6916^{-5}	4.6988^{-6}	1.4743^{-6}	4.2592^{-7}	1.3999^{-7}
24	2.4816^{-1}	6.6120^{-2}	2.0717^{-2}	6.0095^{-3}	1.9543^{-3}	5.6252^{-4}	1.7754^{-4}	4.9641^{-5}	1.5407^{-5}	4.2965^{-6}	1.3727^{-6}	4.0345^{-7}	1.3359^{-7}

Below 1000°K this relation is given by $\rho/\rho_0 = 273.16\left(\frac{p}{T}\right)$ (p in atm, T in °K)

Table 11
INTERNAL ENERGY E/RT_0

$T(^\circ K \times 10^{-3})$	Pressure (atm) 10^2	30	10	3	1	3×10^{-1}	10^{-1}	3×10^{-2}	10^{-2}	3×10^{-3}	10^{-3}	3×10^{-4}	10^{-4}
.15	-145.76	Liquefaction of CO_2			-145.76	-145.76	-145.76	-145.76	-145.76	-145.76	-145.76	-145.76	-145.76
.2	-145.26			-145.26	-145.26	-145.26	-145.26	-145.26	-145.26	-145.26	-145.26	-145.26	-145.26
.235	-144.88		-144.88	-144.88	-144.88	-144.88	-144.88	-144.88	-144.88	-144.88	-144.88	-144.88	-144.88
.25	-144.72		-144.72	-144.72	-144.72	-144.72	-144.72	-144.72	-144.72	-144.72	-144.72	-144.72	-144.72
.3	-144.13	-144.13	-144.13	-144.13	-144.13	-144.13	-144.13	-144.13	-144.13	-144.13	-144.13	-144.13	-144.13
.4	-142.83	-142.83	-142.83	-142.83	-142.83	-142.83	-142.83	-142.83	-142.83	-142.83	-142.83	-142.83	-142.83
.5	-141.40	-141.40	-141.40	-141.40	-141.40	-141.40	-141.40	-141.40	-141.40	-141.40	-141.40	-141.40	-141.40
.6	-139.84	-139.84	-139.84	-139.84	-139.84	-139.84	-139.84	-139.84	-139.84	-139.84	-139.84	-139.84	-139.84
.7	-138.19	-138.19	-138.19	-138.19	-138.19	-138.19	-138.19	-138.19	-138.19	-138.19	-138.19	-138.19	-138.19
.8	-136.46	-136.46	-136.46	-136.46	-136.46	-136.46	-136.46	-136.46	-136.46	-136.46	-136.46	-136.46	-136.46
1.0	-132.80	-132.80	-132.80	-132.80	-132.80	-132.80	-132.80	-132.80	-132.80	-132.80	-132.80	-132.80	-132.80
1.5	-122.91		-122.90		-122.88		-122.83		-122.73		-122.53		-122.54
2	-112.08		-111.68		-110.81		-108.99		-105.06		-96.848		-80.071
3	-77.328		-63.624		-38.568		1.8227		54.976		89.722		97.824
4	-5.6133		36.361		85.414		110.88		116.85		121.29		133.34
5	73.880		116.57		134.08		144.38		169.77		257.21		459.32
6	132.77		156.09		180.10		261.23		463.70		603.88		658.74
7	173.92		213.76		345.64		557.58		649.94		716.98		862.14
8	231.56	286.47	373.14	493.74	585.62	644.38	676.49	710.52	754.63	828.81	925.99	1062.2	1219.5
9	354.66	471.77	576.10	650.20	688.81	724.38	767.16	839.36	937.93	1085.4	1263.4	1531.9	1834.3
10	523.19	628.04	685.59	726.00	763.67	824.21	909.87	1048.2	1222.4	1483.3	1785.8	2103.0	2286.0
11	653.03	714.83	753.22	800.15	864.41	974.61	1123.8	1353.4	1634.2	1981.7	2232.9	2377.1	2428.4
12	732.10	777.66	823.53	899.19	1008.0	1188.1	1421.3	1754.7	2073.6	2321.5	2429.9	2475.2	2490.4
13	792.52	844.30	913.34	1034.0	1203.4	1471.0	1787.5	2140.0	2361.9	2476.4	2515.8	2534.7	2547.2
14	853.92	925.88	1030.4	1211.0	1454.0	1804.2	2137.1	2395.0	2508.0	2556.4	2578.8	2599.7	2650.5
15	924.58	1028.1	1179.5	1432.1	1746.7	2125.0	2389.0	2537.2	2591.6	2623.5	2650.0	2728.4	2891.6
16	1009.6	1154.6	1362.6	1689.0	2043.5	2374.0	2544.8	2624.8	2659.0	2701.1	2787.1	2991.2	3277.4
17	1111.7	1307.2	1576.4	1958.7	2299.5	2542.8	2645.2	2696.7	2741.3	2844.2	3042.4	3370.0	3693.8
18	1232.4	1484.8	1810.3	2210.1	2493.8	2657.0	2723.7	2779.5	2872.6	3088.9	3398.4	3785.2	4189.4
19	1372.0	1682.5	2046.6	2420.4	2633.9	2744.4	2804.3	2901.3	3086.6	3425.9	3804.5	4293.6	4901.7
20	1529.2	1891.6	2266.5	2584.7	2739.3	2826.5	2909.3	3090.2	3387.7	3820.5	4294.7	4989.1	5748.1
21	1700.5	2100.1	2457.0	2711.8	2828.6	2921.9	3061.8	3357.1	3753.8	4292.0	4934.2	5776.6	6403.4
22	1880.4	2296.5	2614.9	2815.2	2917.8	3049.3	3278.2	3691.5	4185.5	4884.3	5664.2	6401.3	6771.4
23	2062.1	2472.9	2744.9	2908.7	3022.2	3225.7	3561.2	4088.0	4709.4	5560.3	6294.6	6778.8	6964.3
24	2239.6	2626.8	2855.5	3004.5	3155.4	3458.2	3902.8	4556.4	5317.2	6181.9	6719.7	6989.7	7078.8

Table 12
ENTHALPY H/RT_0

Pressure (atm)

$T(^{\circ}K \times 10^{-3})$	10^2	30	10	3	1	3×10^{-1}	10^{-1}	3×10^{-2}	10^{-2}	3×10^{-3}	10^{-3}	3×10^{-4}	10^{-4}
.15	-145.21	Liquefaction of CO_2			-145.21	-145.21	-145.21	-145.21	-145.21	-145.21	-145.21	-145.21	-145.21
.2	-144.53			-144.53	-144.53	-144.53	-144.53	-144.53	-144.53	-144.53	-144.53	-144.53	-144.53
.235	-144.02		-144.02	-144.02	-144.02	-144.02	-144.02	-144.02	-144.02	-144.02	-144.02	-144.02	-144.02
.25	-143.80		-143.80	-143.80	-143.80	-143.80	-143.80	-143.80	-143.80	-143.80	-143.80	-143.80	-143.80
.3	-143.03	-143.03	-143.03	-143.03	-143.03	-143.03	-143.03	-143.03	-143.03	-143.03	-143.03	-143.03	-143.03
.4	-141.37	-141.37	-141.37	-141.37	-141.37	-141.37	-141.37	-141.37	-141.37	-141.37	-141.37	-141.37	-141.37
.5	-139.57	-139.57	-139.57	-139.57	-139.57	-139.57	-139.57	-139.57	-139.57	-139.57	-139.57	-139.57	-139.57
.6	-137.65	-137.65	-137.65	-137.65	-137.65	-137.65	-137.65	-137.65	-137.65	-137.65	-137.65	-137.65	-137.65
.7	-135.63	-135.63	-135.63	-135.63	-135.63	-135.63	-135.63	-135.63	-135.63	-135.63	-135.63	-135.63	-135.63
.8	-133.53	-133.53	-133.53	-133.53	-133.53	-133.53	-133.53	-133.53	-133.53	-133.53	-133.53	-133.53	-133.53
1.0	-129.14	-129.14	-129.14	-129.14	-129.14	-129.14	-129.14	-129.14	-129.14	-129.14	-129.14	-129.14	-129.14
1.5	-117.42	-117.42	-117.41	-117.41	-117.39	-117.38	-117.34	-117.31	-117.24	-117.17	-117.02	-117.03	-117.04
2	-104.75	-104.62	-104.33	-104.06	-103.44	-102.88	-101.56	-100.35	-97.513	-94.973	-89.045	-83.855	-71.746
3	-65.723	-61.416	-51.367	-43.488	-25.105	-12.394	17.265	34.010	73.081	84.037	109.60	112.16	118.12
4	13.090	26.531	57.892	73.623	110.33	111.50	137.56	139.47	143.94	145.33	148.57	152.31	161.05
5	102.27	116.21	148.75	154.46	167.78	171.05	178.68	186.63	205.17	232.47	296.16	359.17	506.20
6	170.98	179.68	196.63	204.27	222.11	247.65	307.25	370.86	519.29	563.31	666.01	683.20	723.32
7	220.81	233.63	263.54	305.36	402.93	470.01	626.53	655.73	723.85	744.97	794.25	839.94	946.55
8	288.11	346.78	439.06	567.31	664.94	727.33	761.35	797.32	843.90	922.19	1024.7	1168.1	1333.3
9	425.68	551.47	663.22	742.53	783.76	821.61	867.05	943.69	1048.2	1204.3	1392.3	1675.2	1993.5
10	614.07	727.28	789.29	832.68	872.97	937.59	1029.0	1176.2	1361.4	1637.9	1958.0	2293.5	2487.1
11	762.45	829.55	871.02	921.47	990.42	1108.5	1268.0	1513.1	1812.0	2181.5	2448.5	2601.7	2656.2
12	856.80	906.38	955.96	1037.5	1154.7	1348.2	1598.2	1954.7	2295.4	2560.2	2675.9	2724.3	2740.5
13	931.22	987.58	1062.4	1192.9	1375.9	1664.1	2004.2	2382.5	2620.6	2743.4	2785.7	2805.8	2818.9
14	1006.9	1085.3	1199.0	1395.0	1658.1	2036.2	2395.3	2673.2	2794.9	2847.1	2871.0	2892.9	2946.1
15	1092.9	1206.0	1371.2	1646.1	1987.7	2397.6	2683.3	2843.7	2902.5	2936.7	2964.5	3046.9	3218.0
16	1194.8	1353.9	1581.4	1937.7	2323.8	2683.2	2868.9	2955.8	2992.6	3037.2	3127.6	3342.2	3642.8
17	1315.9	1531.1	1826.5	2245.1	2617.6	2883.2	2994.9	3050.8	3098.2	3206.8	3415.6	3760.5	4100.7
18	1458.1	1736.7	2099.1	2534.4	2845.6	3024.6	3097.2	3157.1	3255.6	3484.2	3810.7	4217.8	4641.4
19	1621.7	1965.7	2368.0	2780.2	3015.4	3136.7	3201.5	3304.7	3501.0	3859.9	4259.3	4773.0	5409.4
20	1805.6	2208.5	2624.3	2976.6	3147.5	3242.9	3331.6	3523.8	3839.3	4297.0	4796.4	5525.0	6320.1
21	2006.1	2452.1	2849.5	3132.7	3261.9	3363.0	3512.4	3826.3	4247.1	4815.7	5491.3	6375.9	7033.6
22	2217.3	2683.6	3039.8	3263.1	3375.9	3517.4	3761.5	4201.3	4724.8	5462.2	6283.3	7058.5	7447.7
23	2431.7	2894.1	3199.6	3382.3	3506.1	3724.2	4082.3	4642.5	5300.6	6198.9	6972.9	7483.1	7678.6
24	2642.6	3080.5	3338.2	3503.7	3667.1	3991.5	4466.0	5160.7	5966.3	6880.1	7448.2	7733.3	7827.4

Table 13
ENTROPY (S/R)

$T(^{\circ}K \times 10^{-3})$	Pressure (atm) 10^{2}	30	10	3	1	3×10^{-1}	10^{-1}	3×10^{-2}	10^{-2}	3×10^{-3}	10^{-3}	3×10^{-4}	10^{-4}
.15	18.476	Liquefaction of CO_2			23.031		25.334		27.636		29.939		32.242
.2	19.494				24.099		26.402		28.704		31.007		33.310
.235	20.124		22.427		24.729		27.032		29.334		31.637		33.940
.25	20.375		22.678		24.980		27.283		29.585		31.888		34.191
.3	21.141		23.444		25.746		28.049		30.351		32.654		34.957
.4	22.447		24.750		27.052		29.355		31.657		33.960		36.263
.5	23.545		25.848		28.150		30.453		32.755		35.058		37.361
.6	24.500		26.803		29.105		31.408		33.710		36.013		38.316
.7	25.349		27.652		29.954		32.257		34.559		36.862		39.165
.8	26.113		28.416		30.718		33.021		35.323		37.626		39.929
1.0	27.451		29.754		32.056		34.359		36.661		38.964		41.267
1.5	30.038		32.343		34.650		36.961		39.283		41.627		43.931
2	32.027		34.392		36.827		39.410		42.316		45.882		50.772
3	36.238		40.040		45.116		51.989		60.584		67.923		72.916
4	42.370		48.580		55.816		61.765		66.435		71.025		76.196
5	47.811		54.177		59.380		64.252		70.072		79.677		96.525
6	51.257		56.572		62.053		70.501		85.448		98.363		107.62
7	53.352		59.353		69.545		83.965		94.225		103.75		116.92
8	55.787	60.185	65.697	72.943	79.151	84.625	88.936	93.692	98.582	105.00	112.10	121.20	130.96
9	60.180	66.751	72.929	78.625	83.002	87.662	92.325	98.376	105.12	114.04	123.87	137.42	152.12
10	65.606	71.834	76.580	81.227	85.567	90.989	96.967	105.05	114.10	126.47	140.11	155.26	166.44
11	69.481	74.507	78.710	83.535	88.616	95.425	103.17	113.79	125.81	140.63	152.94	163.34	170.88
12	71.730	76.334	80.726	86.287	92.511	101.11	111.00	124.28	137.31	149.67	158.38	166.27	172.88
13	73.358	78.107	83.049	89.679	97.339	108.01	119.88	133.64	144.45	153.70	160.79	168.05	174.60
14	74.889	80.084	85.810	93.764	103.04	115.53	127.80	139.55	147.99	155.80	162.51	169.81	177.16
15	76.507	82.356	89.051	98.491	109.25	122.35	133.24	142.77	150.02	157.49	164.27	172.70	182.26
16	78.304	84.960	92.754	103.63	115.18	127.39	136.52	144.75	151.61	159.25	167.14	177.90	189.74
17	80.307	87.891	96.810	108.72	120.05	130.71	138.61	146.32	153.36	162.05	171.90	184.82	197.32
18	82.525	91.099	101.00	113.24	123.62	132.92	140.21	147.98	155.81	166.38	178.06	191.96	205.76
19	84.941	94.480	105.03	116.87	126.13	134.58	141.75	150.16	159.43	171.92	184.68	200.14	217.08
20	87.515	97.881	108.63	119.63	127.98	136.07	143.57	153.22	164.16	178.04	192.20	210.67	229.84
21	90.186	101.13	111.63	121.71	129.50	137.67	145.98	157.25	169.60	184.95	201.45	222.01	239.37
22	92.870	104.07	114.05	123.37	130.95	139.63	149.14	162.01	175.66	193.16	211.51	230.70	244.64
23	95.472	106.63	115.99	124.81	132.53	142.13	153.03	167.36	182.65	202.10	219.90	235.78	247.45
24	97.926	108.80	117.60	126.23	134.40	145.24	157.49	173.39	190.38	210.03	225.43	238.78	249.18

Table 14A

NORMAL SHOCK WAVE CHARACTERISTICS OF A TENTATIVE VENUS ATMOSPHERE

PRESSURE RATIO, P_2/P_1

Velocity (ft/sec)	Altitude (Km)					
	0	23.10	42.16	60	80	100
20×10^2	2.692	4.016	6.773	6.775	6.773	
25×10^2	4.275	6.374	10.745	10.749	10.745	
30×10^2	6.217	9.269	15.638	15.644	15.637	
35×10^2	8.504	12.709	21.457	21.466	21.456	
40×10^2	11.132	16.669	28.208	28.219	28.206	
45×10^2	14.135	21.136	35.838	35.853	35.840	
50×10^2		26.178	44.343	44.365	44.359	
55×10^2		31.840	53.921	53.951	53.952	
60×10^2		37.932	64.381	64.471	64.526	
65×10^2		44.687	75.769	75.943	76.074	
70×10^2		51.941	88.288	88.607	88.799	
75×10^2		59.702	101.501	101.893	102.744	
80×10^2		68.066	115.679	115.945	117.192	116.666
85×10^2		77.092	130.909	130.893	132.296	133.069
90×10^2		86.829	147.284	146.800	148.152	150.660
95×10^2		97.252	164.881	163.811	164.694	168.701
100×10^2		107.835	183.740	182.021	181.840	187.056
105×10^2			203.744	201.498	199.605	206.266
110×10^2			223.790	222.312	217.973	226.280
115×10^2			244.778	244.674	237.744	247.149
120×10^2			266.723	268.396	259.574	268.807
125×10^2			289.673	292.695	282.934	291.282
130×10^2			313.686	316.602	307.874	314.606
135×10^2			338.867	341.410	334.455	339.194
140×10^2			365.240	367.136	362.782	364.812
145×10^2			392.321	393.809	392.937	391.695
150×10^2			419.986	421.469	422.555	420.034
155×10^2			448.384	450.164	452.956	449.700
160×10^2			477.191	479.947	483.937	480.775
165×10^2			506.834	510.883	513.408	513.345
170×10^2			537.374	542.993	543.843	547.574
175×10^2			568.907	575.236	575.691	580.072
180×10^2			600.325	606.519	609.391	607.563
185×10^2			632.794	639.119	643.543	642.936
190×10^2			667.007	674.160	676.304	678.634
195×10^2			702.689	709.215	711.085	712.460
200×10^2			738.494	744.626	747.457	747.360
205×10^2			775.064	781.775	783.186	783.837
210×10^2			812.435	819.664	819.833	822.144
215×10^2			850.412	858.164	857.787	862.758
220×10^2			889.810	897.848	897.297	906.208
225×10^2			930.670	939.077	939.348	952.368
230×10^2			973.108	981.827	983.982	998.529

Table 14 A (cont'd)

Velocity (ft/sec)	Altitude (Km)					
	0	23.10	42.16	60	80	100
235×10^2			1017.023	1025.417	1029.857	1042.823
240×10^2			1062.885	1070.229	1077.403	1087.627
245×10^2			1107.591	1116.307	1126.683	1133.103
250×10^2			1152.523	1163.631	1174.318	1179.510
255×10^2			1197.995	1211.820	1221.943	1226.844
260×10^2			1244.175	1259.769	1270.447	1275.156
265×10^2			1292.193	1308.649	1319.892	1324.633
270×10^2			1342.545	1358.935	1370.325	1375.053
275×10^2			1394.287	1410.496	1421.859	1426.863
280×10^2			1447.309	1463.583	1474.498	1480.148
285×10^2			1501.529	1518.384	1528.308	1535.206
290×10^2			1555.679	1574.651	1583.374	1591.342
295×10^2			1610.311	1629.161	1639.790	1647.116
300×10^2			1666.009	1684.821	1697.658	1704.202
305×10^2					1754.163	1762.225
310×10^2					1810.509	1820.444
315×10^2					1867.597	1877.703
320×10^2					1926.238	1936.733
325×10^2					1987.145	1998.332
330×10^2					2048.959	2061.871
335×10^2					2109.716	2123.668
340×10^2					2171.228	2186.632
345×10^2					2233.716	2250.555
350×10^2					2297.411	2315.431
355×10^2					2362.016	2381.326
360×10^2					2428.009	2448.545
365×10^2						2516.619
370×10^2						2585.719
375×10^2						2655.571
380×10^2						2726.395
385×10^2						2798.288
390×10^2						2871.417
395×10^2						2945.489
400×10^2						3020.505

Table 14B

NORMAL SHOCK WAVE CHARACTERISTICS OF A TENTATIVE VENUS ATMOSPHERE

TEMPERATURE RATIO T_2/T_1

Velocity (ft/sec)	Altitude (Km)					
	0	23.10	42.16	60	80	100
20×10^2	1.222	1.407	1.824	1.824	1.824	
25×10^2	1.383	1.655	2.270	2.270	2.270	
30×10^2	1.566	1.940	2.776	2.776	2.776	
35×10^2	1.776	2.258	3.340	3.340	3.340	
40×10^2	2.009	2.618	3.958	3.958	3.958	
45×10^2	2.264	3.012	4.646	4.645	4.643	
50×10^2		3.438	5.385	5.382	5.370	
55×10^2		3.893	6.174	6.164	6.136	
60×10^2		4.378	6.997	6.942	6.862	
65×10^2		4.892	7.847	7.700	7.503	
70×10^2		5.400	8.711	8.438	8.048	
75×10^2		5.893	9.534	9.208	8.474	
80×10^2		6.367	10.315	9.977	9.034	8.747
85×10^2		6.810	11.034	10.716	9.655	8.796
90×10^2		7.208	11.666	11.402	10.280	8.753
95×10^2		7.551	12.187	12.006	10.901	8.931
100×10^2		7.989	12.571	12.491	11.507	9.368
105×10^2			12.866	12.853	12.087	9.819
110×10^2			13.508	13.066	12.628	10.277
115×10^2			14.137	13.090	13.122	10.737
120×10^2			14.742	12.985	13.516	11.191
125×10^2			15.311	13.013	13.814	11.629
130×10^2			15.830	13.497	13.996	12.043
135×10^2			16.284	13.980	14.034	12.359
140×10^2			16.651	14.457	13.895	12.628
145×10^2			17.092	14.923	13.552	12.851
150×10^2			17.641	15.373	13.524	13.019
155×10^2			18.251	15.799	13.532	13.122
160×10^2			18.983	16.195	13.617	13.152
165×10^2			19.740	16.549	14.317	13.091
170×10^2			20.519	16.867	15.044	12.908
175×10^2			21.317	17.441	15.792	13.215
180×10^2			22.355	18.492	16.555	14.749
185×10^2			23.522	19.656	17.516	16.543
190×10^2			24.747	20.954	18.856	18.088
195×10^2			26.021	22.294	20.440	19.341
200×10^2			27.244	23.672	21.936	20.394
205×10^2			28.651	25.095	23.090	21.224
210×10^2			30.229	26.364	24.089	21.804
215×10^2			31.556	27.404	24.915	22.104

Table 14B (cont'd)

NORMAL SHOCK WAVE CHARACTERISTICS OF A TENTATIVE VENUS ATMOSPHERE

TEMPERATURE RATIO T_2/T_1

Velocity (ft/sec)	Altitude (Km)					
	0	23.10	42.16	60	80	100
220×10^2			32.660	28.290	25.543	22.094
225×10^2			33.574	29.002	25.951	21.734
230×10^2			34.313	29.523	26.108	21.565
235×10^2			34.863	30.085	26.208	21.942
240×10^2			35.216	30.574	26.187	22.411
245×10^2			35.967	30.990	26.029	22.883
250×10^2			36.811	31.344	26.319	23.333
255×10^2			37.654	31.707	26.782	23.755
260×10^2			38.495	32.245	27.230	24.143
265×10^2			39.252	32.727	27.658	24.491
270×10^2			39.774	33.146	28.062	24.791
275×10^2			40.239	33.493	28.425	25.038
280×10^2			40.656	33.758	28.753	25.220
285×10^2			41.036	33.928	29.040	25.318
290×10^2			41.585	34.045	29.281	25.407
295×10^2			42.186	34.638	29.470	25.661
300×10^2			42.770	35.247	29.602	25.926
305×10^2					30.060	26.206
310×10^2					30.771	26.615
315×10^2					31.599	27.401
320×10^2					32.505	28.241
325×10^2					33.481	29.117
330×10^2					34.528	29.993
335×10^2					35.638	30.806
340×10^2					36.821	31.537
345×10^2					38.099	32.255
350×10^2					39.151	32.965
355×10^2					40.126	33.659
360×10^2					40.993	34.267
365×10^2						34.844
370×10^2						35.391
375×10^2						35.949
380×10^2						36.486
385×10^2						36.992
390×10^2						37.463
395×10^2						37.897
400×10^2						38.325

Table 14C

NORMAL SHOCK WAVE CHARACTERISTICS OF A TENTATIVE VENUS ATMOSPHERE

DENSITY RATIO, ρ_2/ρ_1

Velocity (ft/sec)	Altitude (Km)					
	0	23.10	42.16	60	80	100
$20x10^2$	2.201	2.847	3.697	3.697	3.697	
$25x10^2$	3.089	3.844	4.724	4.724	4.724	
$30x10^2$	3.968	4.775	5.625	5.625	5.625	
$35x10^2$	4.772	5.629	6.421	6.421	6.421	
$40x10^2$	5.465	6.353	7.125	7.125	7.125	
$45x10^2$	6.134	6.922	7.675	7.676	7.681	
$50x10^2$		7.490	8.097	8.103	8.122	
$55x10^2$		8.139	8.656	8.666	8.697	
$60x10^2$		8.524	9.095	9.171	9.272	
$65x10^2$		9.064	9.491	9.649	9.837	
$70x10^2$		9.476	10.056	10.362	10.626	
$75x10^2$		9.792	10.332	10.680	11.692	
$80x10^2$		10.163	10.619	10.827	12.169	11.568
$85x10^2$		10.654	10.984	10.932	12.308	13.183
$90x10^2$		11.323	11.491	11.067	12.253	15.171
$95x10^2$		12.137	12.191	11.311	12.025	16.495
$100x10^2$		12.370	13.125	11.728	11.655	16.840
$105x10^2$			14.212	12.340	11.194	17.015
$110x10^2$			14.461	13.202	10.695	17.032
$115x10^2$			14.681	14.509	10.522	16.918
$120x10^2$			14.901	16.220	10.846	16.703
$125x10^2$			15.154	17.651	11.393	16.428
$130x10^2$			15.478	17.750	12.198	16.139
$135x10^2$			15.914	17.804	13.337	16.129
$140x10^2$			16.512	17.838	14.970	16.223
$145x10^2$			16.935	17.879	17.377	16.513
$150x10^2$			17.057	17.955	18.933	17.089
$155x10^2$			17.029	18.093	20.418	17.903
$160x10^2$			16.742	18.318	21.632	19.019
$165x10^2$			16.443	18.662	20.577	20.556
$170x10^2$			16.172	19.131	19.800	22.773
$175x10^2$			15.970	19.037	19.463	22.658
$180x10^2$			15.403	17.971	19.726	18.651
$185x10^2$			14.943	17.280	19.644	19.301
$190x10^2$			14.834	17.319	18.408	19.590
$195x10^2$			14.893	16.972	17.846	18.466
$200x10^2$			14.703	16.477	17.660	17.622
$205x10^2$			14.505	16.331	16.927	17.122
$210x10^2$			14.304	16.130	16.302	17.025
$215x10^2$			14.053	15.860	15.854	17.394
$220x10^2$			13.943	15.696	15.656	18.341
$225x10^2$			13.961	15.682	15.895	20.010

Table 14C (cont'd)

NORMAL SHOCK WAVE CHARACTERISTICS OF A TENTATIVE VENUS ATMOSPHERE

DENSITY RATIO, ρ_2/ρ_1

Velocity (ft/sec)	Altitude (Km) 0	23.10	42.16	60	80	100
$230x10^2$			14.083	15.857	16.501	21.400
$235x10^2$			14.308	15.966	17.194	21.596
$240x10^2$			14.695	16.140	18.096	21.567
$245x10^2$			14.695	16.380	19.258	21.476
$250x10^2$			14.566	16.677	19.645	21.375
$255x10^2$			14.391	16.940	19.697	21.277
$260x10^2$			14.203	16.926	19.741	21.200
$265x10^2$			14.175	16.946	19.783	21.167
$270x10^2$			14.354	17.027	19.837	21.202
$275x10^2$			14.581	17.187	19.931	21.344
$280x10^2$			14.848	17.456	20.062	21.638
$285x10^2$			15.143	17.871	20.245	22.174
$290x10^2$			15.276	18.377	20.499	22.727
$295x10^2$			15.348	18.308	20.846	22.849
$300x10^2$			15.440	18.283	21.312	23.093
$305x10^2$					21.156	23.319
$310x10^2$					20.774	23.314
$315x10^2$					20.394	22.776
$320x10^2$					20.180	22.526
$325x10^2$					20.246	22.698
$330x10^2$					20.289	23.097
$335x10^2$					19.950	22.805
$340x10^2$					19.623	22.611
$345x10^2$					19.332	22.432
$350x10^2$					19.108	22.267
$355x10^2$					18.894	22.129
$360x10^2$					18.761	22.074
$365x10^2$						22.002
$370x10^2$						21.951
$375x10^2$						21.867
$380x10^2$						21.795
$385x10^2$						21.747
$390x10^2$						21.731
$395x10^2$						21.749
$400x10^2$						21.761

Table 14D

NORMAL SHOCK WAVE CHARACTERISTICS OF A TENTATIVE VENUS ATMOSPHERE

VELOCITY RATIO, u_2/u_1

Velocity (ft/sec)	Altitude (Km)					
	0	23.10	42.16	60	80	100
$20x10^2$	.454	.351	.270	.270	.270	
$25x10^2$	.324	.260	.212	.212	.212	
$30x10^2$	.252	.210	.178	.178	.178	
$35x10^2$	.210	.178	.156	.156	.156	
$40x10^2$	.183	.157	.140	.140	.140	
$45x10^2$	.163	.144	.130	.130	.130	
$50x10^2$		.134	.124	.123	.123	
$55x10^2$		.123	.116	.115	.115	
$60x10^2$		.117	.110	.109	.108	
$65x10^2$		.110	.105	.104	.102	
$70x10^2$		.106	.099	.097	.094	
$75x10^2$		.102	.097	.094	.086	
$80x10^2$		.098	.094	.092	.082	.086
$85x10^2$		.094	.091	.092	.081	.076
$90x10^2$		.088	.087	.090	.082	.066
$95x10^2$		.082	.082	.088	.083	.061
$100x10^2$		.081	.076	.085	.086	.059
$105x10^2$			.070	.081	.089	.059
$110x10^2$			.069	.076	.093	.059
$115x10^2$			.068	.069	.095	.059
$120x10^2$			.067	.062	.092	.060
$125x10^2$			.066	.057	.088	.061
$130x10^2$			.065	.056	.082	.062
$135x10^2$			.063	.056	.075	.062
$140x10^2$			.061	.056	.067	.062
$145x10^2$			.059	.056	.058	.061
$150x10^2$			.059	.056	.053	.059
$155x10^2$			.059	.055	.049	.056
$160x10^2$			.060	.055	.046	.053
$165x10^2$			.061	.054	.049	.049
$170x10^2$			.062	.052	.050	.044
$175x10^2$			.063	.053	.051	.044
$180x10^2$			.065	.056	.051	.054
$185x10^2$			.067	.058	.051	.052
$190x10^2$			.067	.058	.054	.051
$195x10^2$			.067	.059	.056	.054
$200x10^2$			.068	.061	.057	.057
$205x10^2$			.069	.061	.059	.058
$210x10^2$			.070	.062	.061	.059
$215x10^2$			.071	.063	.063	.058
$220x10^2$			.072	.064	.064	.055
$225x10^2$			.072	.064	.063	.050
$230x10^2$			.071	.063	.061	.047
$235x10^2$			.070	.063	.058	.046

Table 14D (cont'd)

NORMAL SHOCK WAVE CHARACTERISTICS OF A TENTATIVE VENUS ATMOSPHERE

VELOCITY RATIO, u_2/u_1

Velocity (ft/sec)	Altitude (Km)					
	0	23.10	42.16	60	80	100
$240x10^2$			.068	.062	.055	.046
$245x10^2$			.068	.061	.052	.047
$250x10^2$			.069	.060	.051	.047
$255x10^2$			.069	.059	.051	.047
$260x10^2$			.070	.059	.051	.047
$265x10^2$			.071	.059	.051	.047
$270x10^2$			.070	.059	.050	.047
$275x10^2$			.069	.058	.050	.047
$280x10^2$			.067	.057	.050	.046
$285x10^2$			.066	.056	.049	.045
$290x10^2$			.066	.054	.049	.044
$295x10^2$			.065	.055	.048	.044
$300x10^2$			.065	.055	.047	.043
$305x10^2$					.047	.043
$310x10^2$					.048	.043
$315x10^2$					.049	.044
$320x10^2$					.050	.044
$325x10^2$					.049	.044
$330x10^2$					.049	.043
$335x10^2$					.050	.044
$340x10^2$					.051	.044
$345x10^2$					.052	.045
$350x10^2$					.052	.045
$355x10^2$					.053	.045
$360x10^2$					.053	.045
$365x10^2$						.045
$370x10^2$						.046
$375x10^2$						.046
$380x10^2$						.046
$385x10^2$						.046
$390x10^2$						.046
$395x10^2$						.046
$400x10^2$						.046

Table 15

EQUILIBRIUM CONSTANTS, K_p (atm)

T (°K)	Reaction 1	2	3	4	5
1000	3.022^{-68}	2.525^{-69}	1.4604^{-59}	2.397^{-68}	2.216^{-56}
1500	1.215^{-44}	1.375^{-45}	3.492^{-39}	5.054^{-45}	5.438^{-37}
2000	8.970^{-33}	1.219^{-33}	6.332^{-29}	2.664^{-33}	3.135^{-27}
3000	9.254^{-21}	1.793^{-21}	1.855^{-18}	1.979^{-21}	2.519^{-17}
4000		2.828^{-15}	4.191^{-13}	2.108^{-15}	2.765^{-12}
5000		1.686^{-11}	7.601^{-10}	9.868^{-12}	3.290^{-9}
6000		6.088^{-9}	1.209^{-7}	2.995^{-9}	3.984^{-7}

Table 16

ELECTRON CONCENTRATIONS FOR PURE CO_2, n_{e^-}

(g-moles electrons/44.011 g mixture)

T (°K)	p (atm) 10^2	10	1	10^{-1}	10^{-2}	10^{-3}	10^{-4}
2000	3.32^{-17}	1.52^{-16}	6.98^{-16}	3.21^{-15}	1.48^{-14}	6.79^{-14}	3.06^{-13}
3000	3.56^{-11}	1.58^{-10}	6.84^{-10}	2.61^{-9}	7.27^{-9}	1.15^{-8}	1.48^{-8}
4000	3.59^{-8}	1.29^{-7}	3.20^{-7}	5.19^{-7}	1.08^{-6}	3.40^{-6}	1.63^{-5}
5000	1.77^{-6}	3.93^{-6}	8.26^{-6}	2.61^{-5}	1.4^{-4}	1.1^{-3}	7.4^{-3}
6000	1.33^{-5}	4.41^{-5}	1.8^{-4}	1.2^{-3}	7.9^{-3}	3.3^{-2}	1.1^{-1}

Appendix B

THE COMPUTATION OF TWO-DIMENSIONAL OBLIQUE-SHOCK-WAVE CHARACTERISTICS FROM NORMAL-SHOCK-WAVE DATA

The practical problems usually associated with aerodynamics generally involve heat transfer and aerodynamic forces which arise due to the motion of a body through a fluid. In the present application, both of these problems require a knowledge of the so-called inviscid parameters associated with both shock waves and expansive-type flows such as the Prandtl-Meyer expansion around a corner. The purpose of this appendix is to furnish a practical way to calculate the oblique-shock parameters. Since aerodynamic parameters change only in the direction normal to shock, only the oblique shock angle is required to solve the problem, when the normal-shock solution (Section IV) is known.

The present method may also prove useful for computing oblique-shock characteristics for any selected gas composition once its equilibrium thermodynamic properties are known. While the generally used iteration scheme for obtaining normal-shock data[20] is highly convergent, the iteration scheme for oblique-shock solutions presented in Ref. 20 is not, especially near the detachment point. It is presumed that if it is practical to obtain normal-shock data for a particular composition, the oblique-shock characteristics can be obtained by this method for a particular case.

As previously mentioned, all of the physics of the problem are contained in the normal-shock-wave data and the fact that the velocity component parallel to the shock wave remains constant across the shock (this follows directly from a conservation-of-mass-and-momentum analysis across a flow discontinuity). Therefore, no physical assumptions about the flow are necessary.

What is usually specified in an oblique-shock problem is the flow deflection angle, the upstream thermodynamic state, and the upstream velocity. If the wave inclination angle may be found, all downstream parameters may be calculated. Unfortunately, no explicit expression for the wave inclination angle exists, and a practical iteration scheme which always converges must be found.

Referring to Fig. 12, the following trigonometric relations across an oblique shock become obvious:

$$u_1 = w_1 \sin \beta \tag{39}$$

$$\frac{u_2}{u_1} = \frac{\tan (\beta - \theta)}{\tan \beta} \tag{40}$$

The same conservation equations apply to the normal stream component across a flow discontinuity as apply to the stream across a normal shock wave. Since for a given upstream state u_2/u_1 vs u_1 is usually plotted for a particular gas if normal shock wave data are given, this relation must also hold for the normal stream components across an oblique shock if the upstream thermodynamic state is the same. The general form of the relation is shown in quadrant 2 of Fig. 13. This curve always assumes this form for a perfect gas. Real-gas effects will usually destroy the monotonic nature of this curve and will, in exceptional cases, cause a positive slope in a small u_1 range.[20] However, this presents no problem, as will become evident later.

Equation (39) is very simple and presents no computational problem. Considering Eq. (40), the following equation for β may be developed after some manipulation:

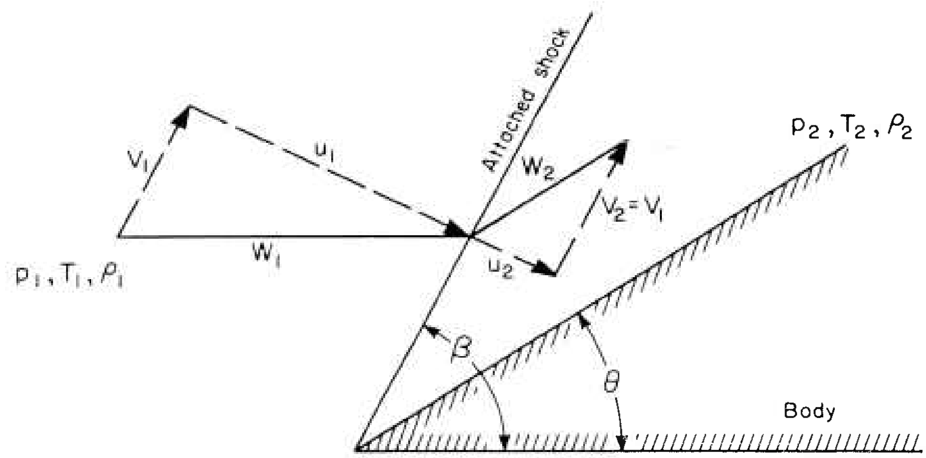

Fig. 12 — Oblique-shock diagram

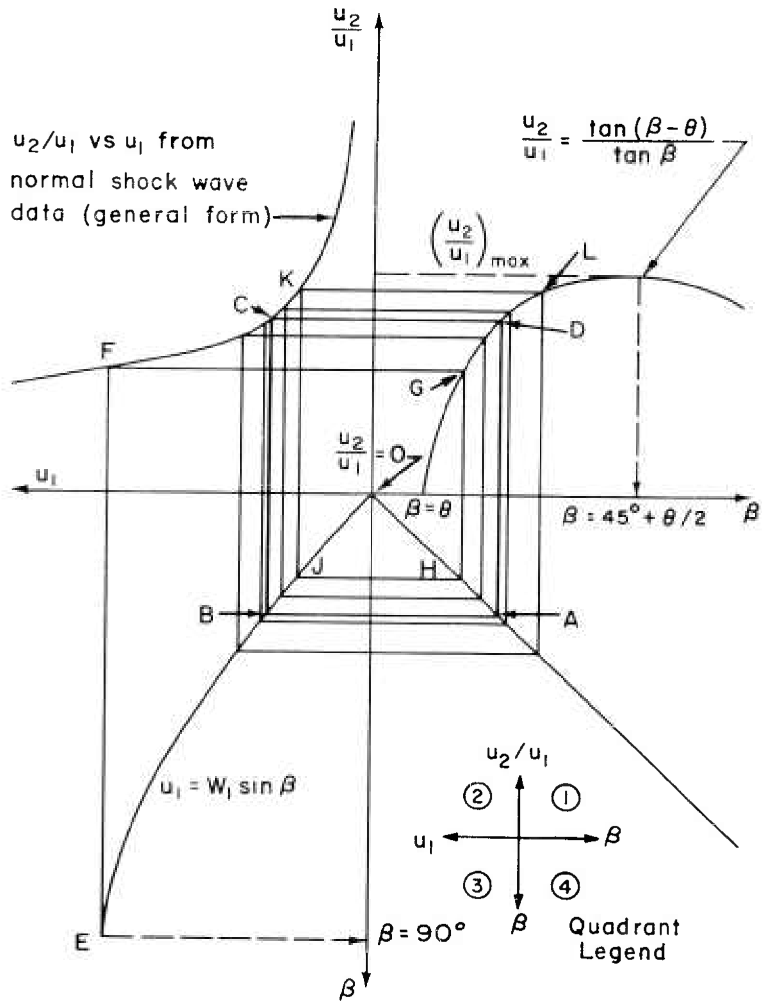

Fig. 13— Graphical solution for u_2/u_1 and β (weak-shock solution)

$$\beta = \arctan \frac{1}{2\left(\frac{u_2}{u_1}\right)\tan\theta}\left[\left(1 - \frac{u_2}{u_1}\right) \pm \sqrt{1 - 2\left(\frac{u_2}{u_1}\right)\left(1 + 2\tan^2\theta\right) + \left(\frac{u_2}{u_1}\right)^2}\,\right] \tag{41}$$

Differentiating Eq. (40), the maximum of u_2/u_1 vs β with θ a fixed parameter occurs at

$$\beta = 45^\circ + \frac{\theta}{2} \tag{42}$$

and

$$\left(\frac{u_2}{u_1}\right)_{max} = \frac{1 - \sin\theta}{1 + \sin\theta} \tag{43}$$

Also, referring to Fig. 13, it is seen that the negative sign in Eq. (41) corresponds to $\theta \leq \beta \leq (45^\circ + \theta/2)$, and the positive sign corresponds to $(45^\circ + \theta/2) \leq \beta \leq 90^\circ$. Note that $0^\circ \leq \beta \leq 90^\circ$ is the only range of interest. For reasons that will become apparent later, it is usually β which must be calculated from a known u_2/u_1, rather than vice versa. Since Eq. (41) requires a rather tedious computation if done by hand in an iteration scheme, Fig. 14 is included for $0 \leq \theta \leq 30^\circ$.

It may be shown that $\beta \leq (45^\circ + \theta/2)$, i.e., $\beta \leq \beta$ corresponding to $(u_2/u_1)_{max}$ for a given θ, must always be in the weak-shock-wave region. Stating this another way: if, for a given upstream state, β were plotted vs θ with upstream velocity as a parameter, $\beta \leq (45^\circ + \theta/2)$ would always be less than the β dictated by the line connecting the maximum θ solutions for a given upstream velocity. This may be seen for a perfect gas by plotting a line $\beta = (45^\circ + \theta/2)$ on pp. 42 and 43 of Ref. 22. The intersection of this

Note: for more detoiled drawings of these curves, see Figs. 14a–14 L.

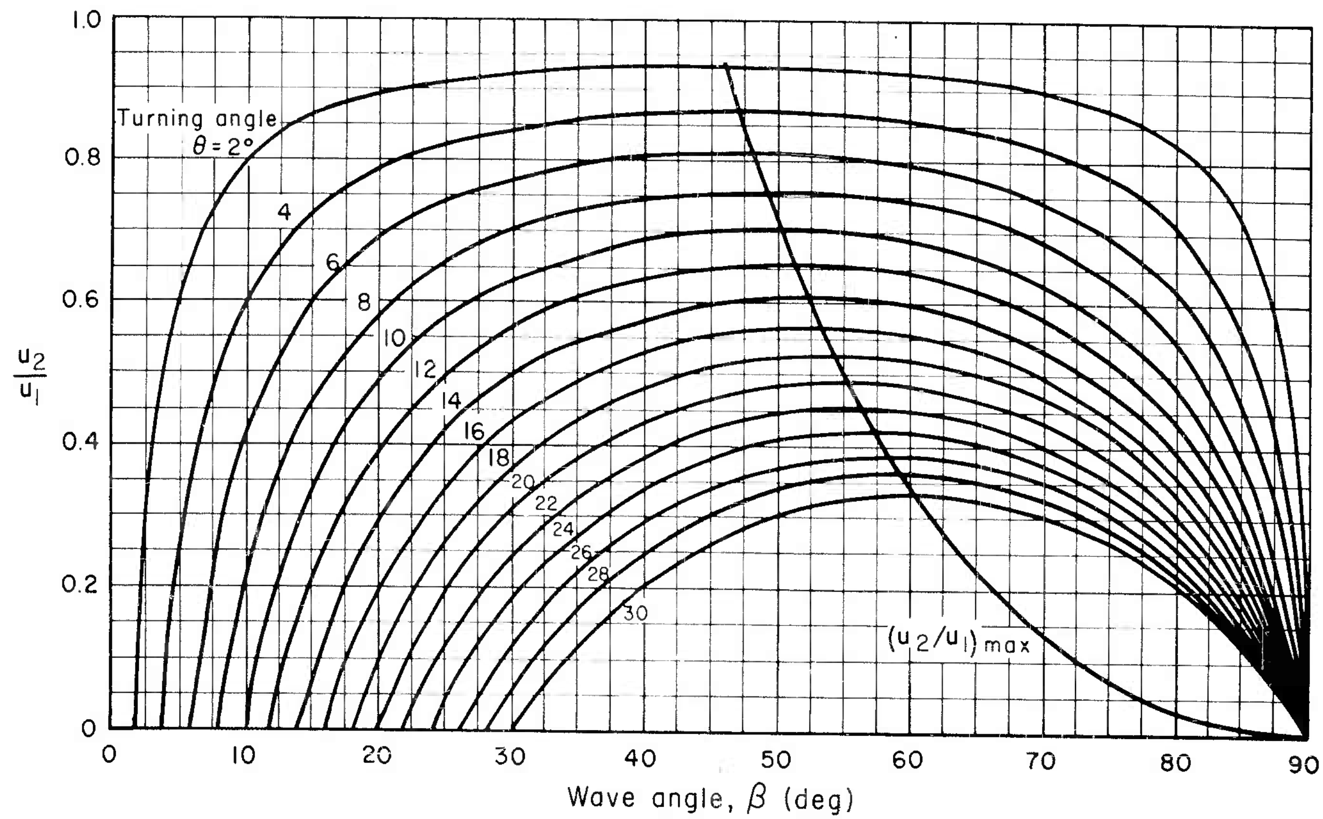

Fig.14— Graphical solution for shock-wave angle

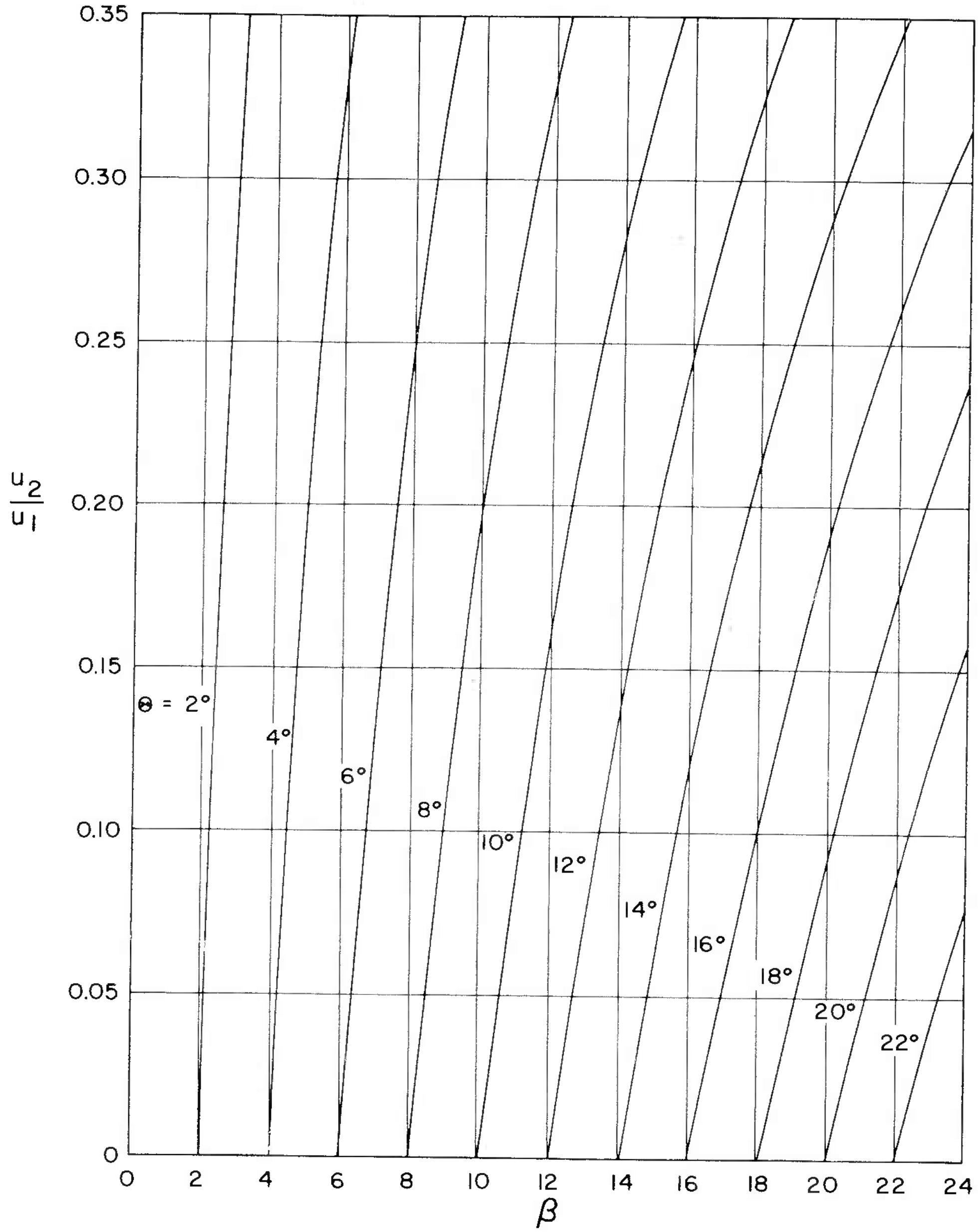

0.35
0.30
0.25
0.20
0.15
0.10
0.05
0
$\frac{u_2}{u_1}$
$\theta = 2°$
4°
6°
8°
10°
12°
14°
16°
18°
20°
22°
0
2
4
6
8
10
12
14
16
18
20
22
24
β

Fig. 14a

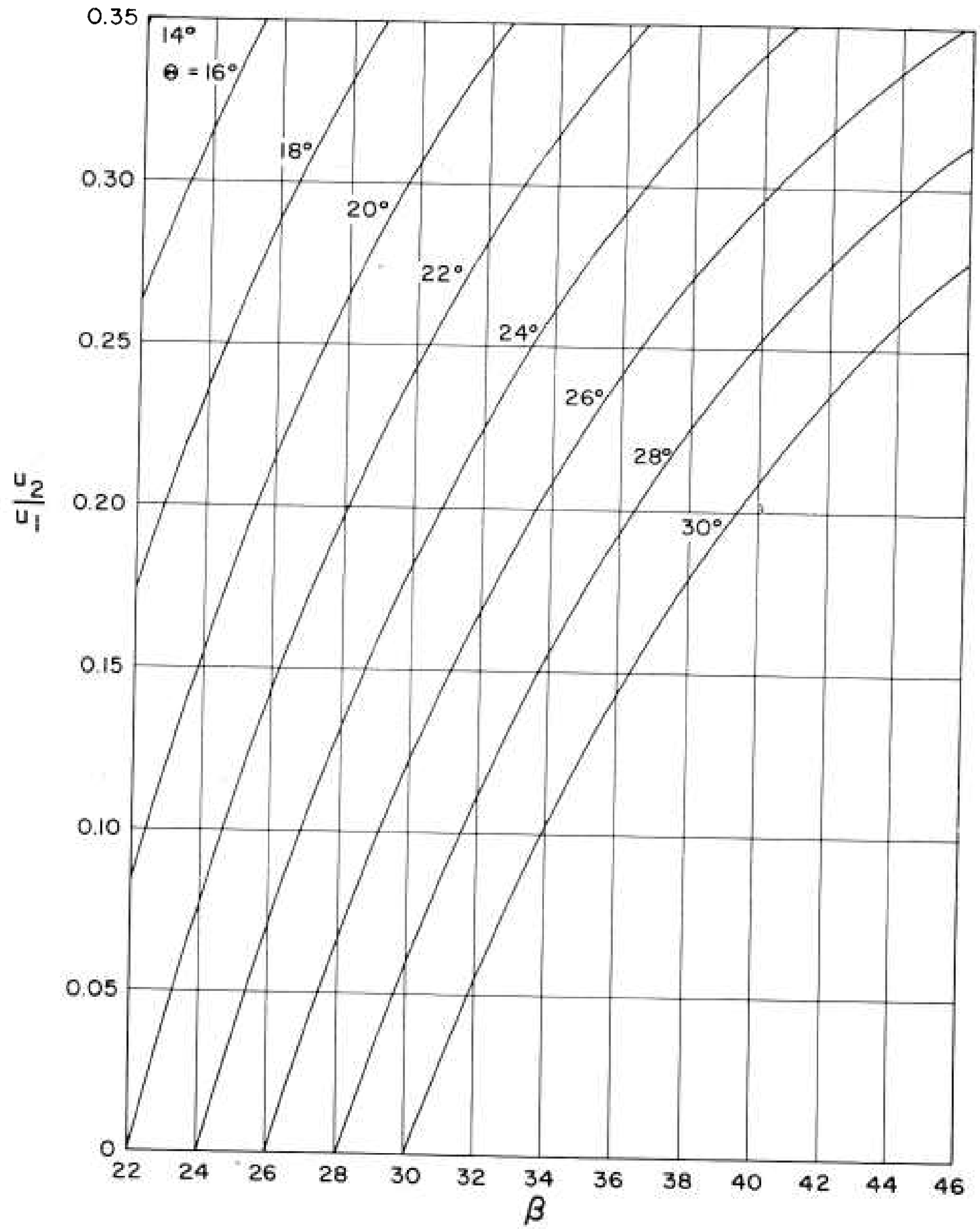
0.35
0.30
0.25
0.20
0.15
0.10
0.05
0
14°
θ = 16°
18°
20°
22°
24°
26°
28°
30°
$\frac{u_2}{u_1}$
22
24
26
28
30
32
34
36
38
40
42
44
46
β

Fig. 14b

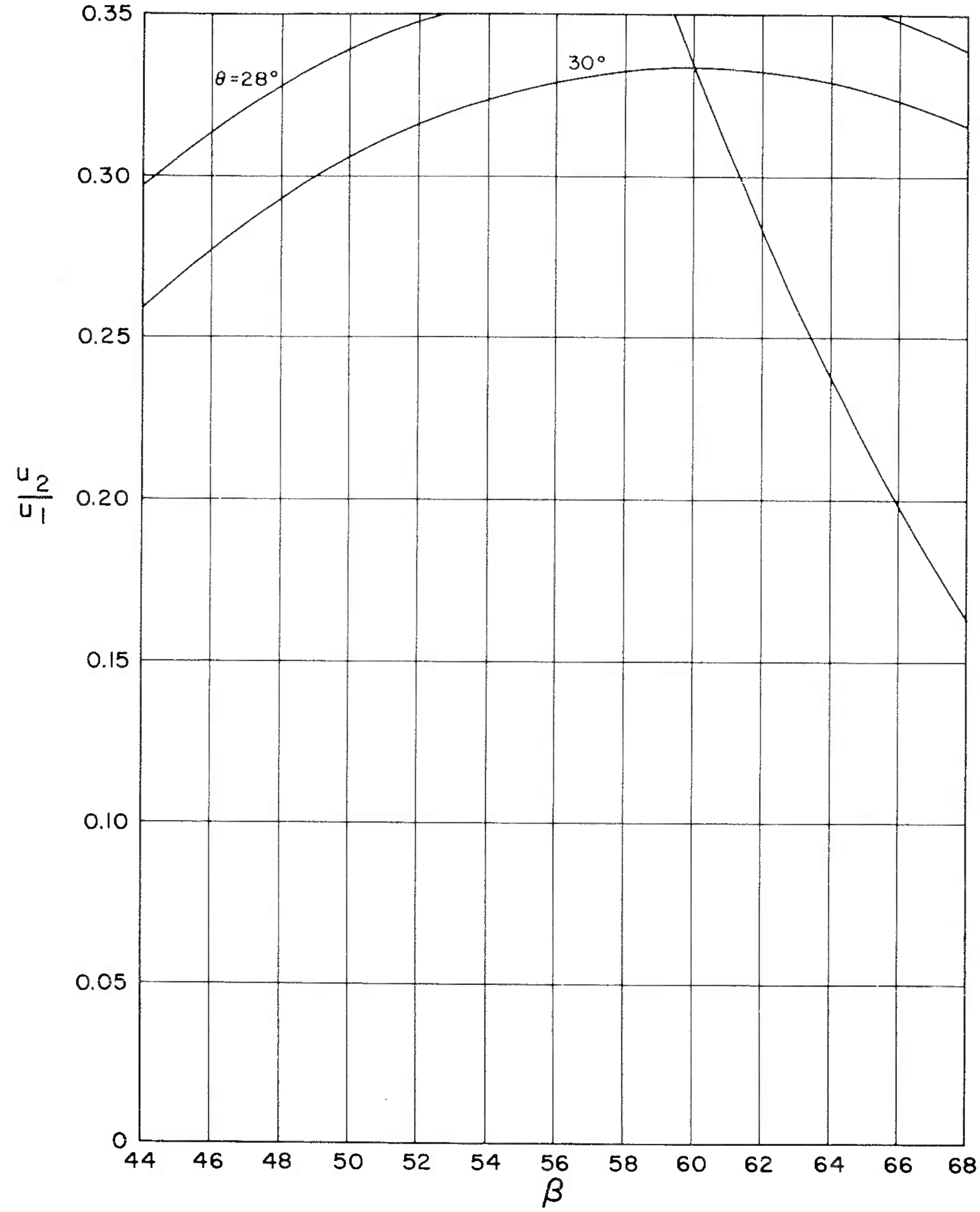

0.35
0.30
0.25
0.20
0.15
0.10
0.05
0
$\frac{u_2}{u_1}$
$\theta = 28°$
30°
44
46
48
50
52
54
56
58
60
62
64
66
68
β

Fig. 14c

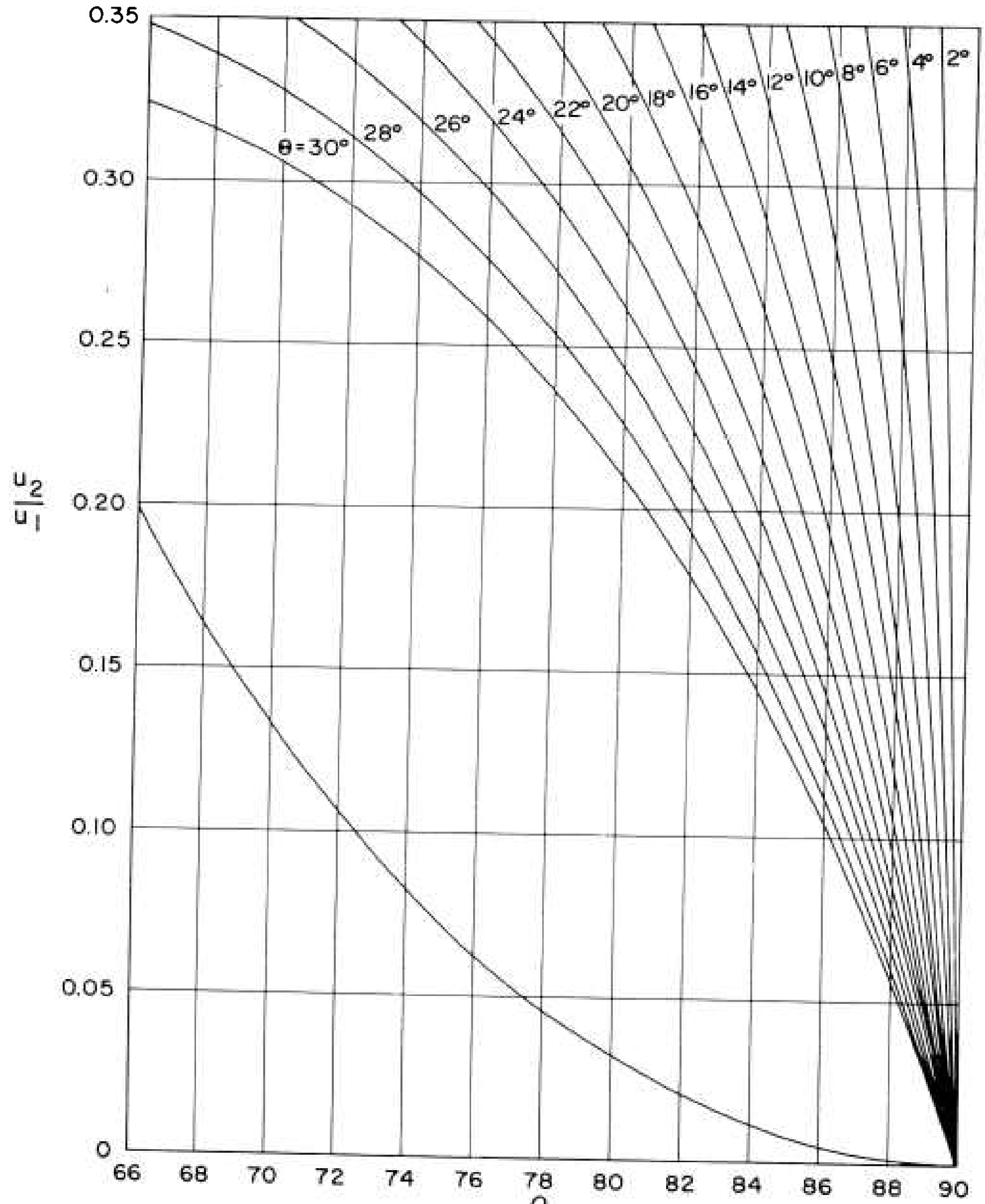
0.35
0.30
0.25
0.20
0.15
0.10
0.05
0
$\frac{u_2}{u_1}$
66
68
70
72
74
76
78
80
82
84
86
88
90
β
$\theta = 30°$
28°
26°
24°
22°
20°
18°
16°
14°
12°
10°
8°
6°
4°
2°

Fig 14d

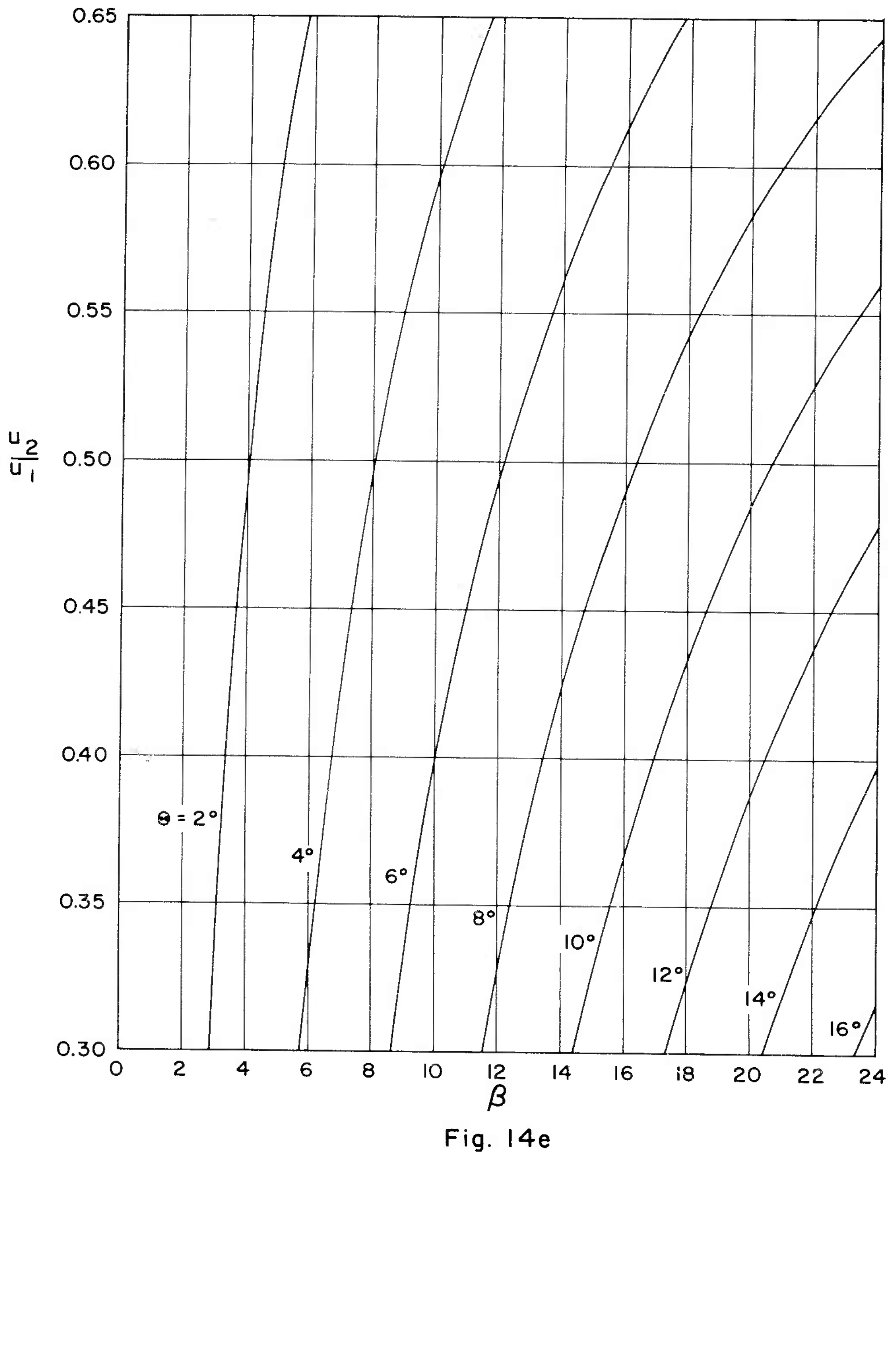
0.65
0.60
0.55
0.50
0.45
0.40
0.35
0.30
$\frac{u_2}{u_1}$
θ = 2°
4°
6°
8°
10°
12°
14°
16°
0
2
4
6
8
10
12
14
16
18
20
22
24
β

Fig. 14e

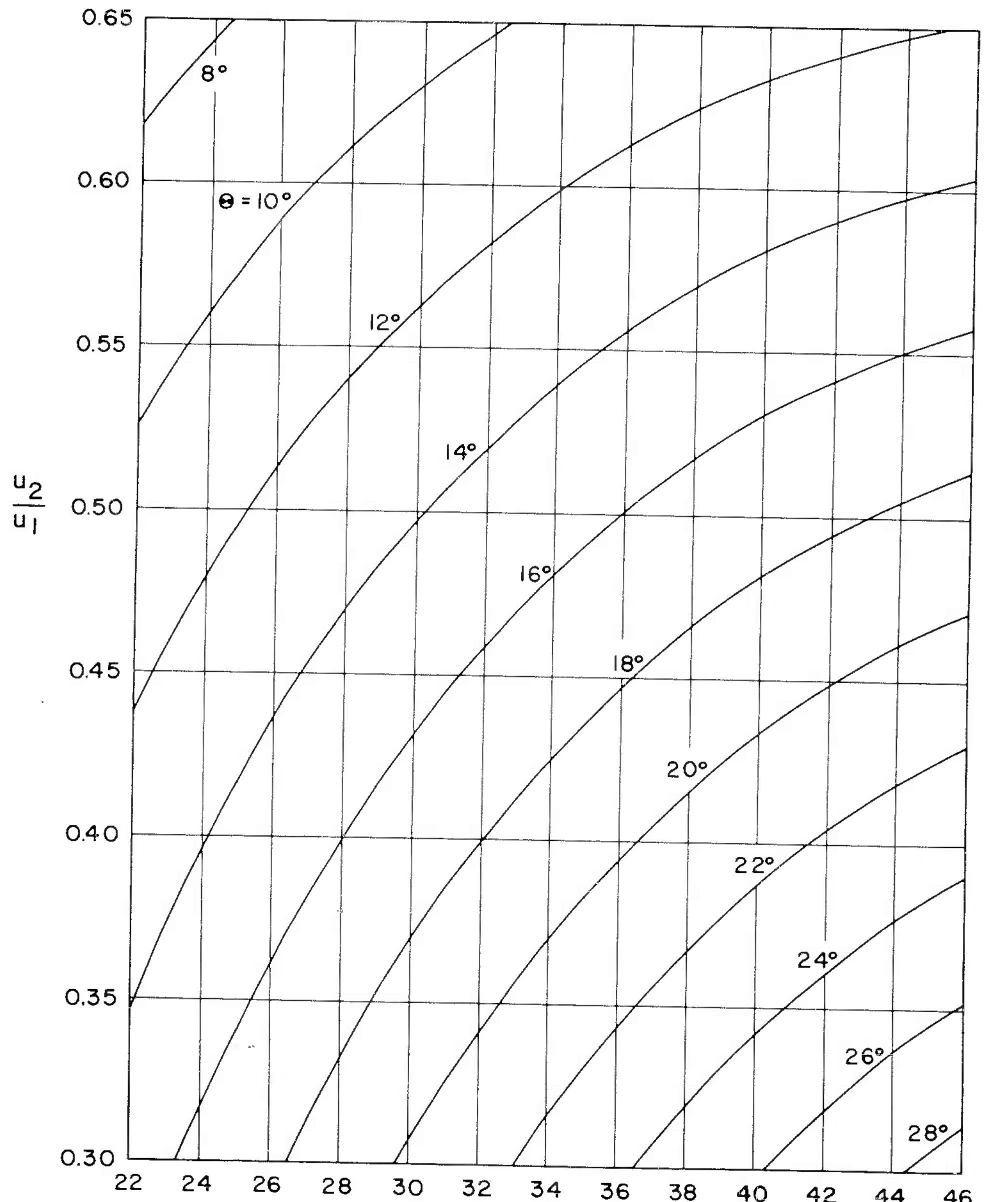
0.65
0.60
0.55
0.50
0.45
0.40
0.35
0.30
u2/u1
22
24
26
28
30
32
34
36
38
40
42
44
46
β
8°
θ = 10°
12°
14°
16°
18°
20°
22°
24°
26°
28°

Fig. 14f

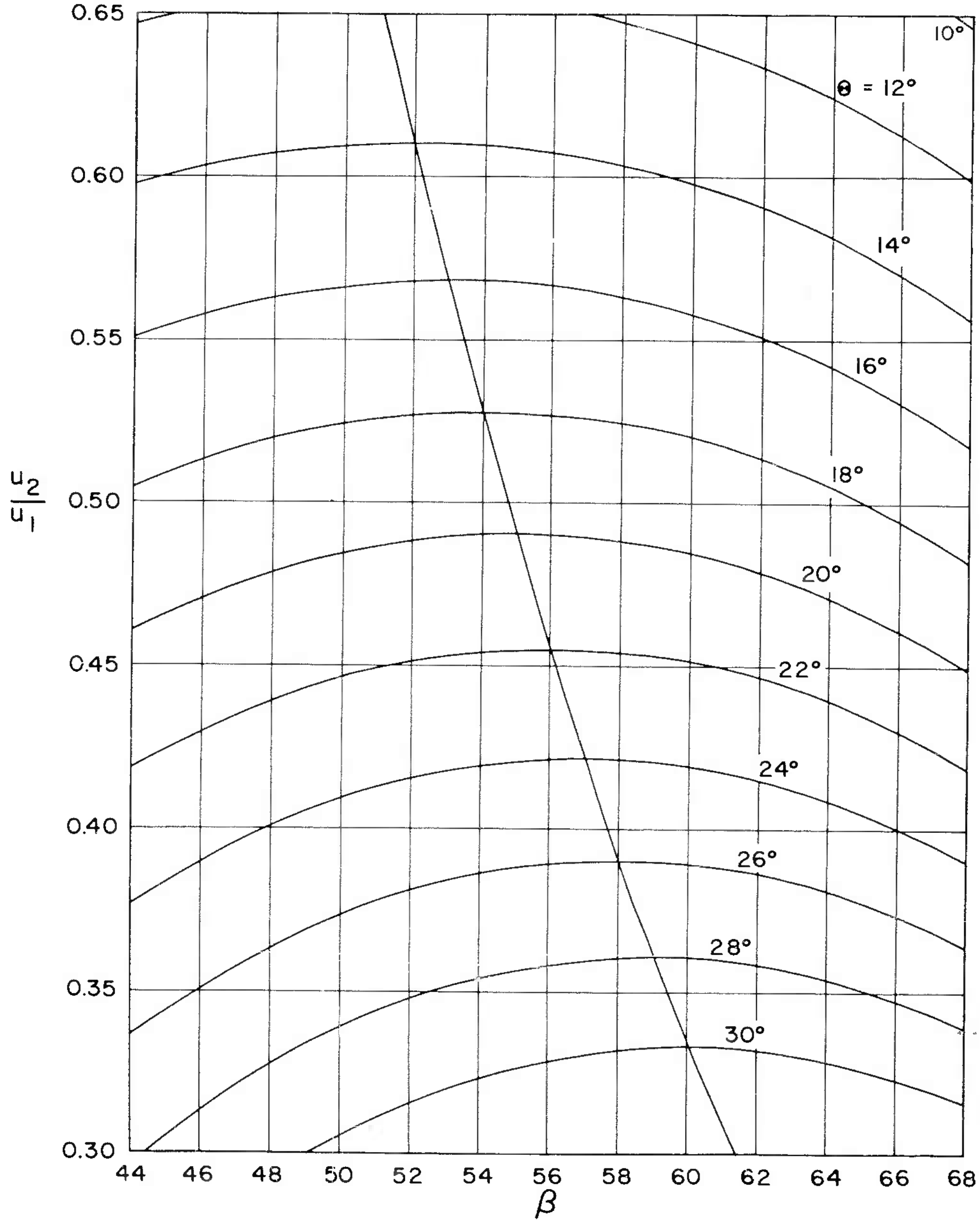
0.65
0.60
0.55
0.50
0.45
0.40
0.35
0.30
$\frac{u_2}{u_1}$
44
46
48
50
52
54
56
58
60
62
64
66
68
β
10°
θ = 12°
14°
16°
18°
20°
22°
24°
26°
28°
30°

Fig. 14g

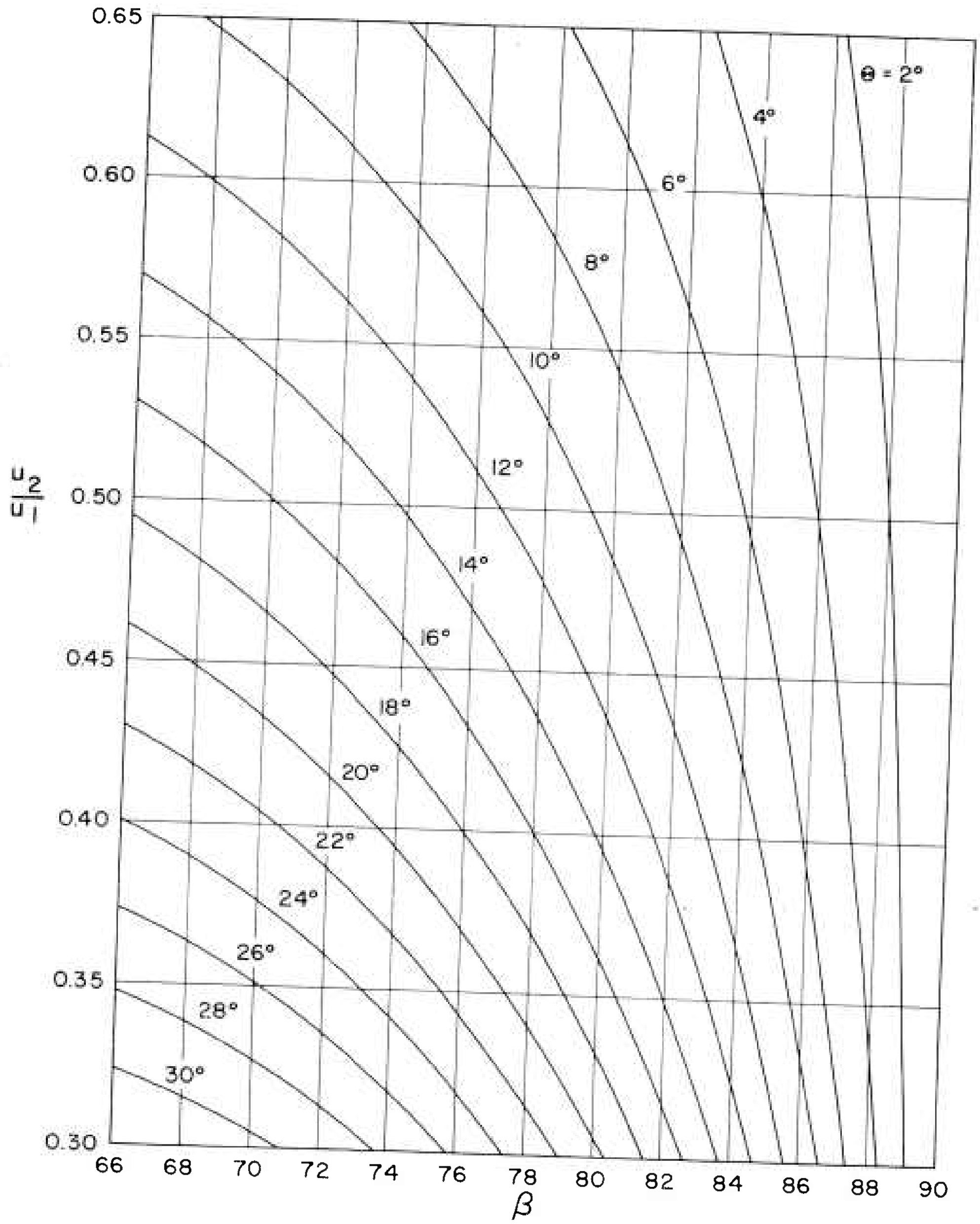
0.65
0.60
0.55
0.50
0.45
0.40
0.35
0.30
$\frac{u_2}{u_1}$
66
68
70
72
74
76
78
80
82
84
86
88
90
β
θ = 2°
4°
6°
8°
10°
12°
14°
16°
18°
20°
22°
24°
26°
28°
30°

Fig. 14h

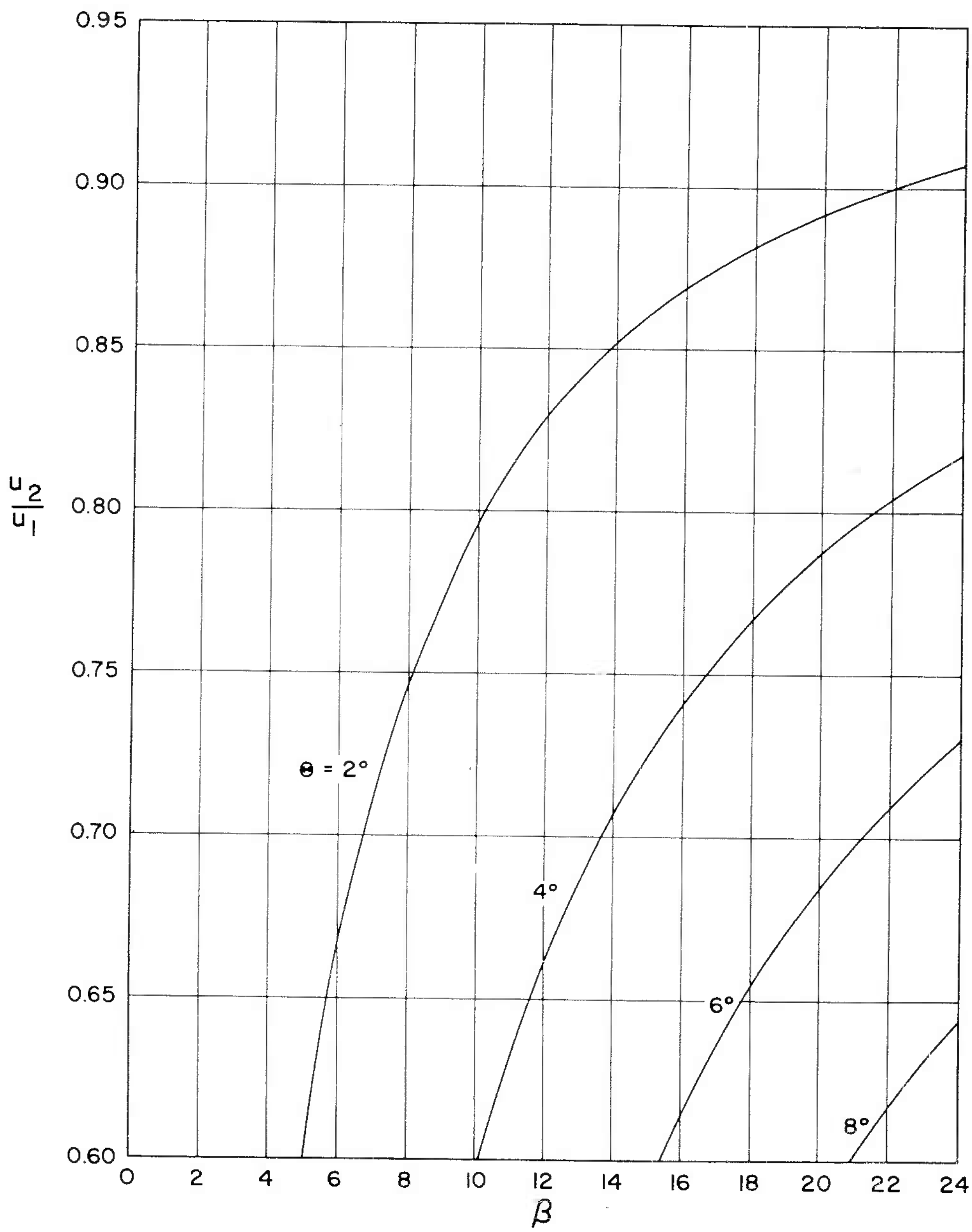
0.95
0.90
0.85
0.80
0.75
0.70
0.65
0.60
$\frac{u_2}{u_1}$
$\theta = 2°$
4°
6°
8°
0
2
4
6
8
10
12
14
16
18
20
22
24
β

Fig. 14i

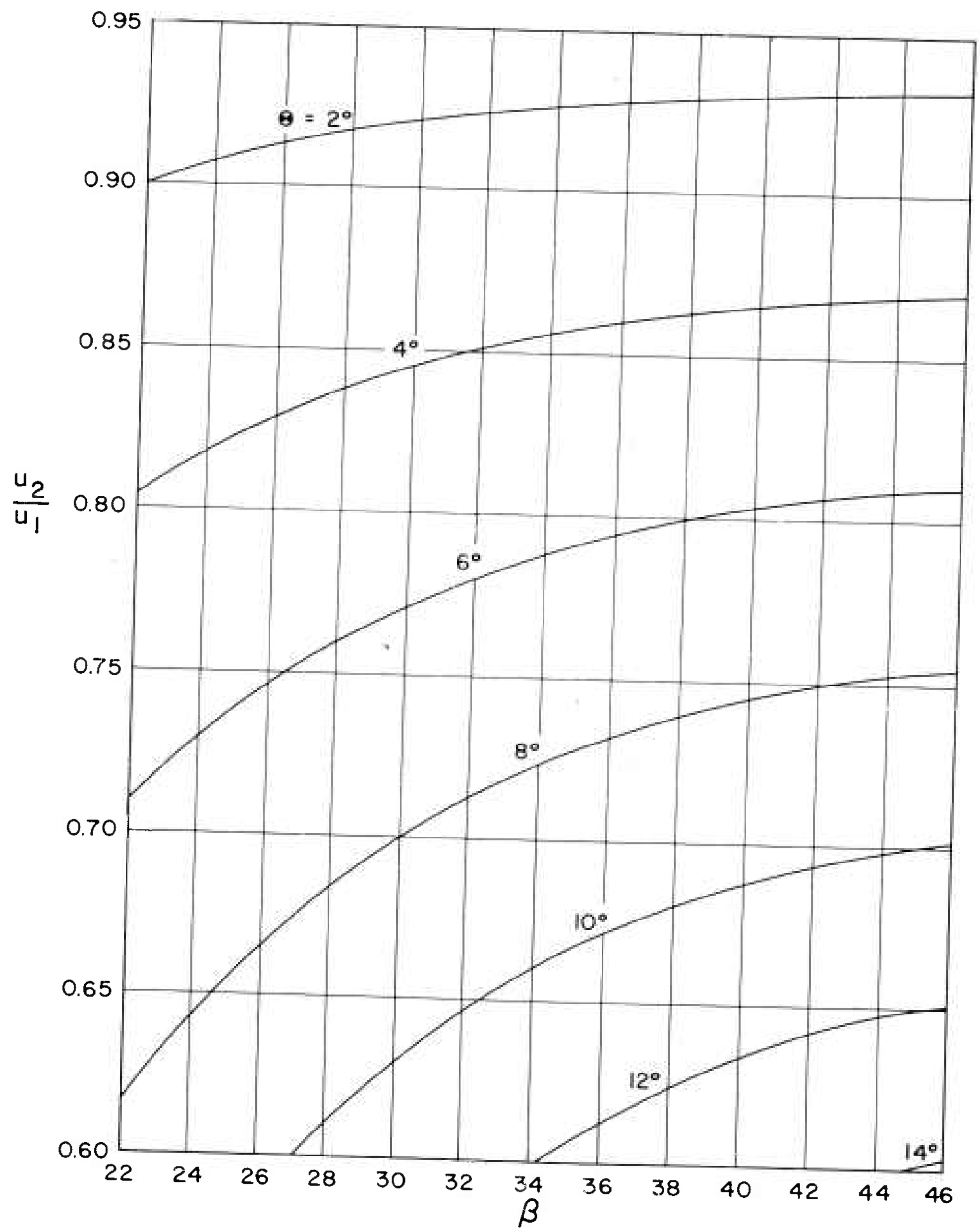
0.95
0.90
0.85
0.80
0.75
0.70
0.65
0.60
$\frac{u_2}{u_1}$
θ = 2°
4°
6°
8°
10°
12°
14°
22
24
26
28
30
32
34
36
38
40
42
44
46
β

Fig. 14j

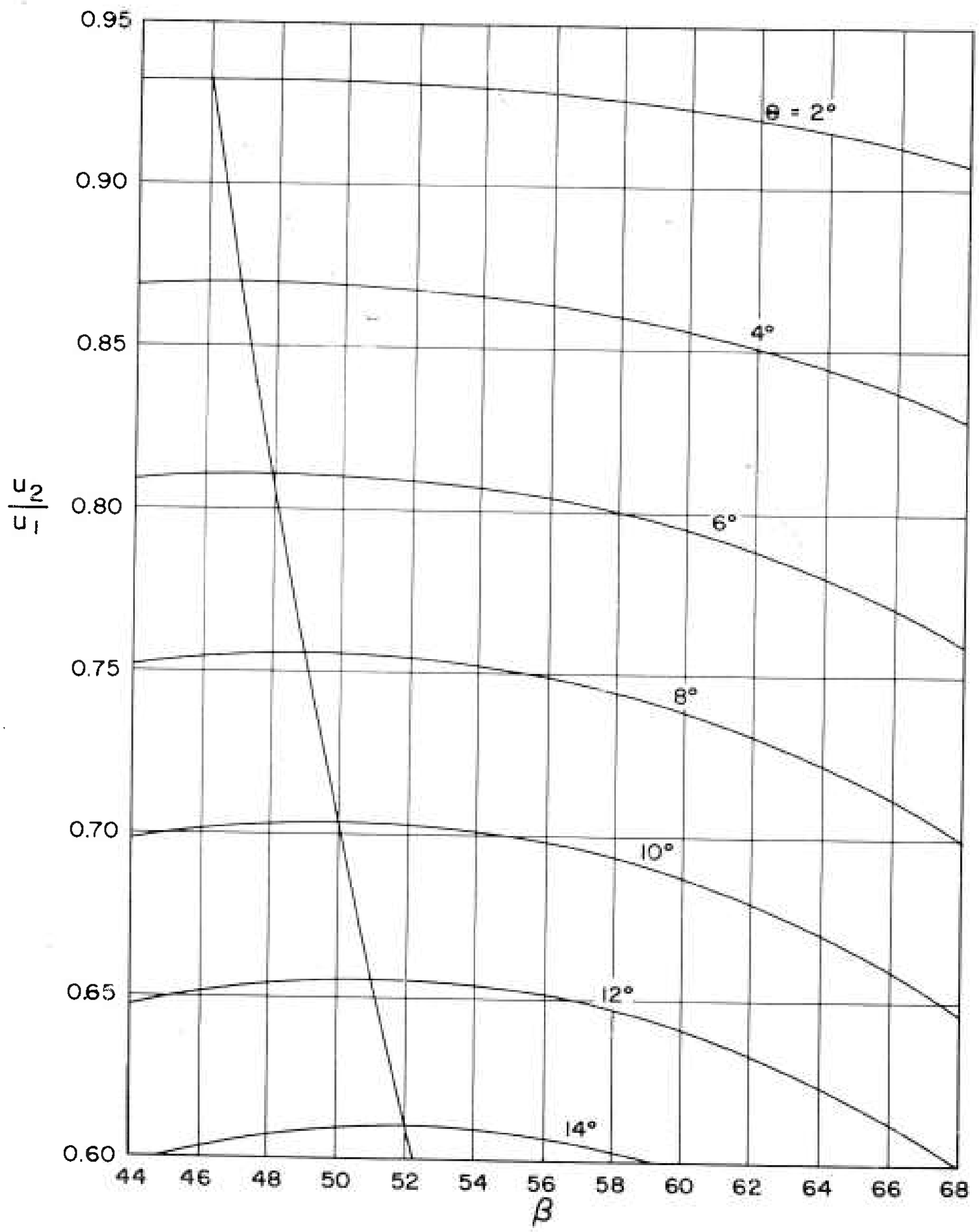

0.95
0.90
0.85
0.80
0.75
0.70
0.65
0.60
$\frac{u_2}{u_1}$
44
46
48
50
52
54
56
58
60
62
64
66
68
β
θ = 2°
4°
6°
8°
10°
12°
14°

Fig. 14k

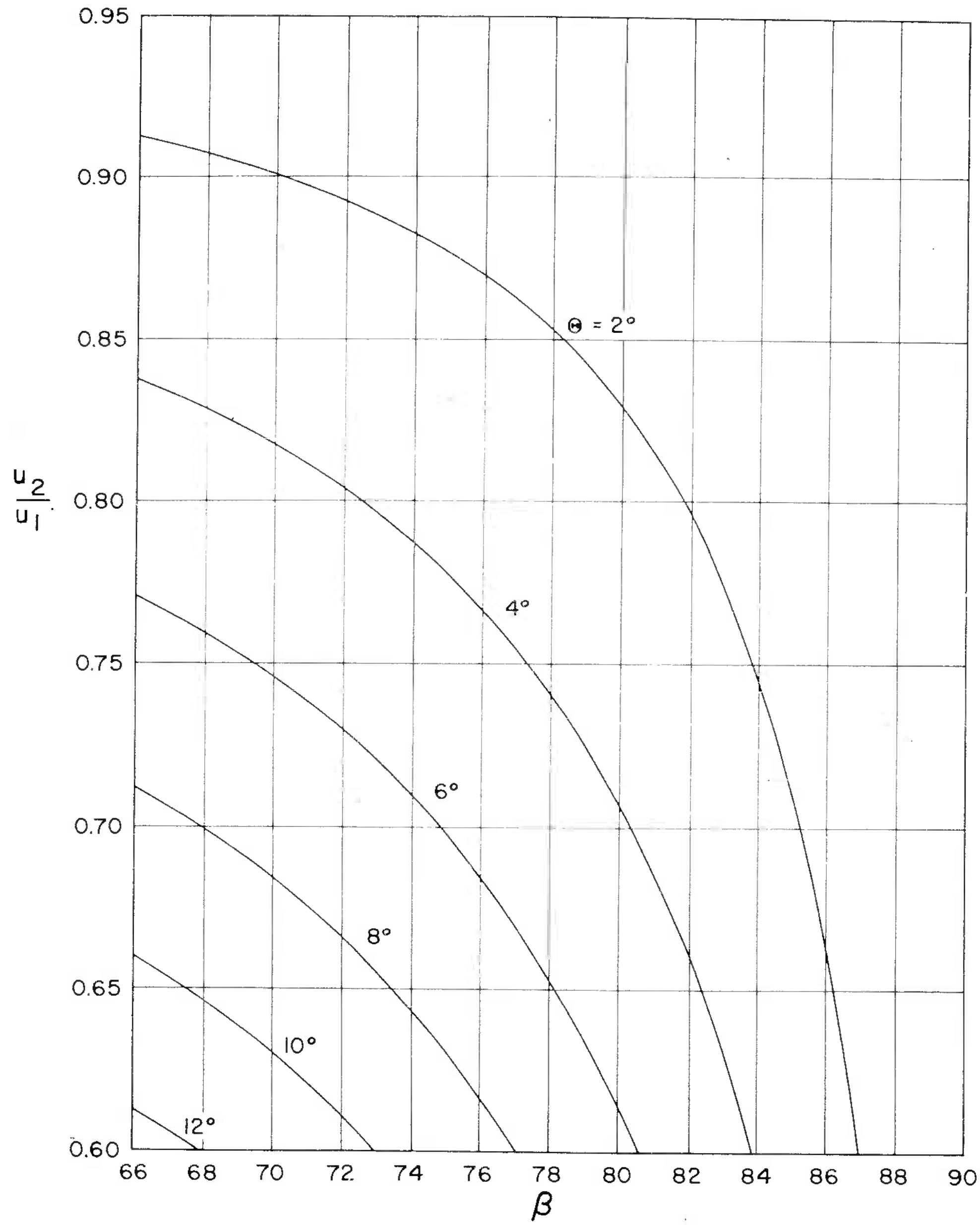
0.95
0.90
0.85
0.80
0.75
0.70
0.65
0.60
$\frac{u_2}{u_1}$
Θ = 2°
4°
6°
8°
10°
12°
66
68
70
72
74
76
78
80
82
84
86
88
90
β

Fig. 14 l

line with $\theta = \theta_{max}$ at Mach = ∞ is not a coincidence, but, as may be shown, a consistent result. The existence of real-gas effects does not alter the original statement, and as the upstream velocity becomes large $\beta = (45^\circ + \theta/2)$ approaches the limit of the weak-shock solutions. At low upstream Mach numbers a large range of weak-shock solutions lies where $\beta > (45^\circ + \theta/2)$, as may be seen on p. 42 of Ref. 22 (at low Mach numbers a gas usually behaves as a perfect gas). At any rate, the majority of physically possible solutions where the upstream Mach number is greater than 2 will occur where $\beta \leq (45^\circ + \theta/2)$; this will turn out to be fortunate, considering convergence of the method.

Now a solution satisfying Eqs. (39) and (40) and the normal shock relation of u_2/u_1 vs u_1 for a given upstream state, w_1 and θ, is desired. A qualitative plot is now constructed in Fig. 13 as follows:

Quadrant 1: A functional relationship between u_2/u_1 and β for the given θ (Eq.(40))

Quadrant 2: The normal-shock relation u_2/u_1 vs u_1 for the given upstream state (contains the physics of the problem)

Quadrant 3: A functional relation between u_1 and β for the given w_1 ($u_1 = w_1 \sin \beta$)

Quadrant 4: A 45° line to graphically convert the β axis in quadrant 1 to the β axis in quadrant 3

Line ABCDA can be seen to represent the weak-shock solution. The procedure to arrive at this solution is as follows:

1. Assume $\beta = 90^\circ$ in quadrant 3 such that $u_1 = w_1$ (point E).
2. From $u_1 = w_1$ find u_2/u_1 in quadrant 2 (point F).
3. From u_2/u_1, find β in quadrant 1 (point G).

4. Carry over this β to quadrant 3 through quadrant 4 (point H). It is now apparent that through the monotonic nature of all the functions the solution has been bracketed between $\beta = 90^{\circ}$ and $\beta_G = \beta_H$.

5. Obtain u_1 in quadrant 3 (point J).

6. Obtain u_2/u_1 in quadrant 2 (point K).

7. Obtain β in quadrant 1 (point L). Again it is obvious that the solution is now bracketed between β_L and $\beta_G = \beta_H$.

8. Continuing in this clockwise fashion, it is seen that the process is rapidly convergent.

It is important to note that any attempt to construct this solution in a counterclockwise manner would have failed, since the process would diverge. It is easily seen that this process converges in the same manner when the normal-shock relation in quadrant 2 contains inflection points but retains negative slope. It will be stated without demonstration that this process also converges when the normal-shock relation contains a small region of positive slope as previously mentioned. In this case, however, the convergence to the solution is from one side only; the solution is not continually being bracketed as above.

One other difficulty may be encountered. On the second iteration point K may correspond to a $u_2/u_1 > (u_2/u_1)_{max}$. In this case the starting point for the third trial is the β corresponding to $(u_2/u_1)_{max}$, i.e., $\beta = (45^{\circ} + \theta/2)$. If on the third trial the ratio u_2/u_1 obtained in quadrant 2 is greater than $(u_2/u_1)_{max}$, the solution must be where $\beta > (45^{\circ} + \theta/2)$.

Figure 15 illustrates the case mentioned immediately above. Following the lines JKLMN and OPQR, it is apparent that the solution must not be where $\beta \leq (45^{\circ} + \theta/2)$. Now starting again at point J and proceeding to K,

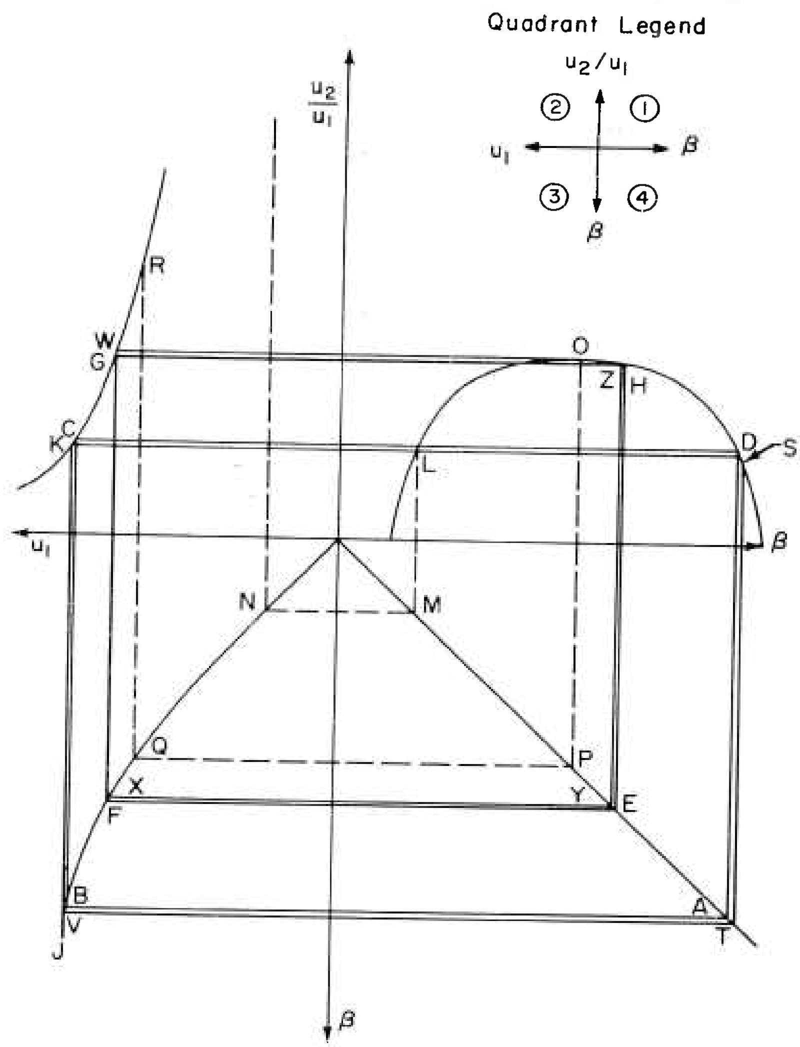

Fig. 15—Graphical solution for u_2/u_1 and β (strong- and weak-shock solution)

continue the KL line to S where $\beta > (45^\circ + \theta/2)$. Continue with a clockwise iteration starting from JKSTV, always selecting $\beta > (45^\circ + \theta/2)$ in quadrant 1; this is seen to converge to the solution ABCDA. Alternatively, starting from $(u_2/u_1)_{max}$ at point O and proceeding counterclockwise, the iteration begun by OWXYZ is seen to be converging to the solution EFGHE. It may also be seen that if β is originally selected such that $\beta_E < \beta < \beta_A$, the clockwise iteration will converge to ABCDA and counterclockwise iteration will converge to EFGHE. It will also be stated without demonstration that these conclusions are not altered if small regions of positive slope occur in the normal-shock relation (quadrant 2). It then becomes apparent that EFGHE is the weak-shock solution and ABCDA is the strong-shock solution.

With all cases now considered, the general method to be followed in obtaining a solution is outlined below.

Given: Upstream state, θ, w_1, and the normal-shock relation between u_2/u_1 and u_1 for the given upstream thermodynamic state.

A. Weak-shock solution

1. Assume $\beta = 90^\circ$, i.e., $u_1 = w_1$
2. From the normal shock relation obtain u_2/u_1
3. From Eq. (41) or the included graphs, obtain a new β, choosing $\beta \leq (45^\circ + \theta/2)$
4. From this β compute a new u_1 from Eq. (39)
5. From the new u_1 and the normal-shock relation obtain a new u_2/u_1
6. If this $u_2/u_1 \leq (u_2/u_1)_{max}$ for the given θ from Eq. (40), repeat this procedure to the desired degree of convergence
7. If this $u_2/u_1 > (u_2/u_1)_{max}$ assume $\beta = 45^\circ + \theta/2$ and compute a

new u_1 from Eq. (39)

8. Using this u_1 and the normal-shock relation obtain a new u_2/u_1

9. If this $u_2/u_1 \leq (u_2/u_1)_{max}$ proceed as in step 6

10. If this $u_2/u_1 > (u_2/u_1)_{max}$, the solution will not lie where $\beta \leq (45^\circ + \theta/2)$; assume $u_2/u_1 = (u_2/u_1)_{max}$; obtain u_1 from the normal shock relation

11. Compute β from Eq. (39) and this u_1

12. Using this β compute u_2/u_1 from Eq. (40) or obtain β from the included charts

13. Using this u_2/u_1 obtain u_1 from the normal-shock charts

14. Repeat steps 11 - 13 until the desired degree of convergence is reached

B. Strong-shock solution

1. Assume $\beta = 90^\circ$, i.e., $u_1 = w_1$

2. From the normal shock relation obtain u_2/u_1

3. From Eq. (41) or the included charts obtain a new β, choosing the $\beta > (45^\circ + \theta/2)$

4. Compute a new u_1 from Eq. (39)

5. Repeat steps 2 - 4 until the desired degree of convergence is reached

It may be shown that if the normal shock solution is obtained by an iteration scheme that is stopped when two consecutive values of u_2/u_1 differ by no more than 0.0001, a consistent degree of convergence in this method is arrived at when two consecutive values of β differ by no more than 0.05 per cent, i.e., $\Delta\beta/\beta \leq 0.0005$; however, this is by no means absolutely true

over the entire range. The rapid convergence of this method is illustrated by three numerical examples for air given below.

It should be kept in mind that this procedure is not particularly useful when a complete set of oblique-shock charts for a known atmosphere is to be constructed. In such a case all that needs be done is to specify a β and iterate the normal-shock equations. The corresponding θ can then be immediately calculated.

EXAMPLES

1. Very Weak Shock

Given: $w_1 = 8000$ ft/sec in air

Altitude = 82,345 ft (1956 ARDC model atmosphere)[23]

$\theta = 20^\circ$

Find: β for the weak-shock solution

Solution: (a) Assume $\beta = 90^\circ$, then $u_1 = 8000$ ft/sec

From the normal-shock data in Ref. 20, $u_2/u_1 = 0.1435$

From Eq. (41), taking the negative sign for $\beta \leq (45^\circ + \theta/2)$

$\beta = 23.58^\circ$

The solution is now bracketed between 23.58° and 90°

(b) Taking $\beta = 23.58^\circ$ and using Eq. (39), $u_1 = 3201$ ft/sec

From the normal-shock data $u_2/u_1 = 0.2407$

From Eq. (41), $\beta = 26.98^\circ$

The solution is now bracketed between 26.98° and 26.16°

Continuing:

(b.1) $u_1 = 3630$ ft/sec

$$\frac{u_2}{u_1} = 0.2198$$

$\beta = 26.16^\circ$

(b.2) $u_1 = 3527$ ft/sec

$$\frac{u_2}{u_1} = 0.2243$$

$\beta = 26.33^\circ$

(b.3) $u_1 = 3548$ ft/sec

$$\frac{u_2}{u_1} = 0.2230$$

$\beta = 26.29^\circ$

(b.4) $u_1 = 3544$ ft/sec

$\frac{u_2}{u_1} = 0.2230$ within the accuracy with which the charts can be read

$\beta = 26.29^\circ$ which is the solution compared with

$\beta = 26.3^\circ$ obtained from Ref. 20

2. Strong-Shock Solution and Illustration of Convergence Difficulties for the Weak Shock

Given $\quad w_1 = 3000$ ft/sec in air

Altitude $= 175,348$ ft

$\theta = 30^\circ$

Find: β for the strong-shock solution

Solution: First, hunting for the weak-shock solution, assume

$\beta = 90^\circ$

$u_1 = 3000$ ft/sec

From the normal-shock data

$$\frac{u_2}{u_1} = 0.2740$$

From Fig. 14 for $\theta = 30^{\circ}$, $\frac{u_2}{u_1} = 0.2740$, and $\beta \leq (45^{\circ} + \theta/2)$

$$\beta = 45.67^{\circ}$$

From Eq. (39)

$$u_1 = 2176 \text{ ft/sec}$$

and from the normal-shock chart

$$\frac{u_2}{u_1} = 0.3866$$

But, as can be seen in Fig. 14, this is greater than

$$\left(\frac{u_2}{u_1}\right)_{max}$$

Therefore, assume

$$\frac{u_2}{u_1} = \left(\frac{u_2}{u_1}\right)_{max} \qquad \beta = (45^{\circ} + \frac{30^{\circ}}{2}) = 60^{\circ}$$

From Eq. (39)

$$u_1 = 2598 \text{ ft/sec}$$

and from the shock chart

$$\frac{u_2}{u_1} = 0.3140$$

which is now less than $\frac{u_2}{u_1}_{max}$ and the process will converge to the weak-shock solution where $\beta < (45^{\circ} + \theta/2)$. Looking for the strong-shock solution, choose $\beta = 90^{\circ}$, $u_1 = 3000$ ft/sec. Then as before $u_2/u_1 = 0.2740$. Now from Fig. 14 pick $\beta > (45^{\circ} + \theta/2)$.

$$\beta = 74.32^{\circ}$$

From Eq. (39)

$$u_1 = 2888 \text{ ft/sec}$$

From the shock charts

$$\frac{u_2}{u_1} = 0.2843$$

From Fig. 14

$$\beta = 73.07^\circ$$

Continuing:

$$u_1 = 2870 \text{ ft/sec}$$

$$\frac{u_2}{u_1} = 0.2848$$

$$\beta = 72.99^\circ$$

$$u_1 = 2869 \text{ ft/sec}$$

$$\frac{u_2}{u_1} = 0.2850$$

$$\beta = 72.96^\circ$$

And since on the last trial

$$\frac{\Delta\beta}{\beta} = \frac{72.99 - 72.96}{72.96} = 0.00041 < 0.0005$$

we stop the process and take the strong-shock solution as

$$\beta = 72.96^\circ$$

3. Weak-Shock Solution on Right Half of u_2/u_1 vs β Curve

Given: Mach number = 1.9 in air which is assumed a perfect gas

Normal-shock relations are taken from Ref. 22. $\theta = 20^\circ$

Find: β for weak shock

Solution: Clearly assuming $\beta = 90^\circ$, $M_{1_{\text{normal}}} = 1.9$ will yield

$$\frac{u_2}{u_1} > \left(\frac{u_2}{u_1}\right)_{max}$$

on the second iteration. Therefore assume

$$\frac{u_2}{u_1} = \left(\frac{u_2}{u_1}\right)_{max}, \ \beta = 55^\circ$$

From Eq. (39), using the Mach numbers instead of velocity

$$M_{1_n} = 1.556$$

From Ref. 23

$$\frac{u_2}{u_1} = \frac{1}{\rho_2/\rho_1} = 0.5109$$

which is greater than $\left(\frac{u_2}{u_1}\right)_{max}$. Therefore, the weak-shock solution must lie where $\beta > (45^\circ + \theta/2)$.

Now, using the previously mentioned counterclockwise solution, choose $\beta = (45^\circ + \theta/2)$ and $\left(\frac{u_2}{u_1}\right)_{max}$

$$\frac{u_2}{u_1} = 0.4903$$

From the normal shock tables

$$M_{1_n} = 1.604$$

and from Eq. (39)

$$\beta = 57.59^\circ$$

From Fig. 14

$$\frac{u_2}{u_1} = 0.4888$$

Continuing:

$$M_{1_n} = 1.608$$

$$\beta = 57.81^\circ$$

$$\frac{u_2}{u_1} = 0.4884$$

$$M_{1_n} = 1.6091$$

$$\beta = 57.87^\circ$$

$$\frac{u_2}{u_1} = 0.4883$$

$$M_{1_n} = 1.6094$$

$$\beta = 57.89^\circ$$

and since

$$\frac{\Delta\beta}{\beta} = \frac{57.89 - 57.87}{57.89} = 0.0003 < 0.0005$$

the process is stopped and

$$\beta = 57.89^\circ$$

compared to the solution in Ref. 22 of

$$\beta = 57.9^\circ$$

Appendix C

CALCULATION OF ELECTRON CONCENTRATIONS AT LOW TEMPERATURES IN THE C-N-O GASEOUS SYSTEM

It is known that strong interference with radio or telemetry transmission from atmospheric-entry vehicles is possible if the transmission frequency is equal to or less than the plasma frequency of the medium surrounding the antenna and if the collision frequency is large enough. Plasma frequency is directly dependent upon the square root of the electron concentration in the surrounding medium, and it may be desired to know this concentration to as low as 10^{-17} g-mole of electrons per g-mole of gas mixture. This concentration corresponds to a transmission frequency of 10 Mc through a medium, for example, at a pressure of 10^2 atm and a temperature of 1000°K in the present tentative Venus atmosphere.

Since the equilibrium composition of gases computed by the method of Ref. 18 does not show the trace constituents, it is not suited to the calculation of electron concentrations at low temperatures if the major constituents of the gas mixture are known. In particular, the present calculations apply to the C-N-O gaseous mixture but the general method may be applied to any arbitrary mixture. The calculated electron concentration is based on an ideal gas mixture in thermodynamic equilibrium when the major constituents of the gas mixture are known. Since the major constituents of the gas are generally computed on the basis of an ideal gas in thermodynamic equilibrium, these conditions are consistent.

For a chemical reaction of ideal gases in thermodynamic equilibrium, the equilibrium constant may be written

$$K_p = \frac{\prod_i p_i}{\prod_j p_j} = \exp\left[-\frac{\Delta E_o^\circ}{RT} + \sum_j \left(\frac{F^\circ - E_o^\circ}{RT}\right)_j - \sum_i \left(\frac{F^\circ - E_o^\circ}{RT}\right)_i \right] \tag{44}$$

where i denotes the products, j the reactants, and Δ the change as measured by products minus reactants. From an examination of the reaction energies for the C-N-O system in Table 4, it is evident that at low temperatures the electrons may to a close approximation be considered to be produced solely by the following reactions:

1. $CO_2 \rightleftharpoons CO_2^+ + e^-$ $\quad \Delta E_o^o = 317{,}731$ cal/g-mole[24]
2. $CO \rightleftharpoons CO^+ + e^-$ $\quad \Delta E_o^o = 323{,}180$ cal/g-mole[9]
3. $O_2 \rightleftharpoons O_2^+ + e^-$ $\quad \Delta E_o^o = 277{,}900$ cal/g-mole[9]
4. $O \rightleftharpoons O^+ + e^-$ $\quad \Delta E_o^o = 314{,}048$ cal/g-mole[9]
5. $C \rightleftharpoons C^+ + e^-$ $\quad \Delta E_o^o = 259{,}842$ cal/g-mole[9]
6. $NO \rightleftharpoons NO^+ + e^-$ $\quad \Delta E_o^o = 213{,}400$ cal/g-mole[9]

Using the law of partial pressures the equilibrium constant for the corresponding reactions may be expressed as

1. $$K_{p_1} = \frac{\left(n_{CO_2^+}\right)\left(n_{e^-}\right)}{n_{CO_2}} \left(\frac{p}{n}\right) \tag{45}$$

2. $$K_{p_2} = \frac{\left(n_{CO^+}\right)\left(n_{e^-}\right)}{n_{CO}} \left(\frac{p}{n}\right) \tag{46}$$

$$3.\quad K_{p_3} = \frac{\left(n_{O_2^+}\right)\left(n_{e^-}\right)}{n_{O_2}} \left(\frac{p}{n}\right) \tag{47}$$

$$4.\quad K_{p_4} = \frac{\left(n_{O+}\right)\left(n_{e^-}\right)}{n_O} \left(\frac{p}{n}\right) \tag{48}$$

$$5.\quad K_{p_5} = \frac{\left(n_{C+}\right)\left(n_{e^-}\right)}{n_e} \left(\frac{p}{n}\right) \tag{49}$$

$$6.\quad K_{p_6} = \frac{\left(n_{NO+}\right)\left(n_{e^-}\right)}{n_{NO}} \left(\frac{p}{n}\right) \tag{50}$$

Since it is assumed that all of the electrons come from the above ionized species

$$n_{e^-} = n_{CO_2^+} + n_{CO+} + n_{O_2^+} + n_{O+} + n_{C+} + n_{NO+} \tag{51}$$

Combining Eqs. (45) - (51), the electron concentration on the basis of n g-moles of the mixture is

$$n_{e^-} = \sqrt{\left(n_{CO_2} K_{p_1} + n_{CO} K_{p_2} + n_{O_2} K_{p_3} + n_O K_{p_4} + n_C K_{p_5} + n_{NO} K_{p_6}\right)\left(\frac{n}{p}\right)} \tag{52}$$

Some equilibrium constants have been calculated and are shown in Table 15 for a range of 1000°K to 6000°K. The amounts n_i of the major constituents are assumed known and may be placed in the computational Eq. (52) along with the equilibrium constants, and the electron concentrations may be determined. It is

suggested, however, that the accuracy obtained by this method be limited to two significant figures at temperatures where electron concentration becomes significant, since the molar constituents assumed in the calculation from Eq. (52) do not account for the presence of electrons.

For illustrative purposes, results of some of these computations for pure CO_2 corresponding to those of Ref. (17) have been made and are presented in Table 16.

REFERENCES

1. Kopal, Z., "Aerodynamic Effects in Planetary Atmospheres," Aerospace Eng., Vol. 19, No. 12, December 1960, p. 10.

2. Kuiper, G. P. (ed.), The Atmospheres of the Earth and Planets, 2d ed., University of Chicago Press, Chicago, 1952, pp. 248, 252, 306, 406.

3. Dole, S. H., The Atmosphere of Venus, The RAND Corporation, P-978, October 12, 1956.

4. Mintz, Y., Temperature and Circulation of the Atmosphere of Venus, The RAND Corporation, P-2003, May 27, 1960.

5. Sagan, C., The Radiation Balance of Venus, Doctoral Dissertation, University of Chicago, 1960.

6. Shaw, J. H., and N. T. Bobrovnikoff, Natural Environment of the Planet Venus, WADC, Phase Technical Note 847-2, February 1959.

7. Vaucouleurs, G., de, Air Force Missile Development Center Technical Note (AFMDC-IN-59-37), Holloman Air Force Base, New Mexico, December 1959.

8. Kaplan, L. D., A New Interpretation of the Structure and CO_2 Content of the Venus Atmosphere, The RAND Corporation, P-2213, May 2, 1961.

9. Gilmore, F. R., Equilibrium Composition and Thermodynamic Properties of Air to 24,000°K, The RAND Corporation, RM-1543, August 24, 1955.

10. Keenan, J. H., and J. Kaye, Gas Tables, John Wiley and Sons, Inc. New York, 1948.

11. Hodgman, C. D. (ed.), Handbook of Chemistry and Physics, 39th ed., Chemical Rubber Publishing Company, Cleveland, Ohio, 1953.

12. Mayer, C. H., "Planetary Radiation at Centimeter Wavelengths," Astronom. J., Vol. 64, March 1959, p. 43.

13. Chamberlain, J. W., and G. P. Kuiper, "Rotational Temperature and Phase Variation of the CO_2 Bands of Venus," Astrophys. J., Vol. 124, 1956, p. 399.

14. Hutchinson, G. E., "The Biochemistry of the Terrestrial Atmosphere," in G. P. Kuiper (ed.), The Earth as a Planet, University of Chicago Press, Chicago, 1954.

15. Barrett, A. H., "Microwave Absorption and Emission in the Atmosphere of Venus," Astrophys. J., Vol. 133, No. 1, January 1961.

16. Summary of the Results of the Moore-Ross Flight of November 1959, Information Release by the Laboratory of Astrophysics and Physical Meteorology, The Johns Hopkins University, Baltimore, Maryland, March 1, 1960.

17. Raymond, J. L., Thermodynamic Properties of Carbon Dioxide to 24,000°K - With Possible Application to the Atmosphere of Venus, The RAND Corporation, RM-2292, November 26, 1958.

18. White, W. B., S. M. Johnson, and G. B. Dantzig, "Chemical Equilibrium in Complex Mixtures," J. Chem. Phys., Vol. 28, No. 5, May 1958.

19. Sweigert, R. L., P. Weber, and R. L. Allen, "Thermodynamic Properties of Gases," Ind. and Chem. Eng., Vol. 38, No. 2, February 1946, p. 185.

20. Normal and Oblique Shock Characteristics at Hypersonic Speeds, Douglas Aircraft Company, Inc., Engineering Report No. LB-25599, December 31, 1957; also R. A. Batchelder, Supplement I to the report.

21. Feldman, S., Hypersonic Gas Dynamic Charts for Equilibrium Air, AVCO-Everett Research Laboratory, Research Report 40, 1957.

22. Equations, Tables, and Charts for Compressible Flow, Ames Research Staff, NACA Report 1135, 1953, pp. 42-43.

23. Minzer, R. A., and W. S. Ripley, The ARDC Model Atmosphere, 1956, AFCRC TN-56-204, December 1956.

24. Tanaka, Y., A. S. Jursa, and F. J. LeBlanc, "Higher Ionization Potentials of Linear Triatomic Molecules. I. CO_2," J. Chem. Phys., Vol. 32, No. 4, April 1960, p. 1199.